

© Copyright 2024

Jessie Kulsuptrakul

CARD8 inflammasome activation upon HIV-1 infection

Jessie Kulsuptrakul

A dissertation

submitted in partial fulfillment of the
requirements for the degree of

Doctor of Philosophy

University of Washington

2024

Reading Committee:

Michael Emerman, Chair

Patrick Mitchell, Chair

Andrew Oberst

Program Authorized to Offer Degree:

Molecular and Cellular Biology

University of Washington

Abstract

CARD8 inflammasome activation upon HIV-1 infection

Jessie Kulsuptrakul

Chairs of the Supervisory Committee:

Michael Emerman and Patrick Mitchell

Department of Microbiology

Inflammasomes are host cytosolic innate immune complexes that assemble upon detection of diverse pathogen-associated cues and play a crucial role in host defense but can also contribute to inflammatory pathogenesis. In prior work, the inflammasome-forming sensor CARD8 was reported to recognize the enzymatic activity of the protease of human immunodeficiency virus type 1 (HIV-1). I demonstrated that human CARD8 has a unique motif among hominoids and Old World monkeys that renders it susceptible to cleavage by HIV-1 protease (HIV-1^{PR}). Furthermore, the protease from the precursor to HIV-1, SIVcpz, can cleave human CARD8, but not chimpanzee CARD8. This indicates that the precursor viruses to HIV-1 were poised to cleave human CARD8 prior to cross-species transmission into human. In addition, I show that CARD8 sensing can happen during acute HIV-1 infection, using multiple modes of infection in cancer and primary cell lines, in a manner dependent on HIV-1^{PR} cleavage of the human-specific motif in CARD8, resulting in a lytic form of cell death called pyroptosis and

the release of proinflammatory cytokines. Genetic knockout of the inflammasome adaptor protein ASC suggests that cell death associated with HIV-dependent inflammasome activation is primarily CARD8-dependent whereas cytokine release may be amplified through secondary modulation by the NLRP3 inflammasome. Additionally, I identified mutant HIV-1 proteases from a panel of protease inhibitor resistant HIV-1 strains that differentially cleave and activate CARD8 compared to wildtype HIV-1.

HIV-1 arose from multiple cross-species transmissions from simian immunodeficiency virus (SIV) infecting other primates. While some non-human primates infected with SIVs exhibit inflammatory pathologies, humans present with the most severe inflammatory pathogenesis, progressing to acquired immunodeficiency syndrome (AIDS) without anti-retroviral therapy. The findings outlined in this thesis suggest a model whereby human-specific activation of the CARD8 inflammasome may contribute to chronic immune activation and may partially explain the heightened pathogenesis of HIV-1 in humans relative to SIV in other non-human primate reservoirs.

TABLE OF CONTENTS

LIST OF FIGURES AND TABLES	IV
ACKNOWLEDGEMENTS	V
CHAPTER 1: INTRODUCTION.....	1
HIV-1 REPLICATION AND THE IMPORTANCE OF HIV-1 PROTEASE	1
POSITIVE SENSE RNA VIRAL PROTEASES	5
THE ORIGINS OF HIV-1	6
HIV AND SIV PATHOGENESIS.....	7
INNATE IMMUNE SENSING AND PROGRAMMED CELL DEATH.....	10
EFFECTOR-TRIGGERED IMMUNITY	13
NLRP1	17
CARD8.....	18
THE ROLE OF PYROPTOSIS IN HIV	20
SUMMARY/THESIS RATIONALE	21
CHAPTER 2: A HUMAN-SPECIFIC MOTIF FACILITATES CARD8 INFLAMMASOME ACTIVATION AFTER HIV-1 INFECTION	22
ABSTRACT	22
INTRODUCTION	23
RESULTS	25
<i>A human-specific motif allows CARD8 to detect protease activity from multiple HIV strains</i>	25
<i>Natural variation in CARD8 alters sensing of SIVcpz protease activity</i>	27
<i>HIV-1 infection activates the inflammasome in primed THP-1 cells in a CARD8-dependent manner.....</i>	29
<i>CARD8-dependent inflammasome activity after HIV-1 infection occurs both early and late in acute infection and depends on the activity of HIV-1^{PR}</i>	34
<i>HIV-1 inflammasome activation is dependent on CARD8 sensing of HIV-1^{PR} activity.....</i>	36
DISCUSSION.....	37
<i>CARD8 as an innate immune sensor of HIV-1^{PR} activity</i>	38
<i>Human CARD8 as a maladaptation to HIV-1 infection</i>	39
<i>Possible links to pathogenesis.....</i>	40

ACKNOWLEDGEMENTS	42
SUPPLEMENTAL INFORMATION	42
METHODS	43
<i>Plasmids</i>	43
<i>Cell Culture</i>	43
<i>Immunoblotting</i>	44
<i>CARD8 cleavage assay</i>	44
<i>FLICA Assay</i>	45
<i>CARD8 and CASP1 knockout generation</i>	45
<i>CCR5+ cell line generation</i>	45
<i>CARD8 complementation</i>	45
<i>HIV-1_{LAI}, HIV-1_{Q23-BG505}, and HIV-1_{LAI-VSVG} production</i>	46
<i>THP-1 priming and HIV-1 infection</i>	46
<i>IL-1R reporter assay</i>	47
CHAPTER 3: EFFECTS OF CELL-TO-CELL TRANSMISSION AND PROTEASE	
VARIABILITY ON CARD8 INFLAMMASOME ACTIVATION AFTER HIV-1 INFECTION	48
ABSTRACT	48
INTRODUCTION	49
RESULTS	51
<i>Cell-to-cell transmission of HIV-1 induces CARD8-dependent inflammasome activation ..</i>	<i>51</i>
<i>CARD8-dependent activation from HIV-1 is mostly ASC-independent.....</i>	<i>57</i>
<i>Protease inhibitor resistant strains of HIV-1 differentially cleave and activate CARD8</i>	<i>60</i>
<i>Protease inhibitor resistant clones exhibit variable protease activation efficiency for CARD8</i>	
<i>cleavage but not altered specificity</i>	<i>63</i>
DISCUSSION.....	67
<i>T cell to macrophage cell-to-cell transmission and implications for HIV-1 pathogenesis ...</i>	<i>67</i>
<i>Inflammasome activation from HIV-1 is largely ASC-independent</i>	<i>68</i>
<i>Protease inhibitor resistant mutants of HIV^{PR} may cleave CARD8 with different efficiencies</i>	
<i>than wildtype HIV^{PR}</i>	<i>69</i>
<i>Ongoing work</i>	<i>70</i>
METHODS	72
<i>Plasmids and Reagents</i>	72
<i>Cell culture</i>	72

<i>HIV-1_{LAI}, HIV-1_{LAI-VSVG}, and HIV-1_{NL4.3-BaL} production</i>	73
<i>Cell-free and cell-to-cell coculture HIV-1 infection</i>	73
<i>Transwell coculture HIV-1 infection</i>	74
<i>Monocyte-derived macrophage isolation/differentiation</i>	74
<i>IL-1R reporter assay</i>	74
<i>ASC KO and CARD8/ASC DKO generation</i>	75
<i>CARD8 cleavage assay</i>	75
<i>HEK reconstitution assay</i>	76
CHAPTER 4: CONCLUSIONS, PERSPECTIVES, AND FUTURE DIRECTIONS	77
SUMMARY	77
CARD8 SENSING OF INCOMING HIV PROTEASE.....	77
CARD8 SENSING OF DE NOVO SYNTHESIZED HIV PROTEASE	79
DIFFERENTIAL CLEAVAGE OF OTHER HOST TARGETS OF HIV PROTEASE	81
EFFECTS OF TISSUE MICROENVIRONMENT ON CARD8 ACTIVATION	83
CARD8 INFLAMMASOME ACTIVATION AS A DRIVER OF HIV-1 PATHOGENESIS	84
EXPLORING OTHER NON-HUMAN PRIMATE CARD8.....	85
THE ORIGINS OF CARD8 INFLAMMASOME ACTIVATION BY HIV-1 PROTEASE	87
CARD8 ACTIVATION FOR HIV CURE	89
CONCLUDING REMARKS	91
BIBLIOGRAPHY	92

LIST OF FIGURES AND TABLES

Figure 1.1: Schematic of HIV replication.....	2
Figure 1.2: HIV proteolytic processing of HIV ^{gagpol}	3
Figure 1.3: Cross-species transmission events preceding HIV-1 and HIV-2	7
Figure 1.4: Hallmarks of lentiviral infection in progressing versus non-progressing hosts	9
Figure 1.5: Canonical inflammasome activation	13
Figure 1.6: Effector triggered immunity by inflammasomes.....	16
Figure 2.1: The F59-F60 motif allows human CARD8 to detect protease activity from multiple HIV strains	26
Figure 2.2: Natural variation in CARD8 alters sensing of SIVcpz ^{PR} activity.....	28
Figure 2.3: SIVmac cleaves wildtype human CARD8.....	29
Figure 2.4: HIV-1 infection activates the CARD8 inflammasome in THP-1 cells	31
Figure 2.5: Functional validation of CARD8 KO THP-1 cells.....	32
Figure 2.6: Incoming and outgoing HIV ^{PR} is responsible for CARD8 inflammasome activation	33
Figure 2.7: HIV-1 inflammasome activation is dependent on a human-specific motif in CARD8	35
Figure 2.8: Human FF motif in chimpanzee CARD8 rescues sensing of HIV/SIV ^{PR}	37
Figure 3.1: Cell-to-cell transmission of HIV induces CARD8 inflammasome activation	54
Figure 3.2: Inefficient cell-free HIV-1 infection yields no CARD8 inflammasome activation	56
Figure 3.3: CARD8-dependent activation from HIV-1 is mostly ASC-independent	59
Figure 3.4: Protease inhibitor resistant strains of HIV-1 differentially cleave and activate CARD8	62
Figure 3.5: Protease inhibitor resistant clones exhibit variable protease activation efficiency ..	65
<hr/>	
Table 3.1: Protease inhibitor resistance mutations and fold resistance	60

ACKNOWLEDGEMENTS

This work would not have been possible without the mentorship, support, guidance, and insight of many individuals. First and foremost, I would like to thank my advisors, Michael Emerman and Patrick Mitchell. To Michael, you are a one-of-a-kind mentor, scientist, and person and have built and fostered an unparalleled utopia for trainees. You inspire me with how dedicated you are to your trainees, providing speedy feedback and advocating for them outright and behind the scenes. Thank you for your unwavering encouragement that has helped me become a more confident scientist. Every time I go into your office feeling stressed over a result, you have never failed to craft a positive spin on my findings, and I always come out of your office feeling more at ease, knowing that you are in my corner. You are beloved and respected by so many, and I am honored to be one of your trainees.

To Patrick, you are one of the most driven people I know. As your first rotation and graduate student, I've watched as you've built your lab from 2 people to 16 people in the span of 3 years and secured remarkable funding to ensure a bright future for your lab. You are a true force of nature and inspire me with your ambition, insatiable thirst for knowledge, and ingenious ideas. Despite pressures to publish in your inaugural lab years, you've remained a kind, supportive, and understanding mentor that values the well-being of his trainees over all else and for that I thank you. Your enthusiasm for science and new data is contagious, and I enjoyed rapidly sending new data to you fresh off the machine, knowing you would be just as (or even more) thrilled than I was to dig into it. From your thorough comments on my drafts to your Slack brainstorming on the potential implications of CARD8 sensing, you've challenged me into becoming a better and more rigorous scientist and pushed me to think more deeply. I am so lucky to have trained with you, and I'm excited to see all you will achieve throughout your research career.

Thank you to my thesis committee – Melody Campbell, Lillian Cohn, and Andrew Oberst – for your insightful feedback on my project and career advice, and a special thank you to Andrew for reviewing this thesis. I am also grateful to my past scientific mentors. Thank you Varuzhan for your kindness and generosity in teaching me the fundamentals of academic research and giving me the opportunity to begin pursuing scientific research when I was an undergraduate. Additionally, I would like to thank Andreas Puschnik who sparked my passion for virology research and inspired me to apply to graduate school.

To current Emerman lab members and alumni, I am so blessed to have experienced such a supportive and close-knit lab environment where I could go to any member of the lab with a question and know I would receive authentic advice without judgment. To Caroline, Terry, Carley, Vanessa, Joy, and Emily, it was a pleasure to be graduate students alongside you all. You all inspire me with your intelligence and determination, and I look forward to hearing about your future epic career achievements. I am immensely grateful for your feedback on my lab meeting presentations and practice talks, and I'll always cherish our daily lab lunch conversations with Michael. To the Mitchell lab, even though I wasn't around day to day, you've always made sure I still felt like I was a part of the lab. I have greatly enjoyed watching the lab grow over my tenure in the Mitchell lab and I am thankful for all your feedback and support (and of course the snacks). I'd also like to thank Quad lab meeting between the Mitchell, Meeske, Guo, and Jordan labs and Thursday Morning Virus Meeting for insightful discussions on my project.

I would also like to thank the very helpful and kind Fred Hutch Flow Cytometry and Genomics core staff including Rebecca Reeves and Elizabeth Jensen for their assistance in processing data. Thank you to the MCB graduate program staff specifically Maia Low, Denise Barnes, and Andrea Brocato for going above and beyond to support graduate students. Thank you to Luna

Yu for IT support and thank you to Jasmine Gonzalez and Hannah Snider for stellar administrative support.

Thank you to the new friends I have made in Seattle and my long-distance friends, who have both supported me from near and far. To Cara and Carley, I am so thankful we decided to impulsively buy flights to Hawaii and make it a yearly tradition. Our spontaneous adventures were a huge highlight of graduate school and I look forward to continuing our annual trips in the future. Thank you to my cat, CRISPR Cats9, who expressed her support by sitting in my lap (or on my laptop) while I wrote this entire dissertation. Thank you to my partner Ryan for never failing to make me smile and feel loved every day of graduate school. You have been my rock through so much, quietly supporting me in kind and thoughtful gestures, and I am so grateful. I am also incredibly lucky to have an amazing family, who, despite not knowing anything about the research field, have always expressed their unconditional support for my scientific career endeavors. Thank you to Kunta, my grandfather, who was eager to fly across the country and visit me in Seattle whenever I gave him an open weekend, and for listening to me on my commute into lab every morning blather on and on about all the experiments I was excited to run that day. Lastly, I would like to thank my mom who raised me and my brother as a single working mother and has always been my biggest cheerleader. This thesis is dedicated to you.

CHAPTER 1: INTRODUCTION

The acquired immunodeficiency syndrome (AIDS) epidemic caused by the human immunodeficiency virus (HIV-1) has killed approximately 40.4 million people as of 2023 (1). HIV-1 disease progression is characterized by chronic inflammation, immune activation, and eventual destruction of the immune system, and despite potent antiretroviral therapy, there is no cure. Thus, understanding how viruses like HIV-1 interact with its human host's immune system is crucial to developing novel therapeutic strategies. This thesis investigates and characterizes an inflammatory immune pathway specifically activated in humans by HIV-1.

HIV-1 REPLICATION AND THE IMPORTANCE OF HIV-1 PROTEASE

HIV-1 is a lentivirus, belonging to the *Retroviridae* family, with an approximately 9kb RNA genome that encodes 15 proteins via overlapping open reading frames (ORFs). The primary targets of HIV-1 are CD4+ T helper cells; however, HIV-1 can also infect macrophages (2,3) and specialized CD4+ T cell subtypes like Th17 cells (4–6) and central memory cells (7–9). To enter target cells, HIV attaches to its host receptor CD4 (10,11) and either CXCR4 (12) or CCR5 (13–17) as a co-receptor to initiate membrane fusion between the virus and the host. HIV-1 strains that use CXCR4 are called X4 viruses whereas those that use CCR5 are called R5 viruses. While both X4 and R5 viruses infect T cells, only a subset of R5 viruses with certain envelope modifications around the CD4 binding residues can infect macrophages, which express low levels of CD4 (18–22). There also exist some dual tropic strains that can use either CXCR4 or CCR5 (23). However, the majority of primary strains of HIV-1 and almost all of the transmitted strains of HIV-1 are R5 viruses (24–26).

Upon entry, the viral capsid is trafficked to the nucleus where the viral genome is reverse transcribed from RNA into DNA by reverse transcriptase (RT) and integrates into the host

genome via HIV-encoded integrase (IN) (27). The integrated viral genome is then transcribed and translated to generate the HIV^{gag} and HIV^{gagpol} polyproteins along with HIV accessory proteins like Vif and Vpu, which antagonize host antiviral factors. HIV-1 then assembles and buds off from the plasma membrane as an immature non-infectious virion enveloped in the host membrane (**Figure 1.1**).

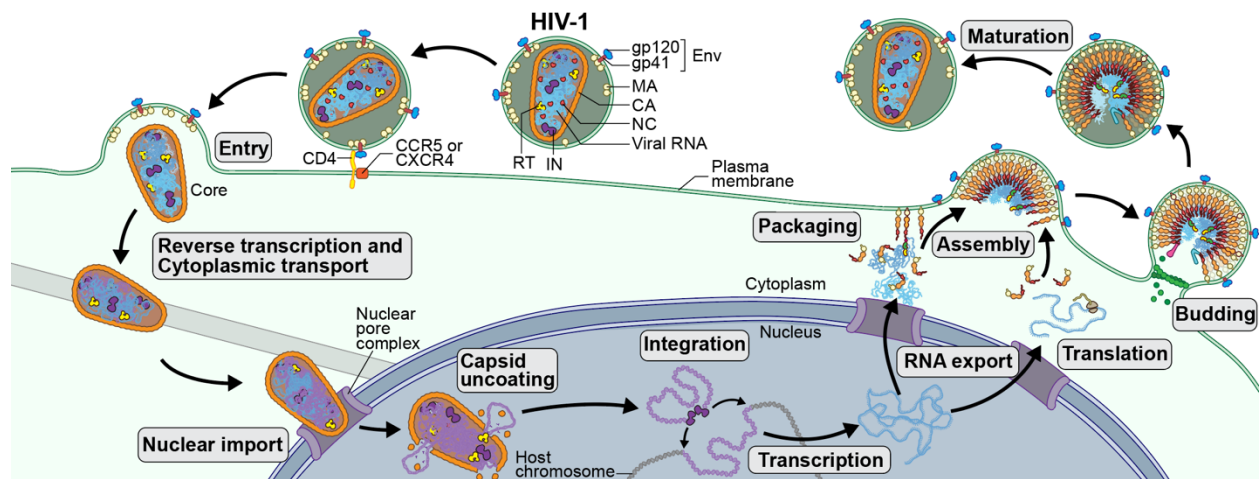


Fig 1.1: Schematic of HIV replication

The HIV-1 replication begins with entry via CD4 then traffics to the nucleus where the capsid uncoats and completes reverse transcription of its RNA genome. HIV is integrated into the host genome, transcribed, and translated. The virus then assembles and buds off the host plasma membrane. HIV protease processes the immature HIV^{gag} and HIV^{gagpol} into a mature infectious virion. This figure is a modified version from (28), used under Creative Commons CC-BY 4.0 license.

The viral polyproteins, HIV^{gag} and HIV^{gagpol} are translated in a 20:1 ratio such that HIV^{gagpol} is translated only when the ribosome slips backward, and the HIV^{gag} stop codon is readthrough (29). HIV^{gag} consists of structural HIV proteins including matrix, capsid, nucleocapsid and p6, whereas HIV^{gagpol} includes both structural proteins and the viral enzymes: RT, HIV protease (HIV^{PR}), and IN (**Figure 1.2A**). In order for HIV to mature and be infectious, HIV^{PR} must recognize and sequentially cleave a range of substrates within HIV^{gag} and HIV^{gagpol} to liberate its functional proteins; proper timing and order of processing are crucial to achieving successful viral maturation (30). HIV^{PR} specificity is determined by the four amino acids before and after the

cleavage site on the HIV^{gag} and HIV^{gagpol} polyprotein, favoring large bulky aromatic residues at the P1 and P1' site immediately flanking the cut site (31) (**Figure 1.2B**).

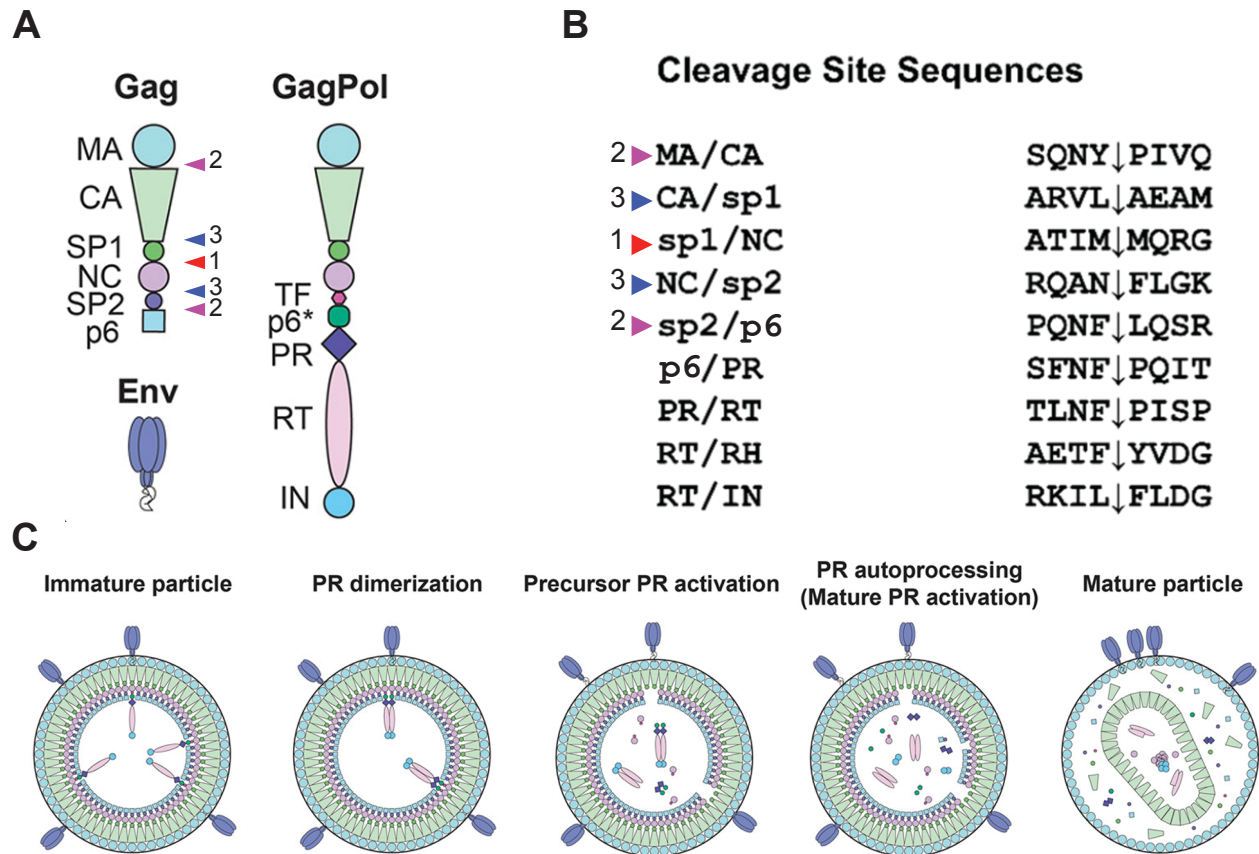


Fig 1.2: HIV proteolytic processing of HIV^{gagpol}

A) Depiction of HIV^{gag} and HIV^{gagpol} showing the proteins that comprise each polyprotein along with the order of HIV^{gag} processing, represented by the colored triangles. B) List of HIV^{PR} cleavage site sequences within HIV^{gagpol} showing the four amino acids before and after the cut site, depicted as a down arrow. C) Schematic showing progressive HIV^{PR} (PR) activation from immature to fully matured HIV particles. **Figure 1.2** was adapted from (32) and (33) under Creative Commons Attribution CC BY 4.0 license.

The first phase of HIV^{gag} processing cleaves between spacer peptide 1 (SP1) and nucleocapsid (NC), which is followed by cuts between spacer peptide 2 (SP2) and p6/transframe (TF) and between matrix (MA) and capsid (CA). In the third phase, CA and NC are liberated by cleaving SP1 and SP2, respectively (**Figure 1.2A**). Timing of HIV^{gagpol} processing and freeing of reverse transcriptase and integrase is presumed to occur late in viral maturation. Activation of the

immature precursor HIV^{PR} embedded in HIV^{gagpol} occurs in *cis* when high HIV^{gagpol} concentration are achieved to allow for dimerization because HIV^{PR} is active only as a dimer. Precursor HIV^{PR} that is present as part of the polyprotein accomplishes the initial cleavage events of HIV^{gag} and HIV^{gagpol} processing, and eventually, the HIV^{gagpol} polyprotein is processed in *trans* to produce free mature HIV^{PR} dimers (**Figure 1.2C**) (34–36). Thus, since HIV^{gagpol} exists at a much lower ratio than HIV^{gag}, HIV^{PR} activation and subsequent processing of HIV^{gag} and HIV^{gagpol} dimerization and subsequent HIV^{PR} activation is canonically thought to only occur during assembly and budding; however, some studies have also shown full HIV^{gag} processing in cytoplasmic lysates of HIV-1 infected cells and recent studies using highly sensitive technology, including nanoscale flow cytometry and instant structured illumination microscopy, have suggested that HIV^{PR} becomes fully activated within infected cells before viral budding (32,37). This thesis investigates the functional consequences of incoming active HIV^{PR} and cytoplasmic HIV^{PR} activation earlier in viral replication.

Given the crucial role of HIV^{PR} in HIV replication, protease inhibitors targeting the enzymatic activity of HIV^{PR} were among the second generation of antiviral treatments for HIV developed in the late 1990's and early 2000's after RT inhibitors. The combination of RT inhibitors with protease inhibitors served as the basis of the first effective combination anti-HIV therapy, at the time known as HAART (highly active anti-retroviral therapy). However, soon after protease inhibitors were introduced, viral variants that were resistant to protease inhibitors arose *in vivo* via mutations near the protease active site permitting polyprotein processing and viral maturation while avoiding drug inhibition. Despite typically having poor overall viral fitness due to less efficient polyprotein processing and replication relative to wildtype HIV-1 in the absence of protease inhibitors, these mutant drug-resistant HIV-1 strains can persist in people living with HIV on HAART, posing a major threat to controlling disease progression (38–41). In addition, most protease inhibitors were associated with significant side-effects on long-term therapy.

Thus, with the development of more potent antiviral drugs such as integrase inhibitors and better reverse transcriptase inhibitors with minimal resistance mutations, protease inhibitors are no longer routinely included in the drug cocktail used for combination antiretroviral therapy. Nevertheless, this thesis utilizes protease inhibitor resistant strains of HIV-1 for the examination of determinants that underlie HIV^{PR} specificity.

POSITIVE SENSE RNA VIRAL PROTEASES

Like HIV-1, all positive sense RNA viruses, including coronaviruses, picornaviruses, and flaviviruses, also translate their genomes as a large polyprotein precursor and require a virally encoded protease to process its polyprotein into its functional substituents. Utilizing polyprotein precursors is a strategy for viruses to keep their genome more compact, eliminating the need to encode multiple promoters that would be required for expression of each individual protein. Similar to HIV^{PR}, positive sense RNA viral proteases are also regulated in a spatiotemporal manner such that proteolytic processing occurs systematically at discrete stages in viral replication. In addition, precursor or intermediate proteins can also provide supplementary functions and regulation in viral replication. For example, the poliovirus 3AB precursor facilitates membrane remodeling to establish the replication complex while the 3CD protease and polymerase precursor, which has protease but no polymerase activity, modulates RNA polymerase activity and thus polio replication (42,43). However, in contrast to HIV, other positive strand RNA viruses do not package their own protease, which is active only at early stages of replication, and not in the virion. While viral proteases canonically process their own polyprotein, they also have important effects on cleavage of host proteins. For example, the picornavirus protease cleaves host translation initiation factors to shut down host translation and facilitate translation of viral proteins via an internal ribosome initiation site (44,45). This thesis explores the consequences of virion-packaged HIV^{PR} cleaving a host protein resulting in activation of an inflammatory host innate immune pathway.

THE ORIGINS OF HIV-1

HIV-1 is comprised of four lineages known as groups M, N, O, and P, corresponding to four independent cross-species transmission events from simian immunodeficiency viruses (SIVs) infecting chimpanzees (SIVcpz) and gorillas (SIVgor) (**Figure 1.3**) (46). HIV-1 groups M and N originated from SIVcpz whereas group O and P originated from SIVcpz but with an intermediate host in gorillas before transmission to humans. HIV-2 is a related virus that causes milder AIDS pathogenesis than HIV-1 but did not arise from cross-species transmission from chimpanzees, but rather arose from at least nine independent cross-species transmissions from sooty mangabeys (SIVsmm) into humans, giving rise to 9 different subtypes (**Figure 1.3**). The predominant global strain responsible for the AIDS pandemic is HIV-1 group M while HIV-2, and HIV-1 groups N, O, and P occur at lower frequency.

Like HIV-1 and HIV-2, SIVcpz is also the result of cross-species transmission and is a molecular chimera produced from the recombination of SIVrcm, which infects red capped mangabeys, and a group of related SIVs called the SIVmus/SIVgsn/SIVmon group, which infects certain species of monkeys in sub-Saharan Africa called guenons, including the mustached monkey (mus), the greater spot-nosed monkey (gsn), and the mona monkey (mon). SIVrcm contributed the 5' end of the genome including parts of HIV^{gagpol} and the accessory gene *vif*, while SIVmus/SIVgsn/SIVmon contributed the 3' end, consisting of HIV accessory proteins including the LTRs (47,48). SIVcpz circulates in *Pan troglodytes troglodytes* and *Pan troglodytes schweinfurthii*, which are two of the four subspecies of chimpanzees. The lack of SIVcpz in the other two subspecies suggests that cross-species transmission into chimpanzees occurred before either subspecies divergence or the last Ice Age, which separated the sub-species geographically (between 30,000 and 100,000 years ago) (49,50). More recently, SIVcpz was

transmitted to western lowland gorillas in a single cross-species transmission at least 100 to 200 years ago, resulting in SIVgor (51).

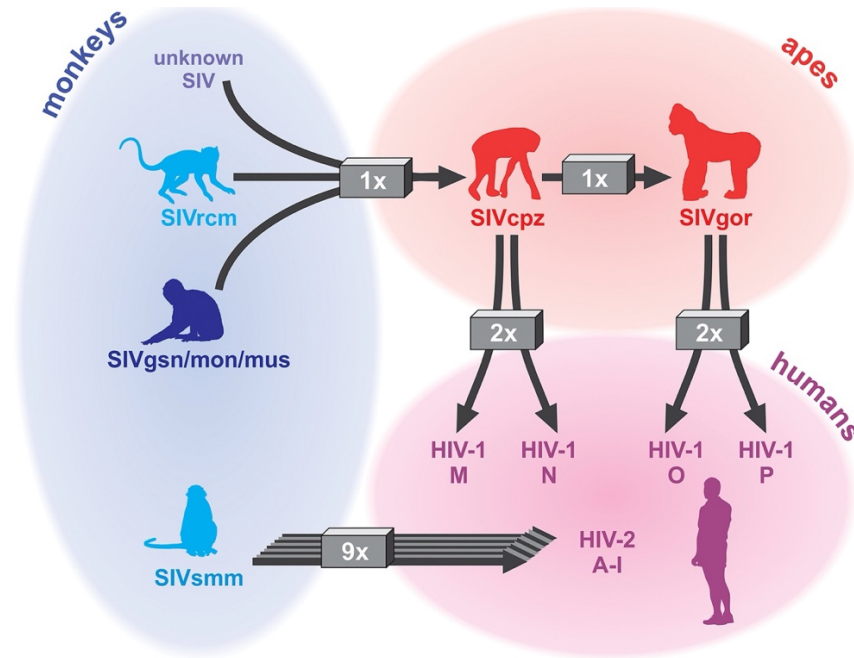


Fig 1.3: Cross-species transmission events preceding HIV-1 and HIV-2

A history of the cross-species transmission events between primates that gave rise to SIVcpz, SIVgor, HIV-1 subgroups, and HIV-2. **Figure 1.3** was adapted from (52) with permission, Elsevier license number 5719210520820.

HIV AND SIV PATHOGENESIS

There are three main stages of HIV-1 disease progression: acute, chronic, and AIDS. The acute phase is characterized by rapid viral replication and dramatic CD4+ T cell depletion, killing 30-60% of gut CD4+ T cells (53). A major hallmark of acute HIV-1 disease is the breakdown of the gut epithelial barrier driven by the depletion of specialized Th17 CD4+ T cell subsets in the gut mucosa. The leaky gut epithelial barrier triggers aberrant microbial translocation and results in systemically circulating microbial ligands like lipopolysaccharides (LPS). These ligands can be sensed by innate pathogen recognition receptors to promote chronic immune activation, leading to dangerously elevated levels of circulating pro-inflammatory cytokines known as “cytokine storm” (4,54–56).

During the chronic phase, there is chronic immune activation as the immune system responds to the aberrant microbial translocation, resulting in immune exhaustion and depletion of CD4+ T cells. HIV-1 continues to replicate, but at lower rates than during acute HIV infection (57,58). Progression from chronic HIV to AIDS can vary person to person, but typically takes ten years or more to advance to AIDS unless their viral load is reduced with effective antiviral therapy. People living with HIV (PLWH) are diagnosed with AIDS when their CD4+ T cell levels fall below 200 cells/mm³. CD4+ T helper cells, a primary target of HIV-1, play a vital role in facilitating cellular and humoral host immune responses to pathogens. Thus, PLWH in AIDS stage are highly susceptible to microbial infection and eventually succumb to opportunistic infections or infection-related cancers that would typically be cleared by healthy individuals but cannot be cleared due to HIV-driven immune destruction. Similarly, chimpanzees infected with SIVcpz also exhibit an AIDS-like immunopathology; however, HIV-1 pathogenesis in humans is notably more severe than chimpanzee AIDS-like pathology (59).

SIVs are endemic in many primate species in Africa and having coevolved with their hosts for millions of years, do not typically cause disease despite replicating to high viral loads. SIVagm and SIVsmm, which infect African green monkeys and sooty mangabeys, respectively, are the best studied examples of SIVs that yield nonpathogenic infection in their natural host. However, when SIVagm and SIVsmm are introduced into non-natural hosts like pig-tailed macaques or rhesus macaques, both SIVagm and SIVsmm induce AIDS-like immunopathology in these non-natural hosts, respectively (60,61). Researchers have tried to recapitulate human-like disease in a natural host model of African monkeys using SIVagm chimeras expressing virulent HIV-1 accessory proteins including Vpu and Nef that can antagonize host antiviral factors to promote immune activation and viral replication. Despite efficient replication and increased immune activation *in vivo*, the HIV-1-like SIVagm chimeras failed to cause accelerated CD4+ T cell

depletion and immunodeficiency even after 5 years of follow-up (62). Thus, pathogenesis associated with lentivirus infection of non-human primates has been hypothesized to be driven by host-derived factors rather than the virus being intrinsically more virulent.

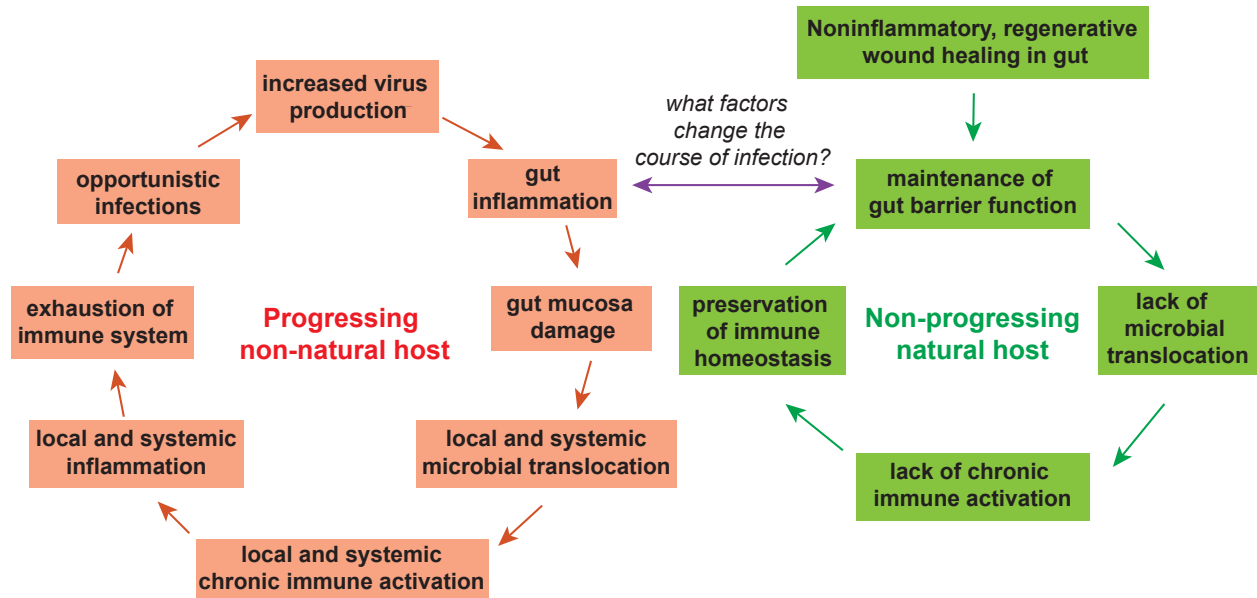


Fig 1.4: Hallmarks of lentiviral infection in progressing versus non-progressing hosts
 A flow chart comparing lentiviral disease progression in non-natural hosts of SIV/HIV like humans and rhesus macaques and non-progressing natural hosts like African green monkeys and vervets. **Figure 1.4** was adapted from (63) under Creative Commons Attribution CC BY 4.0 license.

Various non-human primate studies have implicated the host’s capacity to prevent microbial translocation by regenerating its gut mucosal barrier after initial damage from acute infection as a significant determinant of immune activation, inflammation, and pathogenesis during HIV and SIV infections (**Figure 1.4**) (62–64). For example, unlike humans and macaques, which exhibit severe immunopathogenesis, natural non-progressing hosts like sooty mangabeys and African green monkeys do not exhibit microbial translocation in part due to enhanced gut regenerative capacity facilitated by non-inflammatory macrophage-associated wound healing pathways (**Figure 1.4**) (4,64). However, microbial translocation and immune activation can be recapitulated in African green monkeys during acute SIVagm infection when the gut mucosa is

chemically damaged by dextran sulfate sodium, though microbial translocation is not sufficient to progress nonpathogenic SIV infection into AIDS (65). Taken together, these studies highlight the host immune system as a crucial determinant of primate lentivirus pathogenesis. This thesis investigates the interactions between HIV-1 and its host's immune system and speculates on how activation of a particular host immune pathway can cause disease.

INNATE IMMUNE SENSING AND PROGRAMMED CELL DEATH

In order for the host to mobilize an antiviral response, it must be able to accurately identify a pathogen as “non-self”. To distinguish between self and non-self, the innate immune system is equipped with germ-line encoded pattern recognition receptors (PRRs) that can recognize microbial components known as pathogen-associated molecular patterns (PAMPs). Toll-like receptors (TLRs) are a type of PRR localized to the host cell plasma membrane and endosomes that can detect microbial ligands like LPS and dsRNA. Upon PRR detection of a PAMP, there are multiple effectors that can be elicited by the innate immune system. One such effector is a cytokine known as interferon, which acts in both an autocrine and paracrine fashion to reprogram cells into an antiviral state, transcriptionally upregulating hundreds of interferon-stimulated genes (ISGs) necessary for launching robust host antiviral defense. Another component of the innate immune response is programmed cell death, which inhibits bacterial and viral replication by clearing its replicative niche. The three most well understood forms of programmed cell death are apoptosis, necroptosis and pyroptosis, which are tightly regulated by a cysteine protease family known as caspases. This thesis focuses on the role of pyroptosis in innate sensing of HIV-1, thus apoptosis and necroptosis are described more briefly as a comparison to pyroptosis.

Apoptosis is a non-inflammatory form of programmed cell death essential for homeostatic processes like embryonic development, tissue remodeling, and epithelial cell renewal whereby

dysregulation of cell death can lead to tumorigenesis. It can be activated extrinsically through binding of plasma membrane-bound death receptors or intrinsically by cellular stresses like DNA damage, nutrient starvation, and oxidative stress. Apoptotic cells exhibit a characteristic morphology including membrane blebbing, chromatin condensation, and expression of phagocytic “eat-me” signals like phosphatidylserine to encourage phagocytic clearance of dead cells (66). In contrast, necroptosis is an inflammatory form of lytic cell death that occurs in response to various stimuli including binding death receptors and TLR3 or TLR4, which recognize dsRNA and LPS, respectively. Necroptotic signaling converges on activation of RIPK3 and pore-forming protein MLKL (67). Upon activation, MLKL oligomerizes and localizes to the cell membrane, forming a large pore in the membrane to induce lytic cell death.

Pyroptosis is another form of inflammatory and lytic programmed cell death (68) that is canonically initiated by multiprotein signaling complexes known as inflammasomes.

Inflammasomes are cytosolic innate immune complexes that assemble in response to a range of pathogen-associated signals. Upon pathogen detection, the inflammasome-forming sensor oligomerizes to form a platform for the recruitment and activation of pro-inflammatory caspases, including caspase 1 (CASP1) (69). In addition to canonical inflammasome-driven CASP1 activation, non-canonical pyroptosis can be initiated by direct binding of human caspase 4 and 5 (or caspase 11 in mice) to intracellular LPS. After activation, CASP1 processes pro-inflammatory precursor cytokines into their mature functional form and cleaves and activates a pore-forming protein belonging to the gasdermin superfamily called gasdermin D (GSDMD). GSDMD has a conserved N-terminal pore forming domain and a C-terminal repressor domain. Processing of GSDMD by CASP1 frees the pore-forming domain from the repressor domain to allow for oligomerization of gasdermin, which forms small pores in the cell membrane and initiates pyroptosis, releasing mature inflammatory cytokines interleukin (IL)-1 β and IL-18 (**Figure 1.5**). The final stage of pyroptosis is plasma membrane rupture, which is mediated by a

plasma membrane-bound protein known as NINJ1, resulting in complete cell lysis (70). Thus, the major hallmarks of pyroptosis are activated CASP1, cleaved GSDMD, and proinflammatory cytokine secretion.

Pyroptosis of infected cells destroys the pathogen's replicative niche along with releasing pro-inflammatory cytokines to further amplify the immune response. Pro-inflammatory cytokines like IL-1 β mount a robust immune response by binding to IL-1 receptors on immune cells to promote pathogen clearance and differentiation into specialized immune cells. However, excess circulating pro-inflammatory cytokines (i.e., a cytokine storm) can trigger severe inflammatory pathogenesis and immune exhaustion. Thus, gain of function mutations in inflammasomes lead to constitutive activation, aberrant overproduction of IL-1 β , and are associated with autoimmune and autoinflammatory disease (71,72). In this way, IL-1 inhibitors are clinically used for treatment of autoinflammatory diseases, septic shock syndrome, acute respiratory distress syndrome and other inflammatory malignancies (72–74).

Unlike apoptosis and necroptosis, pyroptosis is not typically initiated by death receptors or extracellular ligands, but instead respond to cytosolic PAMPs and disruptions to homeostasis. Some inflammasomes that can directly sense cytosolic PAMPs include the AIM2 inflammasome, which can detect cytosolic dsDNA (75), the NAIP-NLRC4 inflammasome, which can detect components of bacterial flagellin and type III secretion system proteins (76), and the NLRP6 inflammasome, which can detect lipoteichoic acid associated with gram-positive bacteria (77) (**Figure 1.5**). Other inflammasomes can respond to disturbances in cellular homeostasis like the NLRP3 inflammasome, which can sense potassium ion flux (78) or the pyrin inflammasome, which can sense alterations in Rho GTPase function induced by toxins (79). In this way, inflammasomes that indirectly sense pathogens through detection of pathogen

activities are described as “guards” of cellular homeostasis, one facet of a broader form of innate immune recognition called effector-triggered immunity.

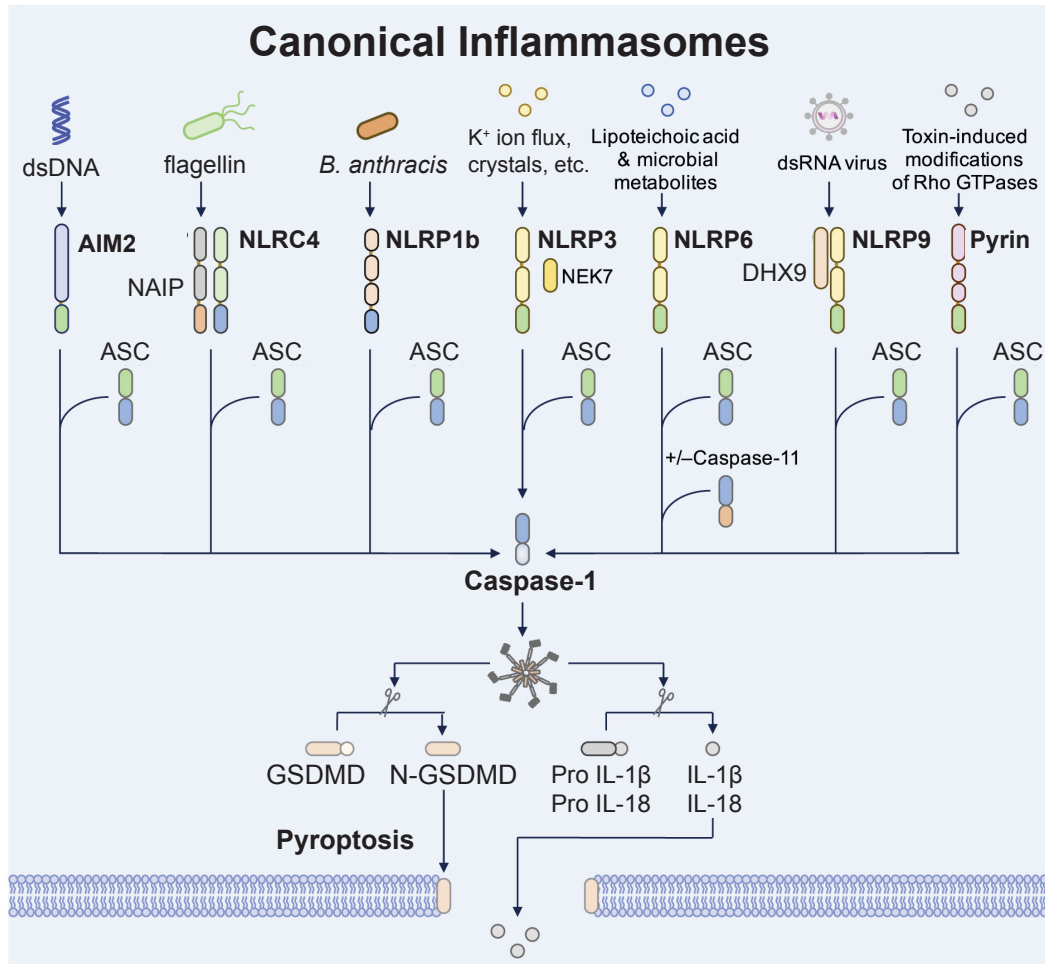


Fig 1.5: Canonical inflammasome activation

Inflammasomes can detect and respond to diverse pathogen stimuli. Upon pathogen detection, these sensors oligomerize to form inflammasomes, which act as a scaffold to recruit and activate caspase-1. Activated caspase-1 processes pro-inflammatory cytokines and gasdermin D (GSDMD) to induce pyroptosis. **Figure 1.5** was modified from (80) with permission, Elsevier license number 5719211109076.

EFFECTOR-TRIGGERED IMMUNITY

In the ongoing arms race between host and pathogen, pathogens have the clear advantage with higher mutation rates, lower generation times, and a larger effective population size; however, innate immune recognition of an essential enzymatic function of a pathogen or its effectors

could help swing the odds in the host's favor. Innate immune sensing of the effector function of a pathogen rather than its microbial architecture is known as effector-triggered immunity (ETI). Together with PAMP-triggered immunity, ETI provides an additional layer of innate host protection from pathogens. Innate sensors of ETI are sometimes referred to as "guards" because they surveil the functional or physical integrity of another host protein or "guardee," and initiate an immune response if it detects disruptions. These disruptions vary widely depending on the circumstances and guard/guardee pairing but can include modification, destabilization, or loss of its host protein guardee (81). Most examples of ETI have been characterized in plants, which use specialized resistance receptors known as R proteins that possess nucleotide-binding and leucine-rich repeat domains, known as NLRs (82–84). Less is known about mammalian ETI, but mammals also have a range of functional NLRs, believed to have been acquired through convergent evolution rather than via a common ancestor with plants (85,86). This thesis focuses on examples of mammalian ETI.

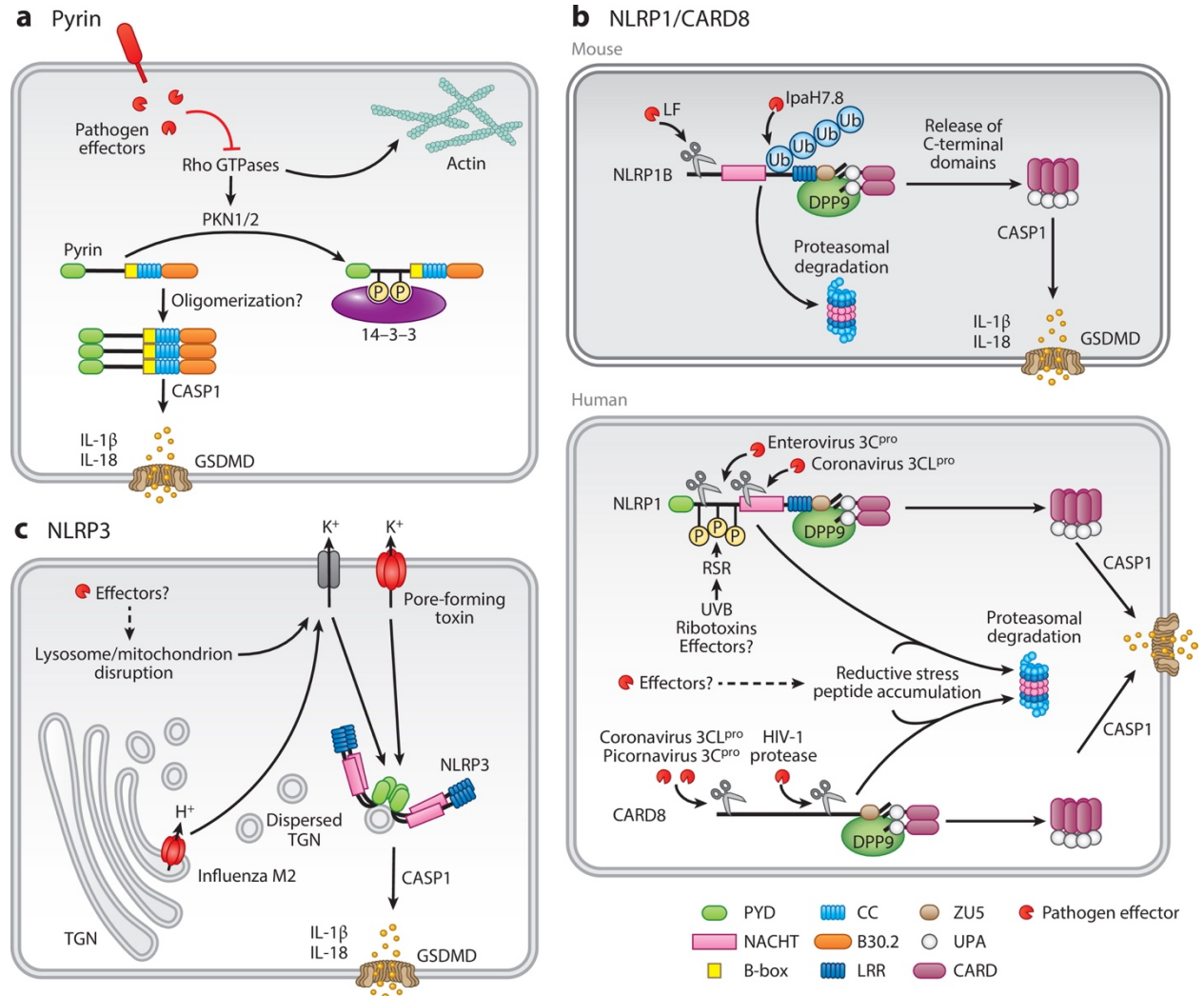
One classic example of a guard/guardee pair is the pyrin inflammasome, a non NLR-containing inflammasome-forming sensor, which guards the function of the small GTPase RhoA. Rho GTPases have diverse cellular functions including regulating the actin cytoskeleton, preserving epithelial barrier integrity, and producing reactive oxygen species and other antimicrobial peptides. Given Rho GTPase's antimicrobial functions, these proteins are oftentimes targeted by bacterial effectors including *Clostridium difficile* TcdB, *Clostridium botulinum* C3, *Vibrio parahaemolyticus* VopS, *Histophilus somni* lbpA, and *Yersinia spp.* Yop E and YopT (79,87,88). Under normal physiological conditions, RhoA is active along with its targets including protein kinase-C related kinases (PKNs). PKNs phosphorylate and inhibit pyrin activation by creating suppressive binding sites for 14-3-3 chaperone proteins such that pyrin is inactive at steady state. However, if RhoA is inhibited by a bacterial effector, RhoA can no longer activate its substrates including PKN, resulting in loss of inhibition by suppressive phosphorylation and

subsequent pyrin inflammasome activation (**Figure 1.6A**). In this way, pyrin can indirectly sense bacterial effectors by guarding the function of RhoA.

Another form of ETI is when disruptions to homeostasis and subsequent cellular stress, incurred by pathogen effectors, can be sensed by host innate sensors. For example, though the exact mechanisms of activation are unknown, the NLRP3 inflammasome activates in response to direct inducers of potassium efflux including *Staphylococcus aureus* alpha-toxin, *Aeromonas hydrophila* aerolysin, and *Streptomyces hygroscopicus* nigericin along with influenza virus M2 protein, which is a proton-selective ion channel that neutralizes the pH of the trans-Golgi network (**Figure 1.6C**) (78,89–93). Of note, the NLRP3 inflammasome requires an initial priming signal of NF- κ B activation to induce expression of NLRP3 and its constituents in order to become fully active. Thus, NLRP3 is sometimes secondarily activated after activation of other innate sensing pathways that induce membrane pores including other inflammasomes and necroptosis (94–96). In this way, NLRP3 acts as an indirect sensor of cellular homeostasis by responding to disruptions in membrane integrity and ion flux.

In another form of ETI, hosts can encode sequence motifs, known as “integrated decoys,” within its innate sensors that mimic the natural substrates of pathogenic effectors such that the pathogen effector inadvertently triggers the innate host response while also accomplishing its effector function (97). For example, the *Arabidopsis* R protein RSS1 encodes a WRKY domain, which canonically acts as an immune defense transcription factor and is oftentimes targeted by pathogen effectors; however, the RSS1 WRKY domain is an integrated decoy that does not exhibit transcription factor function, but rather mimics the WRKY domain to deceive the pathogen effector into unwittingly modifying and activating the decoy in order to elicit an immune response (98,99). While examples of integrated decoys have been well characterized in plants,

mammalian integrated decoys, most notably the NLRP1 and CARD8 inflammasomes, have only recently been reported.



Remick BC, et al. 2023
Annu. Rev. Immunol. 41:453–81

Figure 1.6: Effector triggered immunity by inflammasomes

Schematics depicting the inflammasome activation pathways for the A) pyrin, B) top: NLRP1b bottom: human NLRP1 and CARD8, and C) NLRP3 inflammasome-forming sensors. Upon pathogen effector detection, the sensors oligomerize to form inflammasomes to activate caspase 1 (CASP1) and induce GSDMD-mediated pyroptosis. **Figure 1.6** was reproduced from (81) under a Creative Commons Attribution 4.0 International License.

NLRP1

NLRP1 was the first mammalian NLR to be discovered in 2002. However, the complexities underlying its activation have only been recently elucidated. NLRP1 consists of an N-terminal domain responsible for mediating pathogen detection and a bioactive C-terminal domain, which mediates effector function, including inflammasome assembly and CASP1 activation. Like many canonical inflammasomes, NLRP1 requires adaptor molecule apoptosis-associated speck-like protein (ASC) to recruit and fully activate CASP1 to process pro-inflammatory cytokines (**Figure 1.5**). The NLRP1 C-terminus includes a function-to-find domain (FIIND), consisting of ZU5 and UPA subdomains, and a caspase activation and recruitment domain (CARD), required for CASP1 recruitment and activation. The FIIND self-cleaves between the ZU5 and UPA domains, forming two non-covalently associated fragments (100,101). Pathogen-encoded effector activities can destabilize the N-terminal domain of NLRP1 in a proteasome-dependent manner, resulting in degradation of the N-terminus, release and oligomerization of the C-terminal fragment facilitated by the UPA, and inflammasome assembly (102–106). Thus, NLRP1 functions as a bipartite ‘molecular tripwire’ that can be activated by ETI.

Given the potentially detrimental effects of inappropriate activation of pyroptosis, NLRP1 is also negatively regulated by host serine dipeptidyl peptidases DPP8 and DPP9. DPP8/9 restrict inflammasome activation by sequestering the C-terminal fragments in an inhibitory ternary complex. Thus, Val-boroPro (VbP), a small molecule inhibitor of DPP8/9, can activate the NLRP1 inflammasome, inducing pyroptosis in various cell types (107–110). Gain of function mutations in NLRP1 that bypass negative regulation by the N-terminus and DPP8/9 have been reported to induce autoimmune and auto-inflammatory pathologies (112–119).

The first NLRP1-mediated ETI was reported in NLRP1b, a mouse NLRP1 paralog, which harbors integrated decoy motifs that mimic substrates of bacterial effectors including *Shigella*

E3 ubiquitin ligase IpaH7.8 and *Bacillus anthracis* Lethal Toxin (103). *Shigella* E3 ubiquitin ligase IpaH7.8 ubiquitinates the N-terminus of NLRP1 leading to its functional degradation and subsequent NLRP1 inflammasome activation (**Figure 1.6B top**). Similarly, *Bacillus anthracis* Lethal Toxin is a protease that cleaves within the N-terminus of NLRP1 also leading to its functional degradation by generating an unstable non-methionine neo-N-terminus, which is subsequently degraded via N-end rule, a protein quality control mechanism associated with variations in protein stability depending on the first amino acid of a protein (**Figure 1.6B top**).

Recently, diverse viral proteases were characterized as the first examples of ETI in pathogen recognition by human NLRP1. NLRP1 activates in response to both picornavirus infection of keratinocytes and coronavirus infection of lung epithelial cells by using integrated decoy motifs within its N-terminus that mimic the substrates of their respective viral proteases such that the viral protease cleaves the N-terminus, causing its destabilization, functional degradation and inflammasome activation (**Figure 1.6B bottom**) (104,106). While NLRP1 can directly sense protease and E3 activity, NLRP1 can also indirectly sense cellular stress responses including UVB irradiation and ribotoxins that activate the ribotoxic stress response (RSR), which detects ribosome collisions and other translational aberrances. RSR signaling results in hyperphosphorylation of the NLRP1 N-terminus, which results in functional degradation through an unknown mechanism (**Figure 1.6B bottom**) (119).

CARD8

CARD8 was first identified serendipitously when acute myeloid leukemia cell lines and THP-1 cells, an acute monocytic leukemia cell line, were observed undergoing VbP-mediated pyroptosis in an NLRP1-independent manner (109). To discern the sensor, researchers looked for other host candidate inflammasome-forming sensors containing a FIIND and a CARD that could be modulated by VbP, and CARD8, which lacks most of the characteristic architecture of

NLRs, was the only host candidate gene with a FIIND. Thus, VbP-mediated pyroptosis in myeloid cell lines was found to be CARD8-dependent, and provided the first evidence that CARD8 was an inflammasome-forming sensor.

In contrast to NLRP1, CARD8 inflammasome activation does not require the adapter protein ASC. In ASC-dependent inflammasomes, inflammasome activation induces aggregation of ASC, forming a focus or speck to serve as a platform for recruitment and activation of CASP1 and cytokine processing. Canonically, ASC-independent inflammasomes have been thought to activate pro-CASP1 only partially such that it can process GSDMD to initiate pyroptosis, but not process and mature pro-inflammatory cytokines efficiently (120). However, there have been conflicting reports as to whether or not CARD8 inflammasome activation can fully process pro-inflammatory cytokines even in the same THP-1 cell type treated with VbP (107,121). This thesis investigates this discrepancy in CARD8-dependent cytokine release.

In addition to VbP, CARD8 can also be selectively activated by small molecule inhibitors of M24B aminopeptidases as reviewed in (122). In brief, M24B aminopeptidases catabolize dipeptides, which are the enzymatic product of DPP8/9. When M24B aminopeptidases are inhibited, there is an accumulation of dipeptides, which weakly inhibits DPP8/9 enough to activate CARD8 but not NLRP1; however, the mechanisms surrounding this differential activation and whether pathogenic infection can modulate dipeptide accumulation remain unclear (123).

Like NLRP1, CARD8 can also detect ETI mediated by positive sense RNA viral proteases, including coronavirus 3CL and some picornavirus 3C proteases, via integrated decoy motifs that promote cleavage and functional degradation of its N-terminus (121,124). Interestingly, a polymorphism within the N-terminus of CARD8 can switch host sensitivity from coronavirus

protease to human rhinovirus protease (121). While NLRP1 is expressed primarily in skin and airway epithelium, CARD8 is expressed in T cells and myeloid-derived cells like monocytes and macrophages (125). Due to these expression differences, NLRP1 and CARD8 seem to not exhibit redundancy in most cell types except for immune cells and endothelial cells, which line blood vessels, that express both NLRP1 and CARD8. Intriguingly, despite activated T cells expressing all major components of the CARD8 pathway, CARD8-induced pyroptosis can occur in resting but not activated T cells (110,125,126). To date, while there have been some correlations with disease, there have been no definitive reports of gain of function mutations, like those linked to NLRP1, associated with disease in CARD8.

In addition to positive sense RNA viral proteases, HIV-1 protease (HIV^{PR}) can also activate CARD8 via integrated decoy-mediated functional degradation of its N-terminus (Figure 1.6B bottom) (127). In this study, CARD8 was only able to detect HIV-1^{PR} when a nonnucleoside reverse transcriptase inhibitor (NNRTI) was used to enforce HIV-1^{PR} dimerization. Thus, whether or not CARD8-dependent inflammasome activation could occur in HIV-1 infected cells without NNRTIs, and thus the relevance of HIV-1^{PR} activation of CARD8, was unknown. This thesis centers around characterizing CARD8-dependent sensing of HIV^{PR}.

THE ROLE OF PYROPTOSIS IN HIV

Throughout HIV replication, there are multiple opportunities for innate sensing of HIV-associated PAMPs including dsRNA and endosomal ssRNA, which activate the interferon pathway and provide further immune activation. Despite abundant sources of HIV-dependent immune activation, the mechanisms driving CD4⁺ T cell depletion are less clear. For over 30 years, CD4⁺ T cell depletion observed during HIV disease progression was assumed to be apoptotic; however, a series of papers using human lymphoid-derived CD4⁺ T cells suggested that 95% of CD4⁺ T cells that die are not productively infected with HIV and are instead “bystanders” that

are killed through CASP1-dependent pyroptosis and that cell-to-cell transmission of HIV-1 is crucial to this response (128,129). Henceforth, these studies attributed the pyroptotic death to host innate sensing of accumulated abortive HIV reverse transcripts in resting/nonpermissive bystander CD4+ T cells by the cytosolic DNA-sensing IFI16 inflammasome (130,131). In direct contrast to lymphoid-derived CD4+ T cells, blood-derived CD4+ cells were reported to be naturally resistant to pyroptotic death associated with abortive HIV transcripts (132). However, another research team also investigating blood-derived CD4+ T cells in chronically infected PLWH observed elevated pyroptosis of CD4+ T cells and implicated the NLRP3 inflammasome as the major driver of CD4+ T cell depletion (133). These conflicting reports along with other reports that IFI16 is not an inflammasome-forming sensor, and instead a nuclear transcriptional regulator of antiviral genes including type I interferons and RIG-I (75,134,135), suggests that there may be other mechanisms of CD4+ T cell depletion and HIV-dependent inflammasome activation at play.

SUMMARY/THESIS RATIONALE

HIV-1 remains a major global health problem, inducing severe inflammatory pathogenesis in humans. Many primate studies have emphasized the importance of chronic immune activation in promoting HIV-1 progression to AIDS. Thus, characterizing immune pathways that may partially contribute to overall immune activation from HIV-1 could be crucial to developing novel therapeutics to combat HIV pathogenesis. In this thesis, I characterize the interactions between the CARD8 inflammasome, HIV-1 and its SIV precursors using both an evolutionary and virological lens. I have found that due to a human-specific motif in CARD8, the human but not the chimpanzee CARD8 can uniquely sense HIV-1 protease in various infection contexts and elicit an inflammatory response, implicating CARD8 inflammasome activation as a potential driver of HIV-1 pathogenesis in humans.

CHAPTER 2: A HUMAN-SPECIFIC MOTIF FACILITATES CARD8 INFLAMMASOME ACTIVATION AFTER HIV-1 INFECTION

This chapter was reproduced from the following article:

Kulsuptrakul, J, Turcotte, EA, Emerman M, and Mitchell PS. “A human-specific motif facilitates CARD8 inflammasome activation after HIV-1 infection.” *eLife* 12 (July 7, 2023): e84108.

<https://doi.org/10.7554/eLife.84108>.

ABSTRACT

Inflammasomes are cytosolic innate immune complexes that assemble upon detection of diverse pathogen-associated cues and play a critical role in host defense and inflammatory pathogenesis. Here, we find that the human inflammasome-forming sensor CARD8 senses HIV-1 infection via site-specific cleavage of the CARD8 N-terminus by the HIV protease (HIV-1^{PR}). HIV-1^{PR} cleavage of CARD8 induces pyroptotic cell death and the release of pro-inflammatory cytokines from infected cells, processes regulated by Toll-like receptor stimulation prior to viral infection. In acutely infected cells, CARD8 senses the activity of both *de novo* translated HIV-1^{PR} and packaged HIV-1^{PR} that is released from the incoming virion. Moreover, our evolutionary analyses reveal that the HIV-1^{PR} cleavage site in human CARD8 arose after the divergence of chimpanzees and humans. Although chimpanzee CARD8 does not recognize proteases from HIV or simian immunodeficiency viruses from chimpanzees (SIVcpz), SIVcpz does cleave human CARD8, suggesting that SIVcpz was poised to activate the human CARD8 inflammasome prior to its cross-species transmission into humans. Our findings suggest a unique role for CARD8 inflammasome activation in response to lentiviral infection of humans.

INTRODUCTION

One of the primary selective pressures that shape viral adaptation to a new host, as well as tolerance to persistent infections, is the innate immune system (136,137). One class of innate immune sensors form cytosolic immune complexes called inflammasomes, which initiate inflammatory signaling upon pathogen detection or cellular stress (69). Inflammasome activation is critical for host defense against a wide range of pathogens; however, auto-activating mutations in inflammasome-forming sensors can also initiate inflammatory pathogenesis that drives autoinflammatory and autoimmune disorders (101,138)

The inflammasome-forming sensor caspase recruitment domain-containing protein 8 (CARD8) consists of a disordered N-terminus, a Function-to-Find domain (FIIND), and a caspase activation and recruitment domain (CARD) (101). The FIIND, comprised of ZU5 and UPA subdomains, undergoes self-cleavage resulting in two non-covalently associated fragments (101,139). Proteasome-dependent degradation of the N-terminus leads to the release and assembly of the C-terminal UPA-CARD, serving as a platform for the recruitment and activation of Caspase-1 (CASP1). Activated CASP1 initiates a lytic, programmed cell death called pyroptosis and the release of pro-inflammatory cytokines including interleukin (IL)-1 β and IL-18 (68,69). To prevent aberrant release of the UPA-CARD, the dipeptidyl peptidases 8 and 9 (DPP8/9) form an inhibitory complex with CARD8 (140).

The CARD8 inflammasome can be activated by several triggers. For example, disruptions to protein homeostasis, including direct (e.g., Val-boroPro) and indirect (e.g., CQ31) inhibition of DPP8/9, cause CARD8 inflammasome activation (109,110,123). Several, recent examples also highlight CARD8 inflammasome activation in response to pathogens (121,124), including via its recognition of the enzymatic activity of the HIV-1 protease (HIV-1^{PR}) (127). For example, treatment of HIV-1 latently infected cells with certain nonnucleoside reverse transcriptase

inhibitors (NNRTIs), including efavirenz (127) or doravirine-like analogs including the pyrimidines Pyr01 (141), enforce the cytosolic dimerization of the HIV-1^{PR} and results in CARD8 inflammasome activation in primary CD4+ T cells and humanized mouse models (142). HIV-1^{PR} cleavage of the N-terminus of CARD8 causes proteasome-dependent degradation of the CARD8 N-terminal fragment (127). This 'functional degradation' liberates the UPA-CARD fragment for inflammasome assembly and activation, analogous to viral protease sensing by the inflammasome-forming sensor NLRP1(105,143–145) in which the N-terminus of CARD8 functions as a molecular 'tripwire' to sense and respond to the enzymatic activity of HIV-1^{PR} and other viral proteases (121,124,146).

Here, we report that CARD8 can also sense HIV-1 infection via the detection of HIV-1^{PR} activity. We find that priming of target cells via Toll-like receptor (TLR) agonists prior to HIV-1 challenge enhances CARD8-dependent cell death and is required for IL-1 β secretion. Our evolution-guided studies reveal that CARD8 sensing of HIV-1 and other simian lentiviruses is dependent on a F59-F60 motif in human CARD8 that permits its sensing of HIV-1^{PR}. This motif is absent in other primates that serve as reservoirs of simian immunodeficiency viruses (SIVs), and although both HIV-1^{PR} and SIVcpz^{PR} cleave and activate human CARD8, we find that neither are sensed by chimpanzee CARD8. Thus, our study reveals that the CARD8 inflammasome functions in the innate immune detection of HIV-1 replication. Moreover, our findings suggest that the evolution of the F59-F60 motif in humans gave rise to a human-specific host-virus interaction following the spillover of SIVcpz into humans, which may uniquely shape human innate immune responses to lentiviral infection.

RESULTS

A human-specific motif allows CARD8 to detect protease activity from multiple HIV strains

The HIV-1 protease (HIV-1^{PR}) cleaves human CARD8 between phenylalanine (F) 59 (P1) and F60 (P1') (**Figure 2.1A**) (127). While the amino acid P1 site, F59, is invariant among hominoids, gibbons, and Old World monkeys, only human CARD8 has a phenylalanine at the P1' site, F60 (**Figure 2.1A**). The F59-F60 motif therefore must have arisen in the human lineage after the most recent common ancestor with chimpanzees and bonobos. The F59-F60 motif is also present in *Homo neanderthalensis* (i.e., Neanderthal) CARD8 (**Figure 2.1A**), conservatively dating its emergence within the last million years (147).

In order to assess the significance of the human CARD8 F59-F60 motif, we established conditions required for HIV^{PR} cleavage of CARD8 by co-expression of CARD8 and proviruses from two HIV-1 group M proviruses (HIV-1_{LAI} subtype B and HIV-1_{Q23} subtype A) as well as an HIV-2 isolate, HIV-2_{ROD}. Indeed, we found that wildtype (WT) human CARD8 with a N-terminal mCherry fusion is cleaved upon transfection of HIV-1 and HIV-2 proviruses, resulting in an ~33 kDa product (**Figure 2.1B** and **2.1C**, top blot). The band at ~45 kDa is the result of cleavage by the 20S proteasome and results in a non-functional product (148). Cleavage of CARD8 in these experiments was dependent on the protease encoded by the *Gag-Pol* gene of these proviruses as the HIV^{PR} inhibitor lopinavir (LPV) blocked both Gag processing of p55^{gag} to p41^{gag} and p24^{gag} and CARD8 cleavage (**Figure 2.1C**, top and middle blot). To evaluate the significance of the amino acid variation at the F60 P1' site of CARD8, we next replaced human CARD8 F60 (WT) with either a leucine (L; found in chimpanzee, bonobo, and gorilla) or a serine (S; found in gibbons and Old World monkeys) (**Figure 1A**). HIV^{PR} cleavage of WT human CARD8 (F60) was much more efficient than cleavage of human CARD8 F60L or F60S (**Figure 1D**), consistent with

prior findings that an alanine at position 60 also blocks HIV^{PR} (127). These results indicate that species-specific variation at position 60 impacts CARD8 recognition of HIV^{PR} activity.

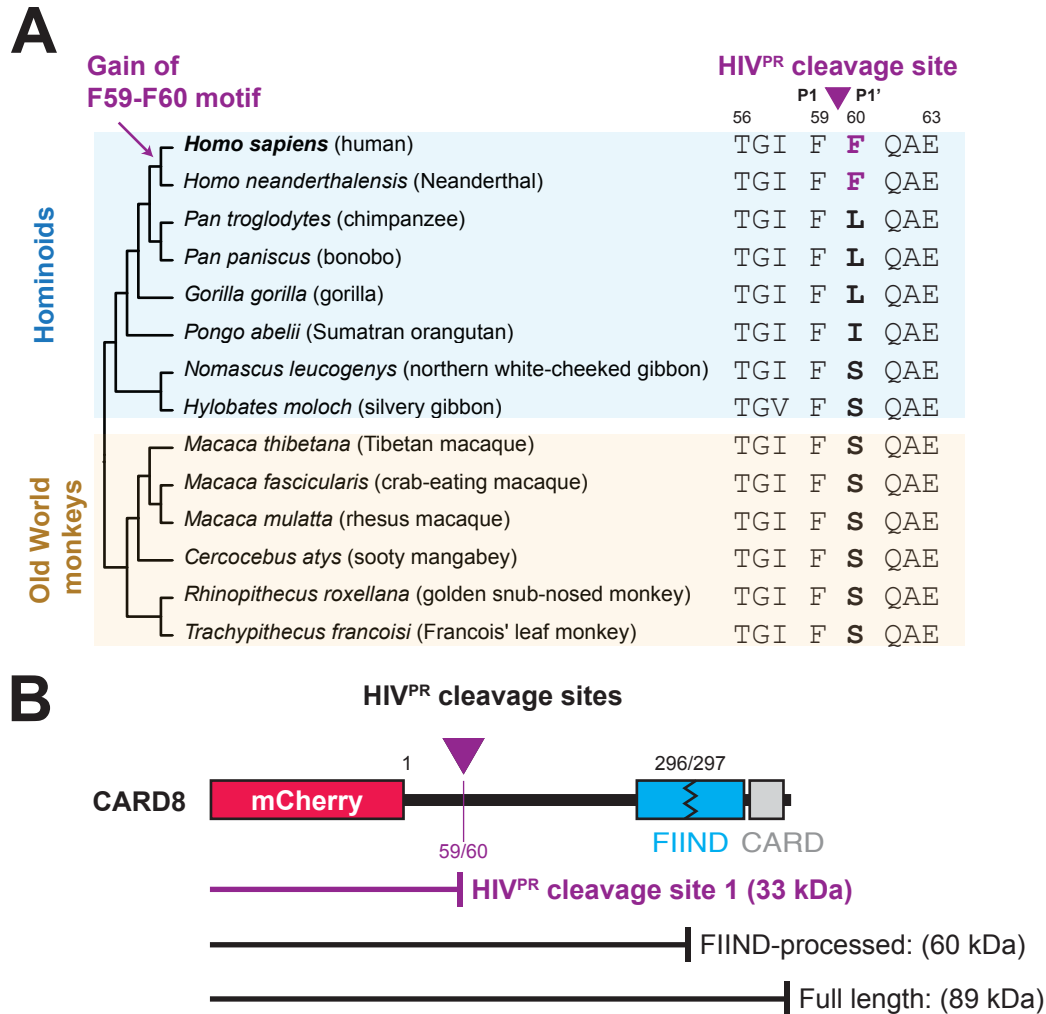


Fig 2.1: The F59-F60 motif allows human CARD8 to detect protease activity from multiple HIV strains

A) Phylogenetic alignment of primate CARD8 protein sequences. The HIV protease (HIV^{PR}) cleavage site is indicated by a purple triangle between F59 (P1) and F60 (P1'). Numbering is based on human CARD8.

B) Depiction of the mCherry-CARD8 used in cleavage assays in C) and D). The predicted molecular weights (kDa) for full length, FIIND-processed, or HIV^{PR} cleavage products are indicated. FIIND, function-to-find domain; CARD, caspase activation and recruitment domain.

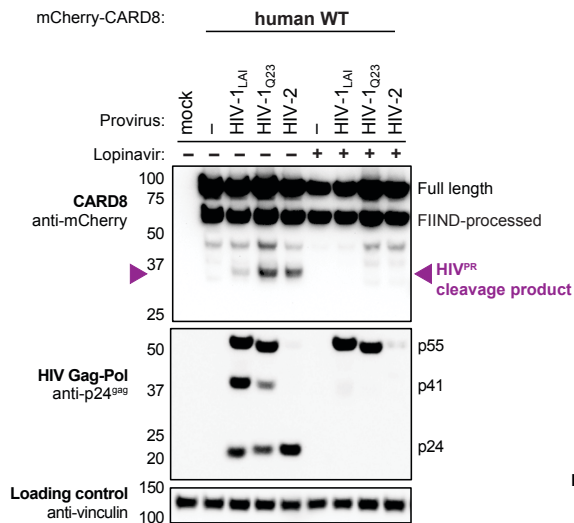
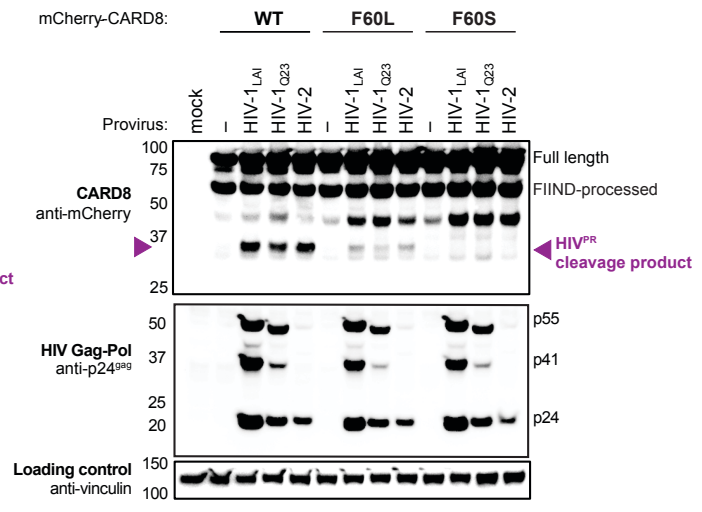
C**D**

Fig 2.1: The F59-F60 motif allows human CARD8 to detect protease activity from multiple HIV strains (continued)

C) HEK293T cells were transfected with a construct encoding N-terminally mCherry-tagged wildtype (WT) CARD8 and indicated HIV proviral constructs, HIV-1_{LAI}, HIV-1_{Q23}, and HIV-2_{ROD}, in the presence (+) or absence (-) of 10 μ M lopinavir, an HIV^{PR} inhibitor. Top: Immunoblotting for anti-mCherry to detect the mCherry-CARD8 fusion protein. The full-length and FIIND-processed bands are indicated as well as the HIV^{PR} cleavage product. The band at ~45kDa is the result of cleavage by the 20S proteasome (148). Middle: Immunoblotting with an anti-p24^{gag} antibody showing Gag cleavage products p41^{gag} and p24^{gag}, and/or full-length Gag, p55^{gag}. Bottom: Immunoblotting with anti-vinculin as a loading control.

D) HEK293T cells were transfected with a construct encoding N-terminally mCherry-tagged WT, F60L, or F60S CARD8 and indicated HIV proviral constructs. Immunoblotting and labeling of the blots as in C. **Figure 2.1** was reproduced from (149) with permission, Creative Commons Attribution 4.0 International License.

Natural variation in CARD8 alters sensing of SIVcpz protease activity

We next asked if HIV^{PR} cleavage of CARD8 was an ancestral function of SIVcpz or if that functionality instead emerged following cross-species transmission and adaptation to humans. SIVcpz_{EK505} and SIVcpz_{LB7} represent lineages that gave rise to HIV-1 group N and M viruses, respectively (46,150,151). Like HIV-1 and HIV-2 proteases, we found that both SIVcpz proteases (SIVcpz^{PR}) cleaved human CARD8 (**Figure 2.2A**), suggesting that SIVcpz^{PR} had a pre-existing ability to cleave human CARD8 prior to spillover. To deduce whether or not this cleavage is unique to humans, we also tested SIVcpz^{PR} ability to cleave chimpanzee CARD8

(**Figure 2.2A**) and F60L and F60S human CARD8 variants (**Figure 2.2B**) and found that none of the other CARD8 variants could be cleaved by SIVcpz^{PR}. Moreover, SIVmac₂₃₉^{PR} also cleaved WT human CARD8, an event that was greatly reduced when tested against the human CARD8 cleavage mutant F60A (**Figure 2.3**). These data suggest that SIVcpz^{PR} was poised to cleave human CARD8 prior to its zoonosis to humans. Moreover, the F59-F60 motif that arose in the human lineage renders human CARD8 uniquely susceptible to cleavage at that position by a broad range of primate lentiviral proteases.

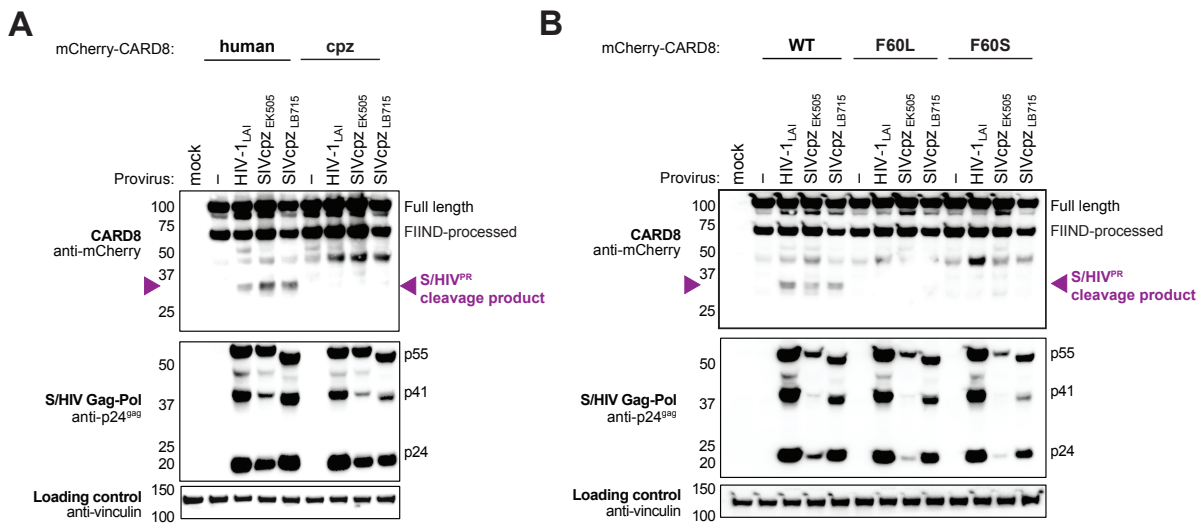


Fig 2.2: Natural variation in CARD8 alters sensing of SIVcpz^{PR} activity

A) HEK293T cells were transfected with a construct encoding N-terminally mCherry-tagged human or chimpanzee (cpz) CARD8 and indicated provirus constructs. Immunoblotting was carried out for CARD8 cleavage, HIV/SIV protease (S/HIV^{PR}) activity, and vinculin (loading control) as indicated. The S/HIV^{PR} cleavage product is indicated by a purple triangle. FIIND, function-to-find domain.

B) HEK293T cells were transfected with a construct encoding N-terminally mCherry-tagged wildtype (WT), F60L, or F60S CARD8 and indicated proviral constructs. Immunoblotting was performed as in A. **Figure 2.2** was reproduced from (149) with permission, Creative Commons Attribution 4.0 International License.

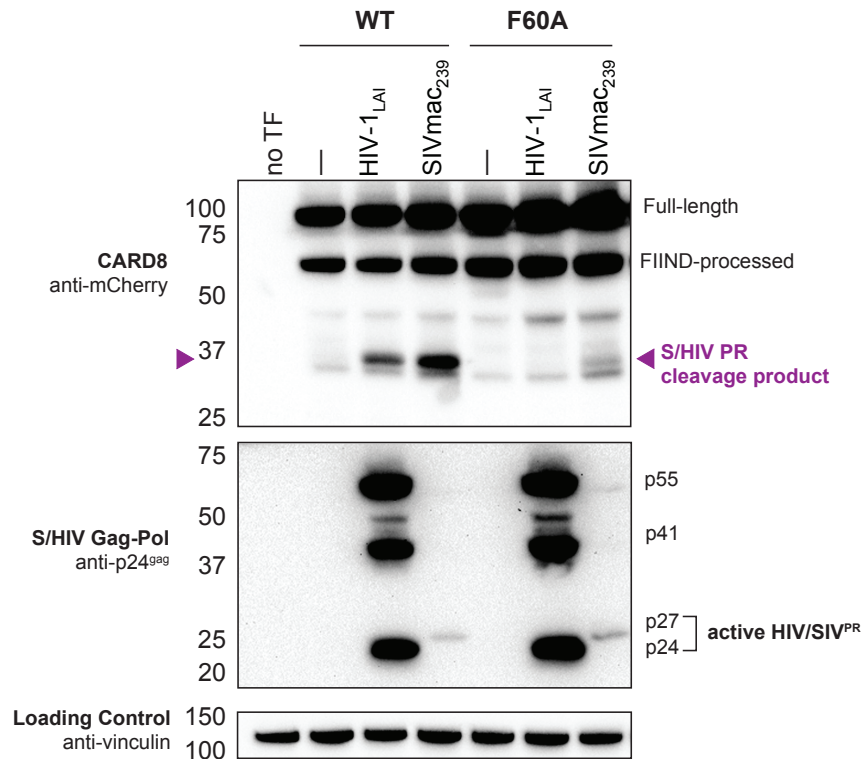


Fig 2.3: SIVmac cleaves wildtype human CARD8

HEK293T cells were transfected with a construct encoding N-terminally mCherry-tagged wildtype (WT) or F60A human CARD8 and indicated provirus constructs. Immunoblotting was carried out for CARD8 cleavage, HIV/SIV protease (S/HIV^{PR}) activity, and vinculin (loading control) as indicated. The anti-p24^{gag} antibody (for S/HIV^{PR} activity) poorly cross-reacts with SIVmac₂₃₉. The S/HIV^{PR} cleavage product is indicated by a purple triangle. We note that SIVmac₂₃₉^{PR} still partially cleaves CARD8 F60A. FIIND, function-to-find domain. **Figure 2.3** was reproduced from (149) with permission, Creative Commons Attribution 4.0 International License.

HIV-1 infection activates the inflammasome in primed THP-1 cells in a CARD8-dependent manner

We next sought to determine the significance of CARD8 cleavage and activation in the context of HIV-1 infection. Treatment with some nonnucleoside reverse transcriptase inhibitors (NNRTIs) induces premature Gag-Pol dimerization and HIV-1^{PR} activity (152,153), which was previously shown to be required for CARD8 activation in HIV-1 latently infected cells (127,142). However, we observed Gag processing of p55^{gag} to p41^{gag} and p24^{gag} in cytoplasmic lysates of THP-1 cells infected with either with either WT HIV-1_{LAI} or HIV-1_{LAI} that was pseudotyped with

the vesicular stomatitis virus glycoprotein (VSV-g) instead of its own envelope (HIV-1_{LAI-VSVG}), consistent with prior studies demonstrating that HIV-1^{PR} is active in the cytoplasm (**Figure 2.4A**) (32,154). To determine if CARD8 inflammasome activation can occur during HIV-1 infection in the absence of small molecule-induced HIV-1^{PR} dimers, we infected the human leukemia monocytic cell line THP-1 at a multiplicity of infection (MOI) <1 and assayed for cell death (**Figure 2.4B-left**) or IL-1 β secretion (**Figure 2.4B-right**). As a positive control for inflammasome activity, uninfected cells were also treated with VbP, which specifically activates the CARD8 inflammasome in THP-1 cells (110). For both HIV-1-infected and VbP-treated THP-1 cells, we observed an increase in cell death compared to mock infected controls as measured by uptake of the membrane impermeable dye propidium iodide (PI) (**Figure 2.4B-left**). However, neither HIV-1 infection nor VbP alone led to an increase in IL-1 β levels (**Figure 2.4B-right**, no prime condition), consistent with prior reports (155,156). We reasoned that the lack of cytokine production may either be an intrinsic property of CARD8 (156), or alternatively, require a signal (e.g., a TLR agonist) to transcriptionally upregulate or 'prime' IL-1 β and/or inflammasome components. Thus, we assessed inflammasome activation by HIV-1 infection or VbP treatment with and without pretreating THP-1 cells with agonists of TLR1/2 (Pam3CSK4), TLR7/8 (CL075), TLR8 (TL8-506), or TLR4 (LPS). We found that VbP treatment and HIV-1_{LAI-VSVG} infection induce cell death independent of priming, although TLR agonists did elevate cell death responses in some instances (**Figure 2.4B-left**). In contrast, the release of IL-1 β after HIV-1 infection or VbP treatment was entirely dependent on TLR priming (**Figure 2.4B-right**). Thus, HIV-1 infection alone (i.e., in the absence of molecules causing premature dimerization of Gag-Pol) is sufficient to induce cell death in THP-1 cells, and priming (e.g., via TLR stimulation) is required for HIV-1 infection induced IL-1 β secretion and elevated levels of cell death.

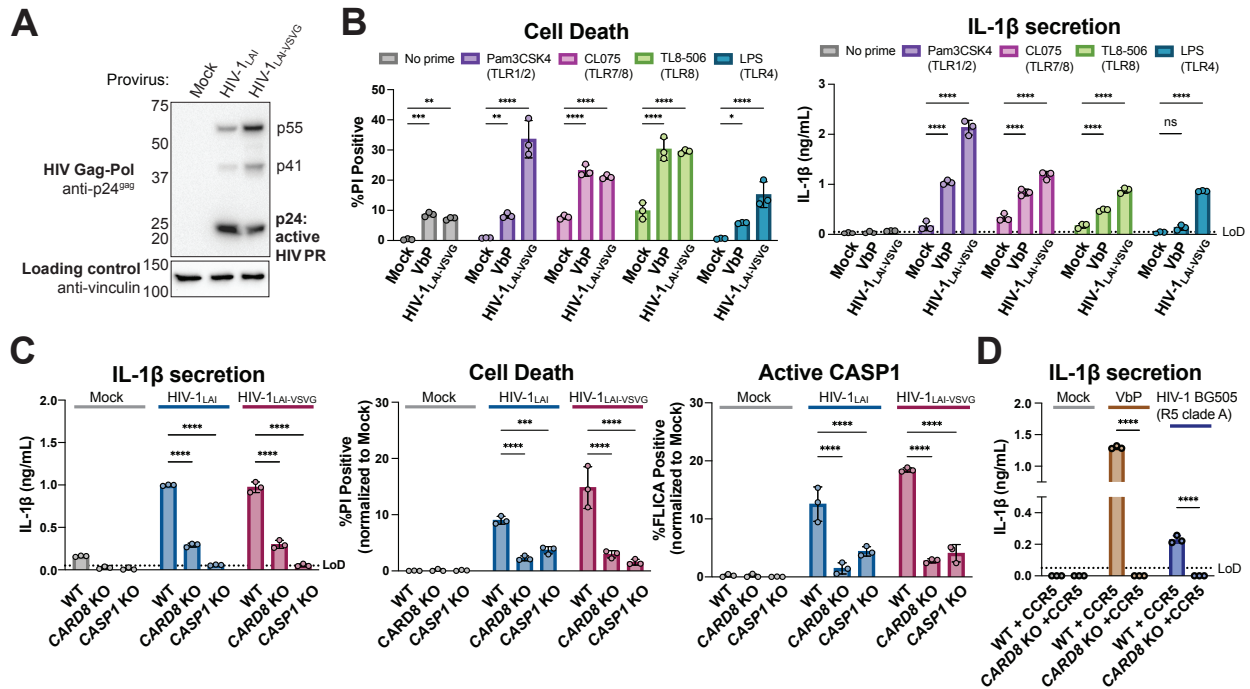


Fig 2.4: HIV-1 infection activates the CARD8 inflammasome in THP-1 cells

A) THP-1 cells were mock infected or infected with HIV-1_{LAI} or HIV-1_{LAI-VSVG}, yielding 8% and 53% p24^{gag}+ cells after 24 hours, respectively. Immunoblotting using cytoplasmic lysates was carried out for HIV protease (HIV PR) activity, and vinculin (loading control) as indicated 24 hours post-infection. **B)** THP-1 cells were either left unprimed or primed with different TLR agonists 4-6 hours before treatment with 10 μM VbP or infection with HIV-1_{LAI-VSVG} at an MOI such that 30-50% were p24^{gag}+ after 24 hours. Inflammasome responses were measured 24 hours following VbP treatment or HIV-1 infection. Left: Cell death is reported as the percent of propidium iodide (PI) positive cells. Right: IL-1β levels were measured using the IL-1R reporter assay. **C)** Wildtype (WT), CARD8 KO, or CASP1 KO THP-1 lines were primed with Pam3CSK4 then challenged with either HIV-1_{LAI} or HIV-1_{LAI-VSVG} at an MOI such that 30-50% of WT cells were p24^{gag}+ after 24 hours. Subsequent inflammasome activation was assayed 24 hours post infection. Left and middle: Cell death and IL-1β levels were measured as in A. Right: Active CASP1 was measured with Caspase 1-specific FLICA dye. **D)** WT or CARD8 KO THP-1s overexpressing CCR5 were primed and treated with 10uM VbP or infected with HIV-1_{BG505} for 24 hours such that ~30% of cells were p24^{gag}+ then probed for inflammasome activation via IL-1β secretion. HIV-1_{BG505} is a CCR5 tropic strain in clade A. The dotted line indicates limit of detection (LoD). Datasets represent mean ± SD (n = 3 biological replicates). P values were determined by 2-way ANOVA with Dunnett's (B-C) or Sidak's (D) test using GraphPad Prism 9. ns= not significant, *p < 0.05, **p < 0.01, ***p < 0.001, ****p < 0.0001. **Figure 2.4** was reproduced from (149) with permission, Creative Commons Attribution 4.0 International License.

To determine if inflammasome activation upon HIV-1 infection is dependent on CARD8, we first generated clonal THP-1 CARD8 knockout (KO) cells via CRISPR/Cas9. We confirmed the

absence of full length (~62kDa) and FIIND-processed (~29kDa) CARD8 in *CARD8* KO THP-1 cell lines by immunoblotting with an antibody specific to the CARD8 C-terminus (**Figure 2.5A**). To functionally test the THP-1 *CARD8* KO cell lines, we primed WT or *CARD8* KO THP-1 cells with Pam3CSK4 then treated with either VbP, which activates the CARD8 inflammasome, or the ionophore nigericin, which specifically activates the NLRP3 inflammasome, and measured cell death and IL-1 β secretion. As expected, WT but not *CARD8* KO THP-1 cells responded to VbP, whereas both cell lines underwent cell death and IL-1 β secretion in response to nigericin, indicating that the *CARD8* KO THP-1 cells retained responsiveness to other inflammasome agonists (**Figure 2.5B**).

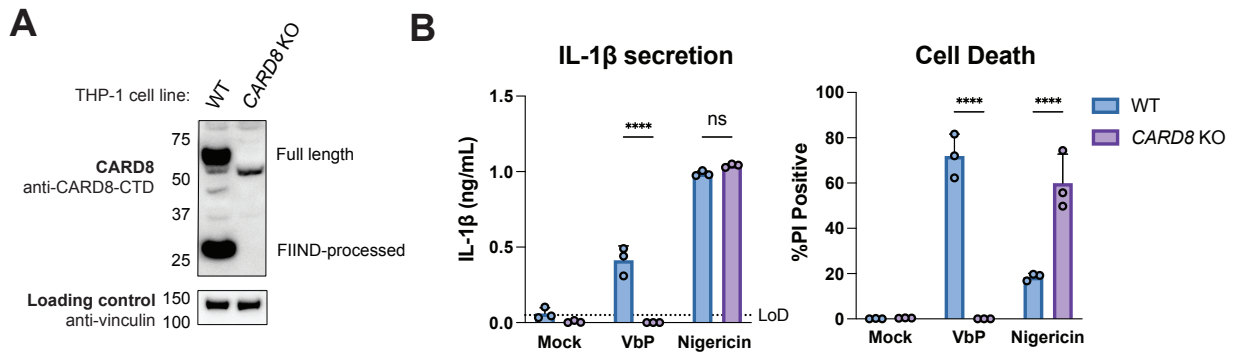


Fig 2.5: Functional validation of *CARD8* KO THP-1 cells

A) Immunoblot of wildtype (WT) or *CARD8* knockout (KO) THP-1 lines was carried out for *CARD8* expression using endogenous antibody against *CARD8* C-terminal domain (CTD) and loading control (vinculin). FIIND, function-to-find domain. **B)** WT or *CARD8* KO THP-1 cells were primed with Pam3CSK4 for 4-6hr then treated with 10 μ M VbP for 24hr or 5 μ g/mL Nigericin for 3 hours before probing for IL-1 β secretion (left) or propidium iodide (PI) dye uptake (right). The dotted line indicates limit of detection (LoD). Datasets represent mean \pm SD ($n = 3$ biological replicates). *P* values were determined by 2-way ANOVA Sidak's test using GraphPad Prism 9. ns= not significant, * $p < 0.05$, ** $p < 0.01$, *** $p < 0.001$, **** $p < 0.0001$. **Figure 2.5** was reproduced from (149) with permission, Creative Commons Attribution 4.0 International License.

We next infected both WT, *CARD8* KO, or *CASP1* KO THP-1 cells with WT HIV-1_{LAI} or HIV-1_{LAI}-vSVG viruses at an MOI that would give 30-50% infection of WT cells. Similar to our observations with VbP, we found that IL-1 β secretion, cell death, and *CASP1* activation (as measured by

FLICA assay) were significantly reduced in *CARD8* KO versus WT THP-1 cells following HIV-1 infection (**Figure 2.4C**). Because responses to HIV-1 infection were reduced to a similar level in both *CARD8* KO cells and *CASP1* KO cells, our findings suggest that the inflammasome response to HIV-1 infection in THP-1 cells is primarily dependent on *CARD8*, but independent of HIV-1 envelope. As different HIV-1 and SIV proviruses were found to cleave human *CARD8* after transfection in 293T cells (**Figure 2.1** and **Figure 2.2**), we also tested a primary isolate of HIV-1 from a different clade and with a different co-receptor usage (HIV-1_{Q23-BG505}, an R5, clade A recombinant virus) in an infection assay in WT and *CARD8* KO THP-1 cells engineered to express the co-receptor CCR5 (**Figure 2.4D**). HIV-1_{Q23-BG505} infection also resulted in IL-1 β secretion in a *CARD8*-dependent manner, suggesting that *CARD8*-dependent inflammasome activation is conserved across HIV-1 strains.

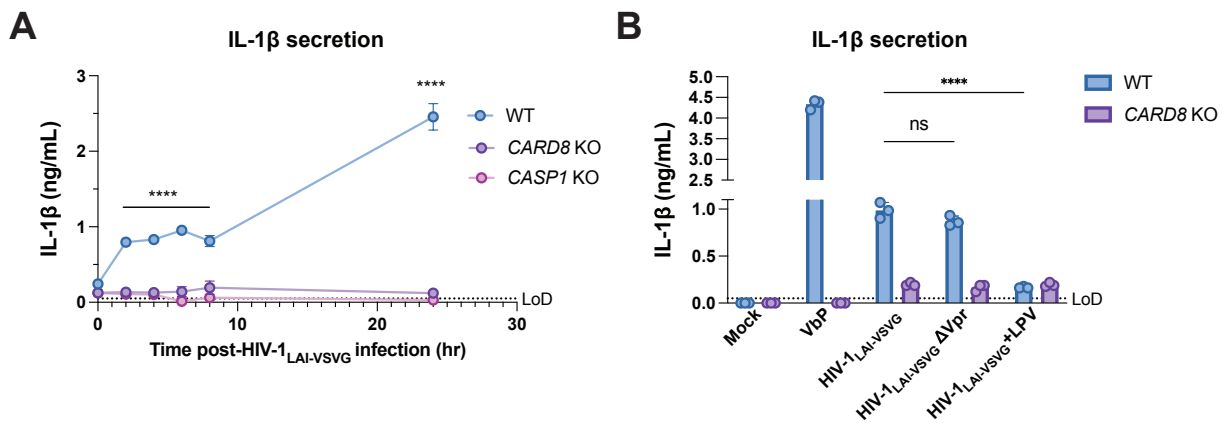


Fig 2.6: Incoming and outgoing HIV^{PR} is responsible for *CARD8* inflammasome activation
A) Wildtype (WT), *CARD8* KO, or *CASP1* KO THP-1 cells were primed overnight with Pam3CSK4 and then infected with HIV-1_{LAI-VSVG}. Supernatant was collected at 0, 2, 4, 6, 8, and 24 hours post-infection to measure IL-1 β secretion. Cells were infected at viral concentration such that ~70% of cells were p24^{gag}-positive after 24 hours. **B)** WT THP-1 cells were primed with Pam3CSK4 were challenged with WT or mutant HIV-1_{LAI-VSVG} or WT virus preincubated in 5 μ M lopinavir (LPV) for 30 min prior to infection. HIV-1_{LAI-VSVG} Δ Vpr has a frameshift mutation in Vpr. Dotted line indicates limit of detection (LoD). Datasets represent mean \pm SD ($n = 3$ biological replicates). P values were determined by 2-way ANOVA with Dunnett's test using GraphPad Prism 9. ns= not significant, * $p < 0.05$, ** $p < 0.01$, *** $p < 0.001$, **** $p < 0.0001$. **Figure 2.6** was reproduced from (149) with permission, Creative Commons Attribution 4.0 International License.

CARD8-dependent inflammasome activity after HIV-1 infection occurs both early and late in acute infection and depends on the activity of HIV-1^{PR}

To gain additional insight into the nature of CARD8 inflammasome responses to HIV-1 infection, we performed a time-course following HIV-1 infection. Unexpectedly, we revealed a statistically significant, CARD8-dependent increase in IL-1 β as early as 2 hours after infection (the first time-point assayed after the initial infection), which plateaued for the next 6 hours and then further increased by 24 hours post-infection (**Figure 2.6A**). As the early timepoints were sampled prior to reverse-transcription and the genesis of *de novo* synthesized HIV-1 transcripts (157), these findings raised the possibility that CARD8 detects the activity of packaged HIV-1^{PR} released into the target cell upon viral entry as well as *de novo* synthesized Gag-Pol. To test this hypothesis, we treated target cells with the HIV^{PR} inhibitor Lopinavir (LPV), which blocked CARD8 inflammasome activation by HIV-1 infection, reinforcing that CARD8 senses HIV-1^{PR} activity. We also considered the possibility that the packaged viral protein R (Vpr) influences CARD8 inflammasome activation. However, we found that a HIV-1 virus lacking Vpr (Δ Vpr) also induces CARD8-dependent inflammasome activation (**Figure 2.6B**). Thus, our findings suggest that HIV-1 infection induces inflammasome activation upon CARD8 detection of HIV-1^{PR} released from the incoming virion as well as newly translated HIV-1^{PR}.

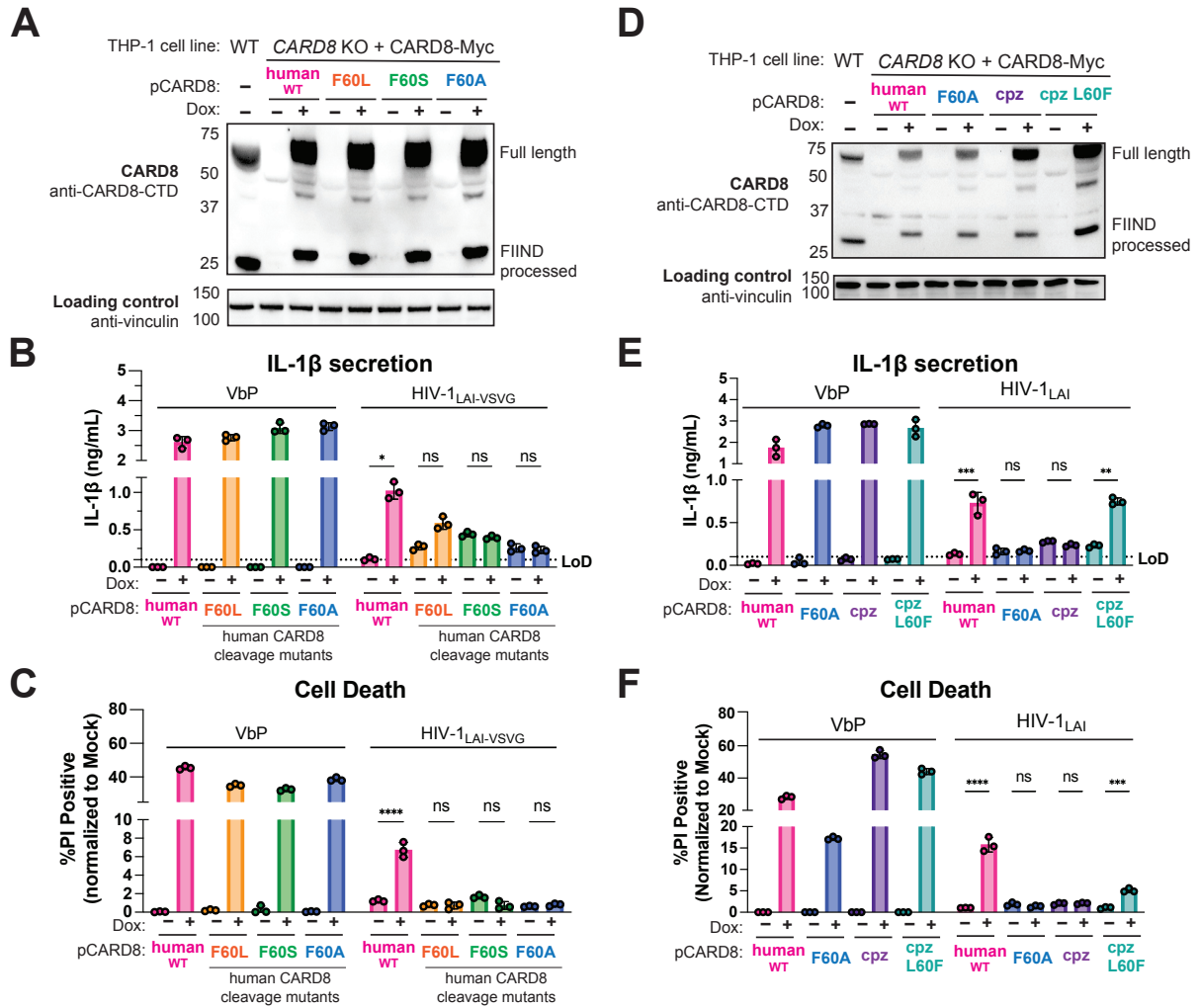


Fig 2.7: HIV inflammasome activation is dependent on a human-specific motif in CARD8
A) CARD8 KO THP-1 lines complemented with different doxycycline (dox)-inducible CARD8 variants (pCARD8) were left uninduced or induced for 18 hours. Immunoblot of wildtype (WT) or complemented CARD8 KO THP-1 lines treated with (+) or without (-) dox was carried out for CARD8 expression using endogenous antibody against CARD8 C-terminal domain (CTD) and loading control (vinculin). FIIND, function-to-find domain. **B-C)** Complementated CARD8 KO lines were left uninduced or dox-induced as described in A and then primed for 4-6 hours with Pam3CSK4 and treated with either 10 μ M VbP or HIV-1_{LAI-VSVG} then assessed for **B)** IL-1 β secretion and **C)** cell death, respectively. **D)** CARD8 KO THP-1 lines complemented with different CARD8 variants were left uninduced or induced for 18 hours. Immunoblot of wildtype (WT) or complemented CARD8 KO THP-1 lines treated with (+) or without (-) dox as described in A. **E-F)** Complementated CARD8 KO lines were induced and primed as described in B then treated with either 10 μ M VbP or HIV-1_{LAI} then assessed for **E)** IL-1 β secretion and **F)** cell death, respectively. All HIV infections were done at a MOI such that 30-50% of cells were p24^{gag}+ after 24 hours. Dotted line indicates limit of detection (LoD). Datasets represent mean \pm SD (n = 3 biological replicates). P values were determined by 2-way ANOVA with Tukey's test using GraphPad Prism 9. ns= not significant, *p < 0.05, **p < 0.01, ***p < 0.001, ****p < 0.0001. **Figure 2.7** was reproduced from (149) with permission, Creative Commons Attribution 4.0 International License.

HIV-1 inflammasome activation is dependent on CARD8 sensing of HIV-1^{PR} activity

To further evaluate the role of the human-derived F59-F60 motif of CARD8 after HIV-1 infection, we used a doxycycline-inducible system to complement *CARD8* KO THP-1 cells with either WT *CARD8* or *CARD8* cleavage mutants (**Figure 2.7A**) and probed for subsequent inflammasome activation. We found that *CARD8* KO THP-1 cells complemented with WT *CARD8* underwent IL-1 β secretion and cell death in response to both VbP and HIV-1 infection in a doxycycline-dependent manner (**Figure 2.7B and 2.7C**), confirming that HIV inflammasome activation is *CARD8*-dependent. In parallel, we complemented *CARD8* KO THP-1 cells with the *CARD8* cleavage mutants F60L, F60S, F60A. All complemented *CARD8* KO THP-1 cells underwent IL-1 β secretion and cell death in response to VbP in doxycycline-treated cells, demonstrating functional *CARD8* expression (**Figure 2.7B and 2.7C**). In contrast, infection with both VSV-g pseudotyped (**Figure 2.7B and 2.7C**) and replication competent (**Figure 2.7E and 2.7F**) HIV-1_{LAI} induced IL-1 β secretion and cell death only in *CARD8* KO THP-1 cells that were complemented with WT human *CARD8*, but not *CARD8* mutants that are resistant to HIV-1^{PR} cleavage. We also found that *CARD8* KO THP-1 cells complemented with chimpanzee *CARD8* restored responsiveness to VbP but not to HIV-1_{LAI} infection, whereas a chimpanzee *CARD8* L60F is cleaved by HIV-1^{PR} and SIVcpz^{PR} (**Figure 2.8**), and can functionally complement human *CARD8* responses to HIV-1 infection (**Figure 2.7D-2.7F**). Thus, human *CARD8* detects the enzymatic activity of HIV^{PR} by encoding a motif that functions as a HIV^{PR} substrate, permitting a human-specific *CARD8* inflammasome response to HIV-1 infection.

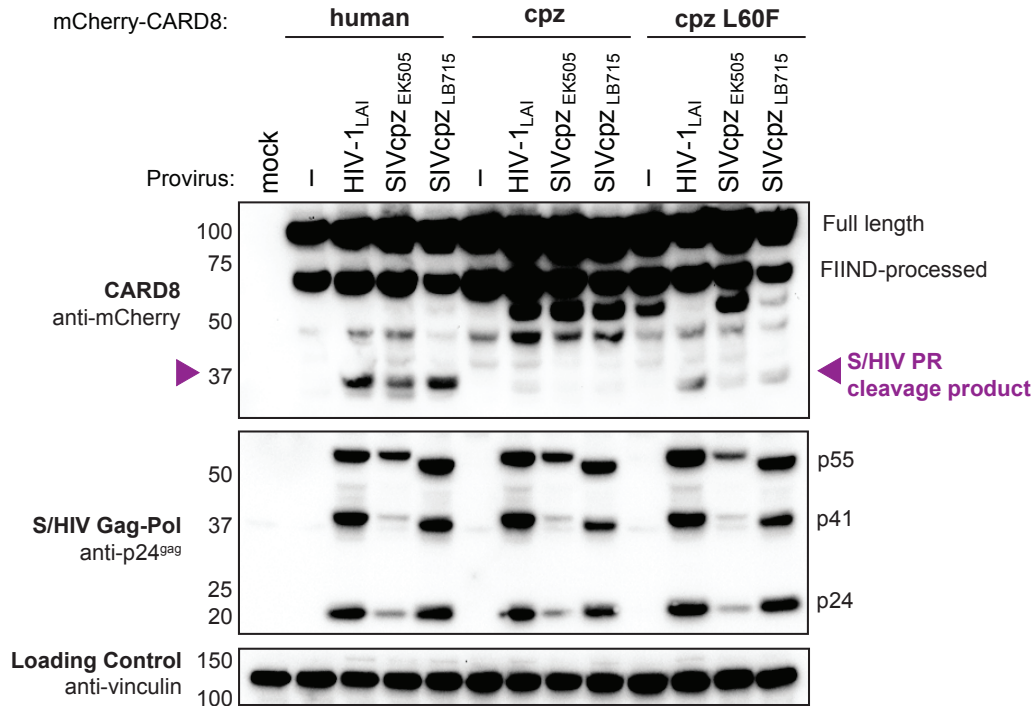


Figure 2.8: Human FF motif in chimpanzee CARD8 rescues sensing of HIV/SIV^{PR}
 HEK293T cells were transfected with a construct encoding N-terminally mCherry-tagged human, chimpanzee (cpz), or cpz with the human FF motif (L60F) CARD8 and indicated provirus constructs. Immunoblotting was carried out for CARD8 cleavage, HIV/SIV protease (S/HIV^{PR}) activity, and vinculin (loading control) as indicated. The S/HIV^{PR} cleavage product is indicated by a purple triangle. FIIND, function-to-find domain. **Figure 2.8** was reproduced from (149) with permission, Creative Commons Attribution 4.0 International License.

DISCUSSION

The ability to selectively induce CARD8-dependent pyroptosis in HIV-1 latently infected CD4+ T cells via NNRTI-enforced dimerization of HIV-1^{PR} has garnered much interest as a means to clear the latent reservoir (141,142,158,159). Here we demonstrate that CARD8 also senses HIV-1 replication in acutely infected cells, which occurs following HIV-1^{PR} site-specific cleavage of a human-specific motif in the CARD8 tripwire. We further show that the unique motif in human CARD8, which is not present in other sampled hominoids and Old World monkeys, enables its sensing of SIVcpz^{PR} – the precursor to HIV-1, indicating that the precursor viruses to HIV-1 were poised to cleave human CARD8 prior to spillover into humans. These results, along with other recent findings (121,124), demonstrate that CARD8 is a *bone fide* innate immune

sensor of viral infection via sensing viral protease activity, and suggest a model for a human-specific inflammatory response to HIV infection.

CARD8 as an innate immune sensor of HIV-1^{PR} activity

Some positive-sense RNA viruses that do not package their viral proteases are sensed following *de novo* synthesized viral protease (121,124). However, as HIV-1 triggers CARD8 inflammasome activation as early as two hours post-infection, well before *de novo* synthesis of viral proteins (**Figure 2.6A**), our findings suggest that HIV-1 entry is also targeted by CARD8 via the innate immune detection of incoming viral protease activity. This conclusion is supported by a recent report that also found that HIV-1 strains lacking RT or integrase function are still sensed by the CARD8 inflammasome in a manner dependent on HIV-1^{PR} activity (160). Based on these findings, we propose that CARD8 can sense HIV-1^{PR} that was packaged into the virion upon its release into the host cytosol upon viral fusion. This idea is consistent with reports that HIV-1^{PR} can function intracellularly to cleave host targets, and not solely in the context of Gag-Pol dimerization during virion assembly and maturation (32,154). We speculate that for HIV-1 this may be particularly relevant for cell-to-cell infection. Thus, our present findings, along with other recent examples of innate immune detection of viral protease activity (121,124), suggest that CARD8's broad antiviral sensing capacity is predicated on its detection of the ubiquitous and essential function of viral proteases, which are evolutionarily constrained by their requirement to target both viral polyprotein and host targets.

We find that inflammasome responses downstream of CARD8 are modulated by TLR stimulation. For example, CARD8-dependent cell death is modestly enhanced by TLR priming by an unknown mechanism (**Figure 2.4**). On the other hand, IL-1 β secretion following HIV-1 infection is strictly dependent on TLR priming, consistent with its established role for transcriptional upregulation of IL-1 β (161). These findings may offer a potential explanation for

conflicting reports as to whether or not primary CD4⁺ T cells undergo pyroptosis and induce IL-1 β secretion in response to HIV-1 infection (128,132). Our findings that several TLR agonists effectively prime CARD8 inflammasome responses (**Figure 2.4B and 2.4C**) suggest that HIV-1 pathogen-associated molecular patterns (i.e., viral nucleic acids) and/or circulating microbial ligands from gut epithelial breakdown, a hallmark of acute HIV-1 disease (162), are potential sources for priming of HIV-1 target cells *in vivo*. Moreover, given the exciting potential of combinatorial host- and virus-directed strategies of HIV-1 reservoir clearance by lowering CARD8 activation threshold (via VbP) and enforced HIV^{PR} cytosolic activity (141), our findings may also guide therapeutic strategies that leverage HIV^{PR}-dependent CARD8 inflammasome activation, which may be bolstered by adjuvants that induce TLR signaling (127,158,163).

Human CARD8 as a maladaptation to HIV-1 infection

Several adaptations of SIVcpz have occurred following its spillover in humans, including Vpu antagonism of human Tetherin/Bst2 (52,164), a mutation in MA that allows infection of human tissues (165), and the adaptation of Vif to antagonize one of the human polymorphisms in APOBEC3H (166). However, other host-virus interactions important for permitting the establishment of the HIV/AIDS pandemic, such as that of SIVcpz Vif with APOBEC3G, arose in intermediate hosts where no further adaptations were required for passage to humans (167,168). Our findings suggest that the interaction of HIV-1^{PR} with human CARD8 is distinct from these scenarios, as SIVcpz^{PR} already had the capacity to cleave human CARD8 before its cross-species transmission to humans, despite the fact that chimpanzee CARD8 is not itself cleaved by SIVcpz^{PR} due to the lack of the FF motif at amino acid 59/60 (**Figures 2.1 and 2.2**).

The F59-F60 motif that confers human CARD8 with the unique capacity to sense HIV/SIVcpz^{PR} is conserved across all humans based on publicly available datasets, as well as being present in a Neanderthal genome, suggesting a genetic sweep occurred in favor of a phenylalanine at

position 60. HIV-1 emerged within the past century (48) and therefore could not have driven the evolution of the HIV-1^{PR} cleavage site in human CARD8. However, human *CARD8* is highly polymorphic, and multiple residues of the N-terminus of *CARD8*, including those that allow *CARD8* sensing of extant human pathogenic viruses including coronaviruses and picornaviruses, show strong evidence of positive selection, an evolutionary signature consistent with a history of host-pathogen conflict (121,136). Indeed, the HIV-1^{PR} cleavage site in *CARD8* overlaps with a site that is cleaved by the coronavirus 3CL protease (121). Although it is possible that the human-specific F60 was fixed stochastically or as a passenger mutation, we favor a scenario in which human *CARD8* sensing of HIV-1^{PR} arose as a consequence of *CARD8* adaptation to another virus (121,124). Thus, we speculate that an ancient infection of our human ancestors may be responsible for our modern day maladaptation to HIV-1.

Possible links to pathogenesis

HIV-1 disease progression to AIDS is characterized by dramatic depletion of CD4⁺ T cells including via pyroptosis (128) and chronic inflammation accompanied by high levels of plasma cytokines including IL-1 (169,170). As such, multiple inflammasomes have previously been implicated for HIV-dependent inflammasome activation, although the exact mechanisms have remained unclear (131,171). Here, we show that HIV infection induces pyroptotic cell death and IL-1 β secretion via *CARD8* recognition of HIV^{PR} activity. Our finding that HIV-1 infection is sufficient to induce inflammasome activation, along with the presence of *CARD8* in relevant T cell populations (110,142,155), also suggests that *CARD8* contributes to HIV pathogenesis. Consistent with this hypothesis, recent publications show that HIV-1 infection drives *CARD8*-dependent pyroptotic cell death both in primary human CD4⁺ T cells *ex vivo* and in humanized mouse models of HIV-1 (160). It is also possible that IL-1 β release after HIV-1 dependent *CARD8* activation after HIV-1 infection could contribute to pathogenesis since IL-1 β induces the

differentiation of Th17 cells (172), a highly HIV-susceptible CD4+ T cell subtype, as well the recruitment of other target immune cells (173).

Simian immunodeficiency viruses are believed to be generally non-pathogenic in their reservoir hosts with the SIVsmm in sooty mangabeys and SIVagm in African green monkeys as the best studied examples (63). SIVcpz in naturally infected chimpanzees is pathogenic although not to the extent of HIV-1 group M infection of untreated humans (59). In contrast, SIVs can cause disease in a new species, including experimental SIV infections of macaque monkeys). It is tempting to speculate that these species-specific differences could be, in part, mediated by differential CARD8 inflammasome activation, which in turn influences the extent of CD4+ T cell depletion, chronic immune activation, and bystander cell immunopathology – key pathogenic events that drive the progression to acquired immunodeficiency syndrome (AIDS) in the absence of antiretroviral therapy (59,60,174). Although our data demonstrates that functional HIV and SIVcpz protease recognition motifs outside of the F59-F60 are absent in human and chimpanzee CARD8, it remains possible that other SIVs have distinct protease specificities that allow for cleavage of species-specific recognition motifs in CARD8 in non-human primates. Indeed, the substrate specificity of SIVmac239^{PR} is distinct from HIV-1^{PR} (**Figure 2.3**), which may be relevant to CARD8 inflammasome activation and CD4+ T cell depletion in experimental macaque infections. We suggest that future work determining these host- and virus-specific interactions is an important consideration when evaluating HIV pathogenesis in non-human primate models.

ACKNOWLEDGEMENTS

We thank everyone in the Emerman and Mitchell labs, Amandine Chantharath for assistance with cloning, Abby Felton for assistance with cell sorting, Joy Twentyman for assistance with cell maintenance, Matt Daugherty, Emily Hsieh, and Brian Tsu for critical reading of the manuscript, Janet Young for helpful discussions, Melissa Kane for kindly providing the doxycycline inducible plasmid (pLKO-puro) used for complementation experiments, Liang Shan and his lab members for discussions and sharing of unpublished results, and the Fred Hutchinson Shared Resources Genomics, Flow Cytometry, and Specimen Processing & Research Cell Bank cores. Lopinavir (LPV) (HRP-9481) and p24^{gag} antibody (ARP-3537) were provided by the AIDS Reagent Program, Division of AIDS, NIAID, NIH. This work was supported by grants from the National Institutes of Health (NIH) (DP2 AI 154432-01) and the Mallinckrodt Foundation to P.S.M; NIH grants DP1 DA051110-03 to M.E., and University of Washington Cellular and Molecular Biology Training Grant (T32 GM007270) to JK.

DECLARATION OF INTERESTS

The authors declare no competing interests.

SUPPLEMENTAL INFORMATION

Supplementary File 1a. List of primers, gBlocks and sgRNA sequences

Supplementary File 1b. List of Antibodies/Reagents

Supplementary File 1c: Primate CARD8 gene IDs

Figure 3-source data

Figure 3-supp1-source data

Figure 4-source data

Figure 5-source data

Figure 1-5-source data. Uncropped western blots from Figures 1-5

All supplemental files can be downloaded from:

<https://elifesciences.org/articles/84108/figures#content>

METHODS

Plasmids

psPAX2 and pMD2.G were gifts from Didier Trono (Addgene). The dox-inducible pLKO-puro vector (175) was a gift from Melissa Kane. Infectious molecular clones for SIVcpz_{EK505} and SIVcpz_{LB715} were gifts from Beatrice Hahn (150,151). HIV-1_{Q23} Δ env provirus and the HIV-1_{Q23.BG505} proviruses were gifts from Julie Overbaugh (176,177). HIV-1_{LAI} and HIV-2_{Rod} were previously described (178,179). The HIV-1_{LAI} DVpr mutant has a frameshift mutation that inactivates the *vpr* gene as described (180). CARD8 sequence IDs used for phylogenetic analysis in **Figure 2.1A** can be found in **Supplementary File 1c**. For CARD8 cleavage assays, the coding sequences of human CARD8 (NCBI accession NP_001171829.1) and chimpanzee CARD8 (NCBI accession XM_024351500.1) were cloned into the pcDNA3.1 backbone (Addgene) with an N-terminal mCherry tag using BamHI and EcoRI cut sites. For dox-inducible complementation assays, the coding sequences of human and chimpanzee CARD8 were cloned into the pLKO-puro backbone using the SfiI site. Point mutations were introduced using overlapping PCR. Full list of primer sequences can be found in **Supplementary File 1a**.

Cell Culture

THP-1 cells (ATCC) were cultured in RPMI (Invitrogen) with 10% FBS, 1% penicillin/streptomycin antibiotics, 10 mM HEPES, 0.11 g/L sodium pyruvate, 4.5 g/L D-Glucose and 1% Glutamax. HEK 293T (ATCC) were cultured in DMEM (Invitrogen) with 10% FBS and 1% penicillin/streptomycin antibiotics. All puromycin selections were done at 0.5 μ g/mL. For complemented dox-inducible lines, tetracycline-free FBS (Sigma) was used to prevent background CARD8 expression. All lines routinely tested negative for mycoplasma bacteria (Fred Hutch Specimen Processing & Research Cell Bank).

Immunoblotting

Cells were washed once with 1xPBS before harvesting in NP-40 buffer with protease inhibitor (200 mM NaCl, 50 mM Tris pH 7.4, 0.5% NP-40 Alternative, 1 mM dithiothreitol, and Roche Complete Mini, EDTA-free tablets; catalog no. 11836170001). Cytoplasmic lysates were clarified via centrifugation and combined with 4x NuPage LDS sample Buffer (Invitrogen) containing 10% β -mercaptoethanol and boiled for 5-10 minutes. Samples were run on a 4-12% SDS-PAGE gel using morpholineethanesulfonic acid (MES) buffer, transferred to a nitrocellulose membrane using a Pierce G2 Fast Blotter (Thermo Scientific), blocked in 5% nonfat milk then probed for with primary antibodies diluted in 2.5% milk for mCherry (for CARD8 cleavage), p24^{gag} (for HIV^{PR} activity), CARD8 C-terminus (for knockout validation and complementation), and vinculin (loading control). Blots were washed three times with PBS-T (0.1% Tween-20), incubated with secondary HRP-conjugated antibodies, washed three times again, and then developed with SuperSignal West Femto Maximum Sensitivity Substrate (Fisher Scientific). Further antibody specifications/concentrations and clone info are described in **Supplementary File 1b**.

CARD8 cleavage assay

HEK293T cells were seeded at $1.5-2 \times 10^5$ cells/well in 24-well plates the day before transfection using TransIT-LT1 reagent at 1.5 μ L transfection reagent/well (Mirus Bio LLC). 100 ng of indicated constructs encoding a N-terminal mCherry tagged CARD8 were co-transfected into HEK293T cells with either 400 ng of pcDNA3.1 empty vector ('-'), or 400 ng of HIV provirus or SIVcpz provirus. HIV Δ env proviruses were used for immunoblots in **Figure 2.1** and **Figure 2.3**, while infectious HIV and SIVcpz provirus were used for immunoblots in **Figure 2.2**. Cytoplasmic lysates were harvested 24 hours post-transfection and immunoblotted as described above.

FLICA Assay

Live cells were incubated in media containing FLICA dye (Immunochemistry Technologies, cat. #97) at a dilution of 1:60-1:100 for 30 min at 37°C then washed and fixed according to manufacturer's protocol. Stained cells were flowed for analysis on a BD Celesta within 18 hours post-staining.

CARD8 and CASP1 knockout generation

CARD8 and *CASP1* knockout THP-1 cells were generated similarly to *NLRP1* knockouts described previously (145). Briefly, a *CARD8* or *CASP1* specific sgRNA was designed using CHOPCHOP (181), and cloned into a plasmid containing U6-sgRNA-CMV-mCherry-T2A-Cas9 using ligation-independent cloning. THP-1 cells were electroporated using the BioRad GenePulser Xcell. After 24 hours, mCherry-positive cells were sorted and plated for cloning by limiting dilution. Monoclonal lines were validated as knockouts by deep sequencing and OutKnocker analysis, as described previously (182,183). Knockout lines were further validated by immunoblot and functional assays. sgRNA used to generate knockouts are described in **Supplementary File 1a**.

CCR5+ cell line generation

WT or *CARD8* KO THP-1 cells were transduced with pHIV-CCR5/ZsGreen as previously described (184). Cells were sorted 4 days post-transduction on a Sony MA900.

CARD8 complementation

HEK293T were seeded at 2×10^5 cells/well in 6-well plates the day before transfection using TransIT-LT1 reagent (Mirus Bio LLC) at 5.8 μ L transfection reagent/well. Cells were co-transfected with pLKO-CARD8, psPAX2, and pMD2.G and media was replaced the next day.

Virus was harvested two days post-transfection and underwent one freeze thaw cycle at -80°C before transducing *CARD8* KO THP-1 cells. *CARD8* KO THP-1 cells were seeded at 2×10^5 cells/well in 6-well plates and transduced with 800 μL virus in the presence of 1 $\mu\text{g}/\text{mL}$ polybrene via spinoculation at 1100 x g for 30 minutes at 30°C then puro-selected 24 hours post-transduction.

HIV-1_{LAI}, HIV-1_{Q23-BG505}, and HIV-1_{LAI-VSVG} production

293T cells were seeded at 2×10^5 cells/well in 6-well plates the day before transfection using TransIT-LT1 reagent (Mirus Bio LLC) at 3 μL transfection reagent/well as previously described (185). For HIV-1 production, 293Ts were transfected with either 1 $\mu\text{g}/\text{well}$ HIV_{LAI} proviral DNA or 1 $\mu\text{g}/\text{well}$ HIV_{LAI} Δenv DNA and 500 ng/well pMD2.G for HIV-1_{LAI} and HIV-1_{LAI-VSVG}, respectively. One day post-transfection, media was replaced. Two or three days post-transfection, viral supernatants were collected and filtered through a 20 μm filter and aliquots were frozen at -80°C . HIV-1_{LAI} and HIV-1_{LAI-VSVG} proviruses were previously described (179,186,187). HIV-1_{Q23-BG505} was produced in the same way as HIV-1_{LAI}.

THP-1 priming and HIV-1 infection

THP-1 cells were seeded at 1×10^5 cells/well in 96-well U-bottom plates in media containing TLR agonist (**Supplementary File 1b**) for 4-6 hours or overnight then treated with either Val-boroPro (10 μM) or nigericin (5 $\mu\text{g}/\text{mL}$) or infected with HIV-1_{LAI}, HIV-1_{Q23-BG505} or HIV-1_{LAI-VSVG} in the presence of 20 $\mu\text{g}/\text{mL}$ DEAE-Dextran via spinoculation at 1100 x g for 30 minutes at 30°C . All infections were done at an MOI <1 . 24 hours post-infection or VbP treatment (two hours for nigericin), supernatants were collected for IL-1 β quantification (see IL-1R reporter assay) and cells were stained with propidium iodide or FLICA dye then fixed and stained with p24^{gag}-FITC for flow cytometry.

IL-1R reporter assay

To quantify the IL-1 β secretion, HEK-Blue IL-1 β reporter cells (Invivogen) were used whereby binding of IL-1 β to the surface receptor IL-1R1 results in the downstream activation of NF- κ B and subsequent production of secreted embryonic alkaline phosphatase (SEAP) in a dose-dependent manner as previously described (145). SEAP levels were detected using a colorimetric substrate assay, QUANTI-Blue (Invivogen), by measuring an increase in absorbance at OD655. Culture supernatant from treated or infected THP-1 cells was transferred to HEK-Blue IL-1 β reporter cells plated in 96-well format in a total volume of 200 μ L per well at 5×10^5 cells/well. On the same plate, serial dilutions of recombinant human IL-1 β (Peprotech) were added to generate a standard curve for each assay. After 24 hours, SEAP levels were assayed by adding 50 μ L of the supernatant from HEK-Blue IL-1 β reporter cells to 150 μ L of QUANTI-Blue colorimetric substrate along with 0.25% Tween-20 to neutralize HIV virions in supernatant before readout. After incubation at 37°C for 15–30 minutes, absorbance at OD655 was measured on an Epoch Microplate Spectrophotometer (BioTek) and absolute levels of IL-1 β were calculated relative to the standard curve.

Data Availability

All data generated or analyzed during this study are included in the manuscript, Figure 3-source data, Figure 4-source data, and Figure 1-4-source data.

CHAPTER 3: EFFECTS OF CELL-TO-CELL TRANSMISSION AND PROTEASE VARIABILITY ON CARD8 INFLAMMASOME ACTIVATION AFTER HIV-1 INFECTION

ABSTRACT

Inflammasomes are cytosolic innate immune complexes that assemble upon detection of diverse pathogen-associated cues and play a critical role in host defense and inflammatory pathogenesis. Our previous work demonstrated that CARD8 detects HIV infection by sensing the enzymatic activity of the HIV protease, resulting in CARD8-dependent inflammasome activation and cell death. Here, we sought to understand CARD8 responses to HIV when the virus is transmitted from infected cells to target cells via a viral synapse (cell-to-cell), a physiologic and important mode of HIV spread. To assess HIV-dependent inflammasome responses during cell-to-cell transmission of HIV-1, we developed HIV coculture systems with a panel of immortalized and primary cells, including human monocyte-derived macrophages. We observed that cell-to-cell transmission of HIV induces CARD8 inflammasome activation in immortalized and primary human monocyte-derived macrophages. Genetic knockout of the adaptor protein ASC and treatment with the NLRP3 inhibitor MCC950 suggest that cell death associated with HIV-dependent inflammasome activation is primarily CARD8-dependent whereas cytokine release may be amplified through secondary modulation by the NLRP3 inflammasome. To evaluate the viral determinants of CARD8 sensing, we tested a panel of HIV protease inhibitor resistant clones to establish how variation in HIV protease affects CARD8 activation. We identified mutant HIV-1 proteases that differentially cleave and activate CARD8 compared to wildtype HIV-1. These data implicate CARD8 activation as a major contributor of pyroptosis by multiple modes of HIV infection, thus providing further physiological relevance for the possible role CARD8 inflammasome activation in HIV pathogenesis.

INTRODUCTION

Human Immunodeficiency Virus (HIV-1) can be transmitted from one cell to another via two main mechanisms: cell-free infection through binding of free HIV-1 virions to target cells, and cell-to-cell infection through direct contact whereby infected cells transmit virus to an uninfected target cell via the formation of a transient viral synapse (129,188,189). Cell-to-cell transmission of HIV-1 has been reported between multiple HIV-1 target cell types including between active and resting CD4⁺ T cells (190,191) and between CD4⁺ T cells and macrophages (192–194). Cell-to-cell transmission delivers a large influx of virus to target cells, resulting in a high multiplicity of infection (MOI) (195–198), which has been proposed to enhance viral fitness by overcoming many host innate antiviral pathways including Tetherin/Bst-2 (199,200), SAMHD1 (201), and TRIM5 α (202), and evading adaptive immune responses like broadly neutralizing antibodies (203,204) and antiretroviral therapy (198,205,206).

The high number of virions that infect cells via cell-to-cell spread compared to cell-free infections makes HIV-1 protease (HIV^{PR}), which is activated when high concentrations of HIV^{gagpol} are achieved, an intriguing target of innate immune recognition during cell-to-cell infection (195–198). While HIV^{PR}'s canonical function is to cleave viral polyproteins within the virion, HIV^{PR} was previously shown to also cleave the host cell protein CARD8 in its N-terminus during acute cell-free HIV-1 infection, leading to its proteasomal degradation and subsequent inflammasome activation, characterized by a form of lytic cell death known as pyroptosis (68) and the release of pro-inflammatory cytokine interleukin (IL)-1 β (127,142,149). In this way, the CARD8 N-terminus serves as a “molecular tripwire” to recognize the enzymatic activity of HIV^{PR} and other viral proteases (121,124,146). Moreover, HIV^{PR} cleavage of CARD8 occurs rapidly after infection such that HIV^{PR} inhibitors and fusion inhibitors, but not reverse transcriptase inhibitors can prevent CARD8 inflammasome activation, implying that virion packaged HIV^{PR} can cleave CARD8 in the infected cells (127,149). Previously, both the NLRP3 and IFI16

inflammasomes have been implicated as innate sensors of HIV-1 infection, and drivers of CD4+ T cell depletion using blood and lymphoid-derived CD4+ T cells, respectively, and cell-to-cell transmission was reported to be crucial for IFI16 sensing of abortive HIV transcripts (128,129,131,133). However, innate sensing of HIV^{PR} during cell-to-cell transmission of non-lymphocytic HIV-1 target cell types has not been investigated.

Given the important role of HIV^{PR} in replication, early combination antiretroviral therapy for people living with HIV (PLWH) included protease inhibitors along with reverse transcriptase inhibitors. However, resistance mutations to protease inhibitors quickly arose in PLWH through mutations around the HIV^{PR} active site allowing for polyprotein processing and viral maturation while avoiding drug inhibition. Despite typically having poor overall viral fitness due to less efficient polyprotein processing and replication relative to wildtype HIV-1 in the absence of protease inhibitors, these mutant drug-resistant HIV-1 strains can persist in people living with HIV on HAART, posing a major threat to controlling disease progression (38–41). To compensate for mutations in HIV^{PR} that change its substrate specificity, HIV^{gag} sometimes evolves mutations around HIV^{PR} cleavage sites to permit proper polyprotein processing (207).

Here, we assessed CARD8-dependent inflammasome responses upon cell-to-cell transmission of HIV-1 in myeloid cells as well as the effects of naturally occurring mutations in HIV^{PR} on CARD8 sensing. We found that CARD8 inflammasome activation can readily occur in the context of cell-to-cell transmission in both THP-1 cells, an acute myeloid leukemia cell line, and in primary monocyte-derived macrophages. In contrast to other host innate immune pathways, which are ineffective during cell-to-cell transmission, our findings suggest that CARD8 sensing of HIV^{PR} could be an important innate sensing failsafe to cell-to-cell transmission of HIV-1. In addition, we observed that HIV-infected cells lacking ASC, an adaptor protein crucial to the formation of many inflammasomes including NLRP3 and IFI16, exhibited similar levels of cell

death but reduced cytokine release relative to wildtype cells. These data suggest that while HIV-dependent cell death is ASC-independent, ASC-dependent inflammasomes may partially contribute to cytokine release in these cell types. We also identified various HIV^{PR} inhibitor resistant clones that can differentially cleave and activate the CARD8 inflammasome, providing a powerful tool for investigating the effects of CARD8 inflammasome activation on viral replication. Functional characterization of HIV^{PR} inhibitor resistant clones suggests that differences in the capacity for mutant HIV^{PR} resistant strains to activate CARD8 is likely not due to changes in specificity for CARD8 but rather, in part, from variations in capacity for these mutant HIV^{PRs} to dimerize and activate.

RESULTS

Cell-to-cell transmission of HIV-1 induces CARD8-dependent inflammasome activation

In order to achieve adequate levels of viral infection, cationic polymers like DEAE-dextran are often used to facilitate host and viral membrane fusion and thus enhance viral infection; however, we observed that DEAE-dextran alone can induce inflammasome activation in some THP-1 cell lines (data not shown). As a cationic polymer, DEAE-dextran alters electrostatic interactions between membranes, which may prompt inadvertent potassium efflux from host cells that would be consistent with sensing by the NLRP3 inflammasome. Therefore, we established conditions to test whether or not CARD8 dependent inflammasome activation could occur in models of HIV-1 infection that lack cationic polymers.

We designed an *in vitro* coculture infection system to mimic cell-to-cell transmission of HIV-1 using SUPT1 cells, a T-cell lymphoma line, as a viral producer line and either THP-1 cells, an acute monocytic leukemia line, or primary monocyte-derived macrophages (MDMs), as target lines (**Figure 3.1A**). Infected SUPT1 cells were cocultured with THP-1 cells for 48 hours, and IL-

IL-1 β secretion was used as a proxy for inflammasome activation. In previous work, we showed that toll-like receptor (TLR) priming was crucial to stimulating cytokine release in THP-1 cells (149), thus all target cells were treated with the TLR1/2 agonist Pam3CSK4 before starting the coculture.

We observed that coculture of wildtype (WT) THP-1 cells with HIV-1_{LAI}-infected but not mock-infected SUPT1 cells results in robust inflammasome activation as indicated by IL-1 β secretion. Since SUPT1 cells infected with HIV-1_{LAI} do not elicit IL-1 β secretion and lack functional CARD8 inflammasome responses, we could infer that inflammasome activation in the coculture is attributed entirely to the THP-1 cells or MDMs following cell-to-cell spread (**Figure 3.1B**). To determine the potential role of CARD8 in inflammasome activation during cell-to-cell transmission of HIV-1, we cocultured HIV-1_{LAI}- or mock-infected SUPT1 cells with either WT or CARD8 KO THP-1 cells and compared subsequent inflammasome activation. Unlike WT THP-1 cell cocultures, cocultures with CARD8 KO THP-1 cells displayed no significant activation (**Figure 3.1B**). These data demonstrate that CARD8 is the primary sensor that drives inflammasome activation in HIV-1 cell-to-cell transmission in THP-1 cells.

We also interrogated whether or not the inflammasome activation we observe in our coculture system is solely from cell-to-cell transmission or if cell-free infection may also contribute. We demonstrate that cell-free HIV-1 infection without the use of cationic polymers like DEAE-dextran produces inefficient infection and does not elicit CARD8-dependent inflammasome activation in THP-1 cells (**Figure 3.2A-B**). Additionally, in an orthogonal approach, we conducted a similar coculture experiment with HIV-1_{LAI}-infected SUPT1 cells and target THP-1 cells either allowing cell-to-cell transmission (mixed) or preventing cell contact by using a virus-permeable transwell (**Figure 3.2C**). We observed no significant activation, as measured by IL-

IL-1 β secretion, when the infected SUPT1 cells were separated from the target THP-1 cells by the transwell unless DEAE-dextran was added upon starting the coculture (**Figure 3.2D**). Despite equal amounts of available cell-free virus in the transwell and mixed condition, the transwell condition treated with DEAE-dextran exhibited significantly less inflammasome activation than the cell-to-cell (mixed) condition (**Figure 3.2D-E**). These data suggest that our coculture system, which lacks DEAE-dextran, measures inflammasome activation induced by only cell-to-cell infection, not secondary cell-free infection.

We then examined cell-to-cell HIV-1 transmission using primary MDMs as a target cell in the coculture system. We cocultured TLR-primed MDMs with SUPT1 cells mock-, HIV-1_{LAI}-, or HIV-1_{NL4.3-BaL}-infected and assayed for inflammasome activation (**Figure 3.1C**). HIV-1_{LAI} is a CXCR4 tropic strain unable to infect macrophages whereas HIV-1_{NL4.3-BaL} is a CCR5 and macrophagic tropic strain. We observed inflammasome activation, as measured by IL-1 β secretion, in MDMs cocultured with HIV-1_{NL4.3-BaL}-infected SUPT1 cells but not in MDMs cocultured with HIV-1_{LAI}- or mock-infected SUPT1 cells. Thus, MDMs cocultured with an envelope that confers macrophage-tropism exhibited inflammasome activation, demonstrating that viral entry is necessary for this activation and indicating that this phenotype is not from fusion of the donor and target cell.

To elucidate additional determinants of inflammasome activation in primary macrophages, SUPT1 cells infected with HIV-1_{NL4.3-BaL} were incubated with various antiretroviral drugs prior to coculture, including lopinavir and nevirapine, which inhibit HIV-1 protease (HIV-1^{PR}) and HIV-1 reverse transcriptase (HIV-1^{RT}), respectively. Consistent with our prior results with cell-free HIV-1 infections, inflammasome activation following cell-to-cell spread was abrogated by lopinavir, demonstrating that HIV^{PR} activity is necessary for CARD8-dependent activation (**Figure 3.1C**).

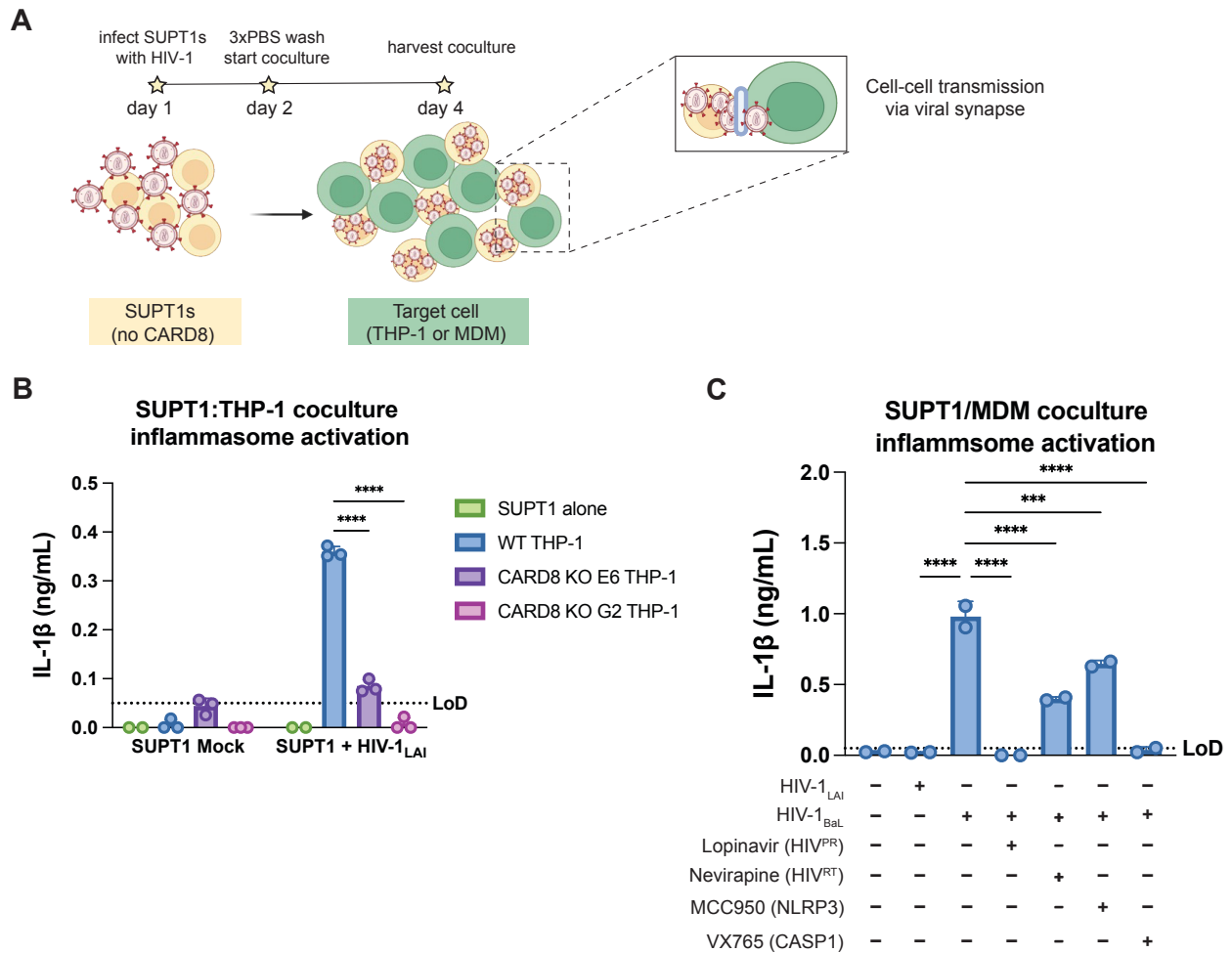


Fig. 3.1: Cell-to-cell transmission of HIV induces CARD8 inflammasome activation

A) Schematic of coculture experimental setup. SUPT1 cells were infected for 24 hours prior to coculturing with target cells. The coculture was harvested 48 hours later to probe for IL-1 β secretion in the coculture supernatant via IL-1R reporter assay. (B) Wildtype (WT) or CARD8 KO THP-1 cells were cocultured with SUPT1 cells either mock-infected or infected with HIV-1_{LAI} as depicted in (A). THP-1 cells were primed with Pam3CSK4 (500ng/mL) for 16 hours prior to coculture. SUPT1 cells were infected with HIV-1_{LAI} such that 30% of the cells were positive for intracellular p24^{gag} after 24 hours. (C) Monocyte-derived macrophages (MDMs) were cocultured with SUPT1 cells mock-, HIV-1_{LAI}- or HIV-1_{NL4.3-BaL}-infected then assayed for inflammasome activation as in (B). Fifteen minutes before starting the coculture, SUPT1 cells infected with HIV-1_{NL4.3-BaL} were pre-treated with either DMSO, lopinavir (5 μ M), nevirapine (50 μ M), MCC950 (10 μ M) or VX765 (1 μ M), inhibiting HIV-1 protease (HIV^{PR}), HIV-1 reverse transcriptase (HIV^{RT}), NLRP3, or caspase 1 (CASP1), respectively. SUPT1 cells were infected with HIV-1_{LAI} and HIV-1_{NL4.3-BaL} such that 2% and 7% of cells, respectively, were positive for intracellular p24^{gag} after 24 hours. Dotted line indicates limit of detection (LoD). Datasets represent mean \pm SD (B) ($n=3$ biological replicates) or (C) ($n=2$ biological replicates from one donor). p -Values were determined by one-way (C) or two-way (B) ANOVA with Dunnett's test using GraphPad Prism 10. ns = not significant, * $p<0.05$, ** $p<0.01$, *** $p<0.001$, **** $p<0.0001$.

Previously, we had observed that CARD8 could sense both active HIV-1^{PR} released into the host cytosol following viral fusion, which we refer to as “incoming” HIV-1^{PR}, and *de novo* translated HIV-1^{PR} in our cell-free infection system using DEAE-dextran and spinoculation (149). To ascertain whether or not both incoming and *de novo* translated HIV-1^{PR} could also contribute to inflammasome activation in our coculture system, we used a reverse transcriptase inhibitor, nevirapine, to prevent synthesis of *de novo* translated HIV-1^{PR}, and thus any CARD8-dependent IL-1 β secretion would only be due to incoming HIV^{PR} in the presence of nevirapine. Indeed, we observed HIV-dependent inflammasome activation in the presence of nevirapine treatment that was added at the time of co-culture, indicating that incoming HIV^{PR} is sufficient to elicit an inflammasome response. However, the amount of IL-1 β in the presence of the RT inhibitor is reduced, suggesting that *de novo* synthesized HIV^{PR} or incoming HIV^{PR} from secondary cell-to-cell spread may also contribute to inflammasome activation in the coculture system (**Figure 3.1C**).

Since NLRP3 had previously been implicated in HIV-dependent inflammasome activation in CD4⁺ T cells, we also assessed the effects of NLRP3 inflammasome-specific inhibitor MCC950 on inflammasome activation in our primary macrophage cocultures. Upon MCC950 treatment, we still observed robust inflammasome activation from MDMs cocultured with HIV-1_{NL4.3-Bal-} infected SUPT1 cells, though the response was reduced relative to DMSO-treated cocultures (**Figure 3.1C**). These findings indicate that NLRP3 is not the primary sensor for HIV-dependent activation in MDM cocultures; however, NLRP3 activation may amplify IL-1 β secretion after primary activation from CARD8. In addition, inflammasome activation was inhibited by VX765, an inhibitor of Caspase 1 (CASP1), indicating that this phenotype is dependent on CASP1, and therefore depends on the downstream effectors of CARD8 activation (**Figure 3.1C**). Taken together, these data suggest that in the context of cell-to-cell transmission, CARD8 in primary macrophages can sense HIV-1 infection via HIV^{PR} activity, resulting in inflammasome activation.

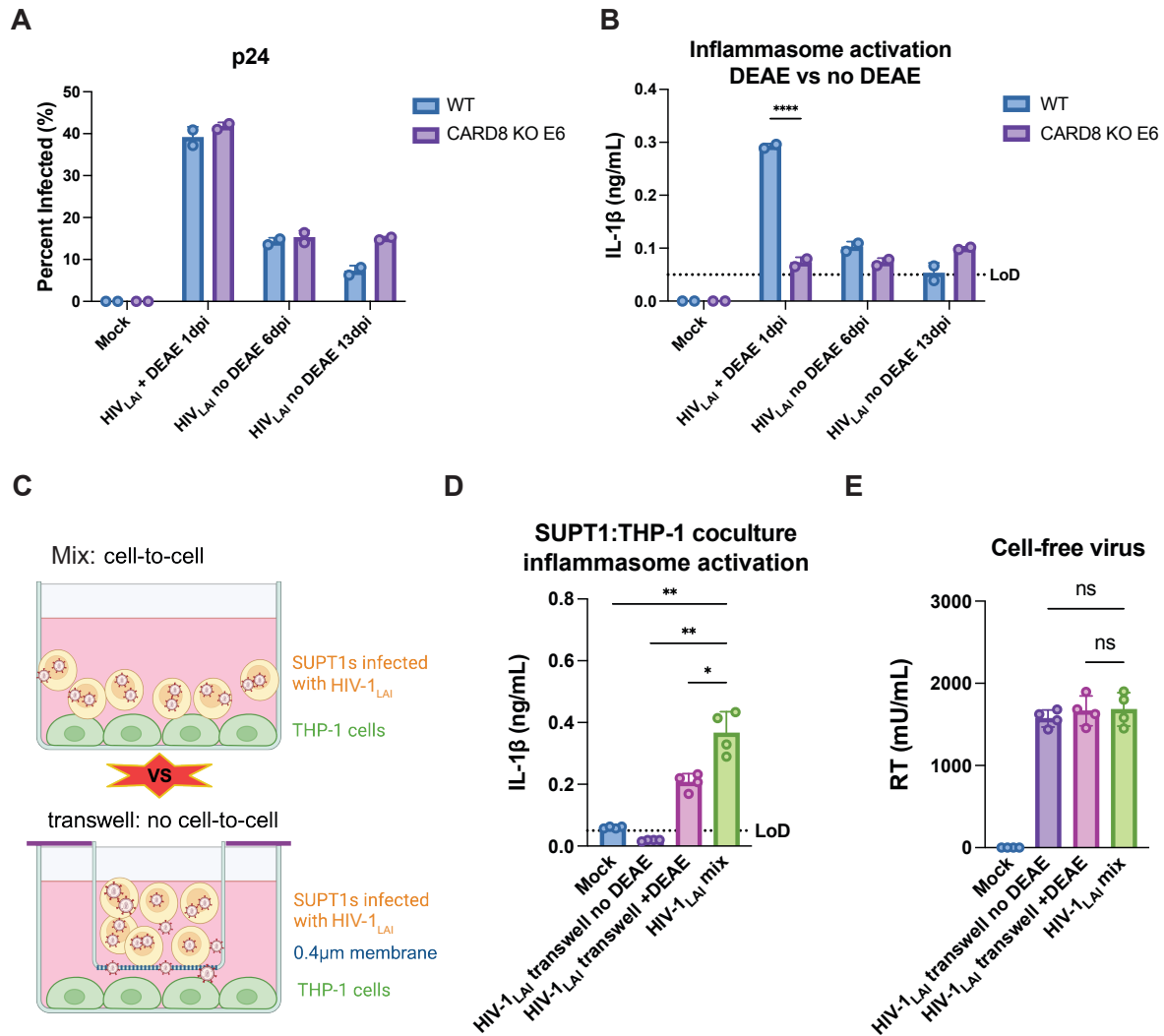


Fig. 3.2: Inefficient cell-free HIV-1 infection yields no CARD8 inflammasome activation
 Wildtype (WT) or CARD8 knockout THP-1 cells were infected with HIV-1_{LAI} at the same MOI in the presence or absence of DEAE-dextran then harvested after the indicated amount of days post-infection (dpi) and assayed for A) intracellular p24^{gag} and B) IL-1β secretion by flow cytometry and IL-1R reporter assay, respectively. C) Schematic illustrating experimental setup for SUPT1/THP1 cell coculture in D and E. THP-1 cells were primed overnight with Pam3CSK4 prior to coculture. SUPT1 cells were either mock infected or infected with HIV-1_{LAI} then cocultured with primed WT THP-1 cells 24 hours post infection. Mock- or HIV-1_{LAI}-infected SUPT1 cells were either mixed with the THP-1s cells or put in a transwell with a virus-permeable membrane in the presence or absence of DEAE-dextran. DEAE-dextran was added to the mock but not the mixed condition. Supernatant from the cocultures were harvested 3 days after starting the coculture and assayed for D) IL-1β secretion as in B) and E) cell-free infectious HIV virions via reverse transcriptase assay. Dotted line indicates limit of detection (LoD). Datasets represent mean ± SD (A-B: n=2; D-E: n=4 biological replicates). A-B: Two-way ANOVA with Sidak's test D-E: One-way ANOVA with Dunnett's test using GraphPad Prism 10. ns = not significant, *p<0.05, **p<0.01, ***p<0.001, ****p<0.0001.

CARD8-dependent activation from HIV-1 is mostly ASC-independent

Since NLRP3 and IFI16 had previously been implicated in HIV-dependent inflammasome activation, we next asked whether or not other inflammasomes contribute to CARD8-dependent inflammasome activation in response to HIV-1 in both modes of infection. ASC, which is encoded by *PYCARD* and will be referred to as ASC from this point forward, is a key adaptor protein necessary for formation of various inflammasomes including the NLRP3 and IFI16, but not the CARD8 inflammasome. Thus, we assessed inflammasome activation using WT THP-1 cells or CRISPR/Cas9-generated clonal *CARD8* KO, ASC KO, or *CARD8*/ASC double KO (DKO) THP-1 cells during cell-free and cell-to-cell HIV-1 infection.

To functionally validate the THP-1 KO cell lines, we treated WT, *CARD8* KO, ASC KO, and *CARD8*/ASC DKO THP-1 cells with either Valbora-Pro (VbP), which is a known CARD8 activator, or the ionophore nigericin, which specifically induces NLRP3 inflammasome activation. As expected, in response to VbP treatment, *CARD8* KO and *CARD8*/ASC DKO did not respond while WT and ASC KO lines induced dramatic cell death, as measured by propidium iodide dye uptake (**Figure 3.3A**). Similarly, VbP treatment did not elicit IL-1 β secretion from *CARD8* KO or *CARD8*/ASC DKO lines but induced IL-1 β secretion from WT and ASC KO lines; however, IL-1 β secretion in the ASC KOs was reduced relative to WT, suggesting that potassium influx induced by CARD8-dependent pyroptosis may secondarily activate the ASC-dependent NLRP3 inflammasome and contribute to overall activation (**Figure 3.3B**). Moreover, WT and *CARD8* KO lines responded to nigericin, inducing cell death and IL-1 β secretion, while ASC KO and *CARD8*/ASC DKO did not respond, indicating that these KO lines are specific and maintain responsiveness to other inflammasome agonists (**Figure 3.3A-B**).

We next infected WT, *CARD8* KO, ASC KO, or *CARD8/ASC* DKO THP-1 cells with VSV-G pseudotyped HIV-1_{LAI} (HIV-1_{LAI-VSVG}) in our cell-free infection system and probed for inflammasome activation 24 hours post-infection. Both WT and ASC KO exhibited high levels of cell death in response to HIV-1_{LAI-VSVG} with no significant difference in cell death while the *CARD8* KO and *CARD8/ASC* DKO both exhibited minimal cell death with no significant difference between the two lines, indicating that HIV-dependent cell death is ASC-independent (**Figure 3.3A**). Along with cell death, as an additional proxy for inflammasome activation, we looked for corresponding IL-1 β secretion in WT versus KO lines in response to HIV-1_{LAI-VSVG} infection. While only minimal IL-1 β secretion was measured from *CARD8* KO and *CARD8/ASC* DKO, we observed significant IL-1 β secretion in the WT and ASC KO lines; however, like during VbP treatment, the IL-1 β secretion was reduced in the ASC KO relative to WT to the same level as VbP treated ASC KO (**Figure 3.3B**). Taken together, these data suggest that cell death associated with HIV-1_{LAI-VSVG} infection is solely *CARD8*-dependent and ASC-independent whereas cytokine release is mostly *CARD8*-dependent, but ASC-dependent inflammasomes may amplify or facilitate IL-1 β secretion in our cell-free infection model.

We next assessed the relative contribution of ASC-containing inflammasomes in HIV-1 cell-to-cell infection, using SUPT1 cells as viral producer cells and THP-1 cells as target cells. We infected SUPT1 cells with HIV-1_{LAI} then after 24 hours, cocultured them with either WT, *CARD8* KO, ASC KO, or *CARD8/ASC* DKO THP1s. Supernatants were harvested 48 hours after the coculture was started to probe for secreted IL-1 β . We observed inflammasome activation from cocultures with WT and ASC KO but not *CARD8* KO or *CARD8/ASC* DKO THP-1 cells, suggesting that activation is *CARD8*-dependent (**Figure 3.3C**). Similar to our cell-free infection, we observed reduced levels of inflammasome activation in the ASC KO relative to WT THP-1 cells (**Figure 3.3C**). These findings are consistent with *CARD8*-dependent cytokine release from

HIV-1 infection being amplified by secondary activation of an ASC-containing inflammasome in both cell-free and cell-to-cell infection models.

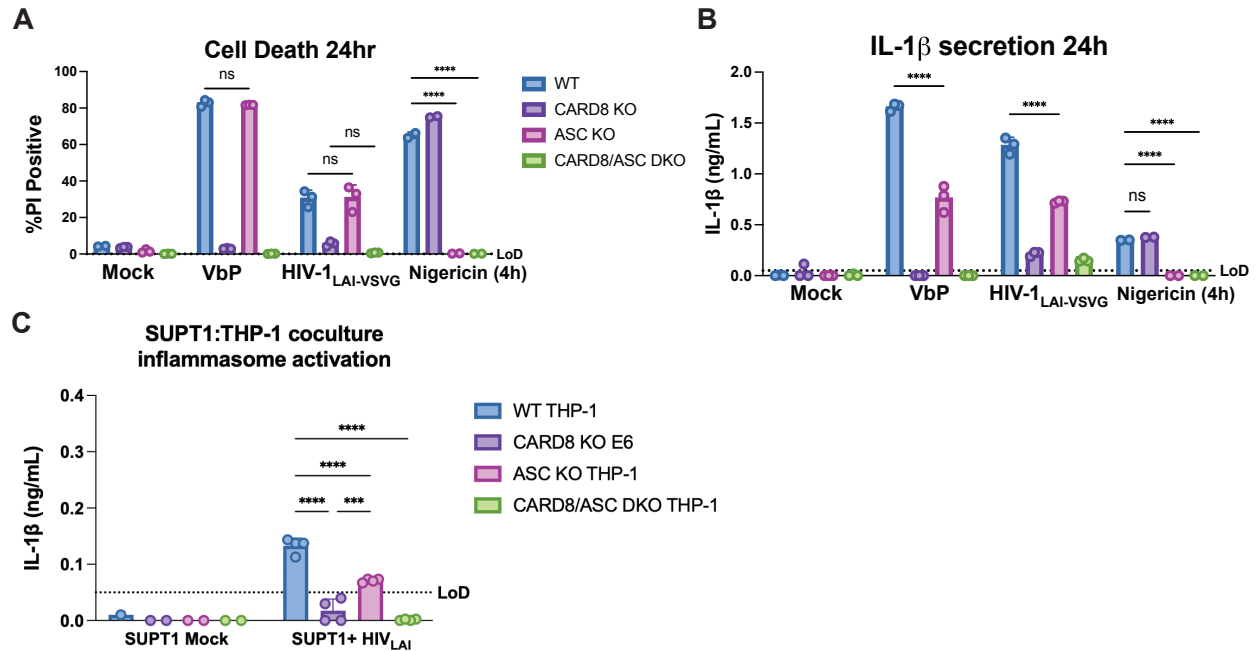


Fig. 3.3: CARD8-dependent activation from HIV-1 is mostly ASC-independent

(A) Wildtype (WT), CARD8 knockout (KO), ASC KO, or CARD8/ASC double knockout (DKO) THP-1 cells were primed with Pam3CSK4 then challenged either HIV-1_{LAI-VSVG} or treated with VbP (5 μ M) or nigericin (5 μ g/mL). Inflammasome activation was assessed after 24 hours for VbP treated and HIV-1_{LAI-VSVG} infected cells and after 4 hours for nigericin treated cells. Cell death is reported as percent of propidium iodide (PI) positive cells. (B) IL-1 β secretion was assessed from the supernatant using IL-1R reporter assay. (C) SUPT1 cells were infected for 24 hours prior to coculturing with target THP-1 cells. The coculture was harvested 48 hours later to probe for IL-1 β secretion in the coculture supernatant via IL-1R reporter assay. Wildtype (WT), CARD8 KO, ASC KO or CARD8/ASC double KO (DKO) THP-1 cells were cocultured with SUPT1 cells either mock-infected or infected with HIV-1_{LAI}. THP-1 cells were primed with Pam3CSK4 (500ng/mL) for 16 hours prior to coculture. SUPT1 cells were infected with HIV-1_{LAI} such that 20% of the cells were positive for intracellular p24^{gag} after 24 hours. Dotted line indicates limit of detection (LoD). Datasets represent mean \pm SD (A-B) (n=3 biological replicates) or (C) (n=4 biological replicates). p-Values were determined by two-way ANOVA with Tukey's (A&C) and Dunnett's (B) test using GraphPad Prism 10. ns = not significant, *p<0.05, **p<0.01, ***p<0.001, ****p<0.0001.

Protease inhibitor resistant strains of HIV-1 differentially cleave and activate CARD8

HIV-1^{PR} inhibitors prevent CARD8-dependent inflammasome activation; however, they also inhibit viral replication due to the essential role of HIV-1^{PR} in viral replication. To decouple CARD8 inflammasome activation from viral replication, we reasoned that naturally occurring HIV-1^{PR} mutants may affect CARD8 cleavage and activation while remaining replication competent. Thus, we assayed a clinically-derived panel of multi-protease inhibitor (PRI)-resistant infectious molecular clones of HIV-1, possessing 4-10 PRI-resistance mutations in HIV^{PR} and one compensatory HIV^{gag} mutation at the junction between nucleocapsid (NC) and p1 (**Table 3.1**) (207). This panel exhibits varying resistance to assorted protease inhibitors as previously determined (207) and summarized in **Table 3.1**.

Clone name	PRI-resistance mutations in HIV ^{PR}	HIV ^{gag} mutation	Fold resistance								
			NFV	FPV	SQV	IDV	ATV	LPV	TPV	DRV	
CA122805	10F, 33F, 43T, 46L, 54V, 82A, 84V, 90M	A431V (NC/p1)	64	62	>200	63	59	127	24	14	
CA96458	10F, 30N, 33F, 43T, 84V, 88D, 90M	A431V (NC/p1)	>200	20	>200	15	99	30	3.1	7.2	
CA96451	32I, 33F, 43T, 46I, 47V, 54M, 73S, 82A, 89V, 90M	A431V (NC/p1)	76	>200	12	88	88	>200	12	112	
CA20392-1	24I, 46L, 54V, 82A	A431V (NC/p1)	27	3.4	7.6	20	19	35	0.8	3.4	

Table 3.1: Protease inhibitor resistance mutations and fold resistance

Table shows the protease inhibitor (PRI) resistant clones assayed with corresponding mutations in HIV protease (HIV^{PR}) and HIV^{gag} along with fold resistance to clinically used protease inhibitors. The HIV^{gag} mutation is at the junction between nucleocapsid (NC) and p1. Fold resistance was previously determined in (207) by Monogram PhenoSenseTM assay. NFV- nelfinavir; FPV- fosamprenavir; SQV- saquinavir; IDV- indinavir; ATV- atazanir; LPV- lopinavir; TPV- tipranavir; DRV- darunavir. The consensus subtype B sequence can be found on the Stanford HIV Drug Resistance Database (HIVDB) (208).

To assess CARD8 cleavage, we co-expressed CARD8 with an N-terminal mCherry tag and either wildtype HIV-1_{LAI} or PRi-resistant HIV-1 proviruses. HIV-1_{LAI} protease cleaves CARD8 between phenylalanine (F) 59 and F60 (127), resulting in a ~33kDa product (**Figure 3.4A**). We identified two PRi-resistant clones, CA122805 and CA96458, that were markedly less efficient at cleaving CARD8 than HIV-1_{LAI}, and two PRi-resistant clones, CA96451 and CA20392-1, that cleave CARD8 more efficiently than HIV-1_{LAI} (**Figure 3.4A**). To assess inflammasome activation downstream of CARD8 cleavage in these PRi-resistant clones, we used HEK293T cells that endogenously express CARD8, but lack the entire inflammasome pathway. We reconstituted the inflammasome pathway into HEK293T cells by transfecting them with human caspase 1 and human IL-1 β and then challenged with either empty vector, HIV-1_{LAI} or the PRi-resistant proviruses. Consistent with the observed CARD8 cleavage by each HIV-1 strain, the clones CA122805 and CA96458, which exhibited less CARD8 cleavage than HIV-1_{LAI}, also induced less IL-1 β secretion than HIV-1_{LAI} (**Figure 3.4B**). Similarly, CA96451 and CA20392-1, which demonstrated enhanced CARD8 cleavage correspondingly elicited more IL-1 β secretion than HIV-1_{LAI} (**Figure 3.4B**). Thus, PRi-resistant HIV-1 clones differentially cleave and activate the CARD8 inflammasome, providing a powerful tool for future studies to establish the relative effects of CARD8 inflammasome activation on viral replication.

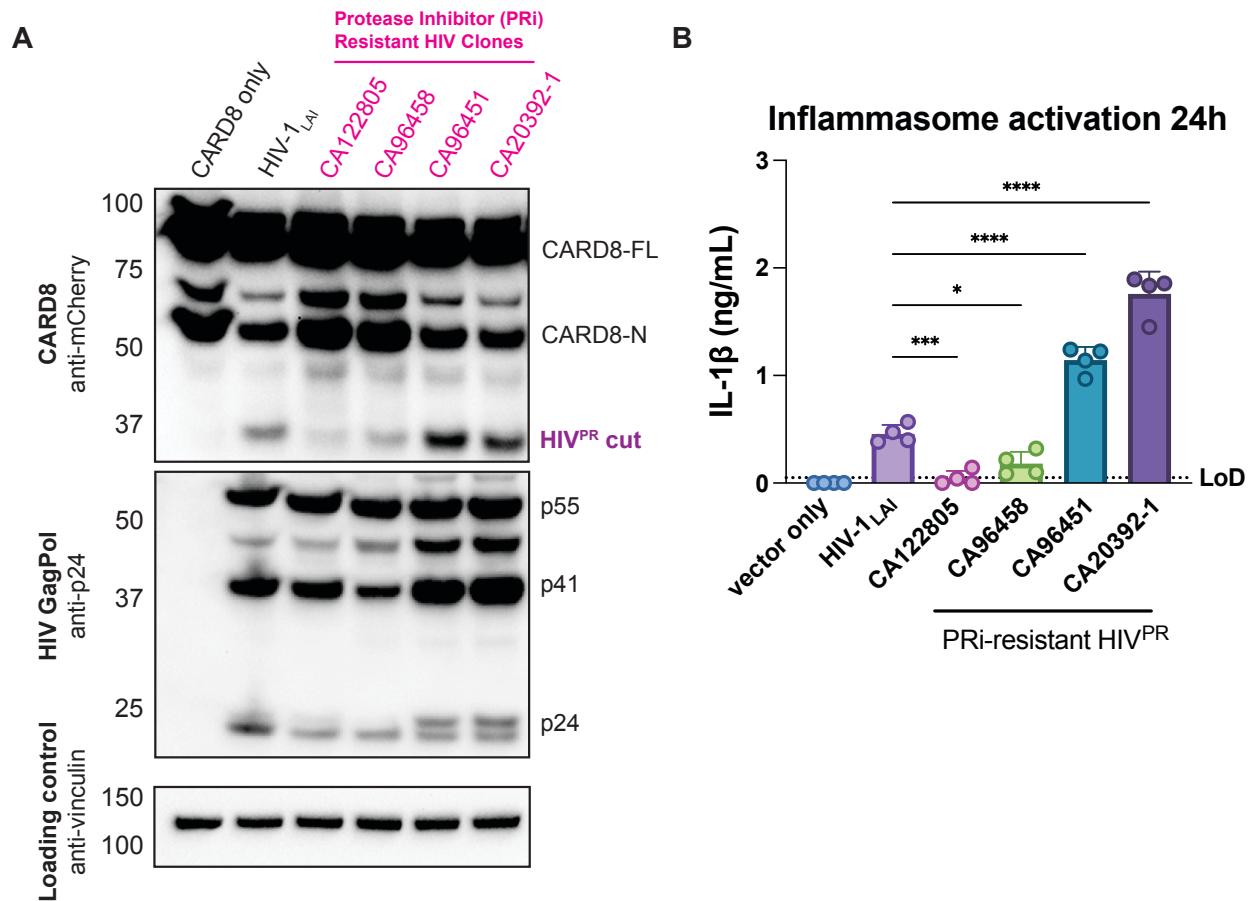


Fig. 3.4: Protease inhibitor resistant strains of HIV-1 differentially cleave and activate CARD8

(A) HEK293T cells were transfected with a construct encoding CARD8 with an N-terminal mCherry tag (mCherry-CARD8) and indicated HIV-1 proviral constructs. Protease inhibitor (PRi) resistant clones of HIV-1 are a subset of a panel expressing prototypical multidrug resistant HIV-1 protease (HIV^{PR}) in an NL4.3 backbone. Top: Immunoblotting using anti-mCherry antibody to detect mCherry-CARD8. The full-length (CARD8-FL) and FIIND-processed (CARD8-N) bands are indicated as well as the HIV^{PR} cleavage product. The band at ~45 kDa is the result of cleavage by the 20S proteasome. Bottom: Immunoblotting with an anti-p24^{gag} antibody showing HIV-1^{gag} cleavage products p41^{gag} and p24^{gag}, and/or full-length HIV-1^{gag}, p55^{gag}. (B) HEK293T cells were transfected with human caspase 1 and human IL-1β, and either carrier vector or indicated HIV-1 proviruses then probed for IL-1β secretion 24 hours post-transfection via IL-1R reporter assay. Dotted line indicates limit of detection (LoD). Datasets represent mean ± SD (n=4 biological replicates). p-Values were determined by two-way ANOVA with Dunnett's test using GraphPad Prism 10. ns = not significant, *p<0.05, **p<0.01, ***p<0.001, ****p<0.0001.

Protease inhibitor resistant clones exhibit variable protease activation efficiency for CARD8 cleavage but not altered specificity

We next investigated the molecular basis for the differential CARD8 activation capacity of PRi-resistant clones. PRi-resistant mutations in HIV^{PR} occur predominantly around the active site of HIV^{PR}, and thus, sometimes modify the proteolytic processing capacity of HIV^{PR}. To compensate for mutations in HIV^{PR} that change its substrate specificity, mutations in HIV^{gag} that permit proper polyprotein processing are selected for. Thus, since PRi-resistant HIV^{PR} exhibit differences in specificity for its own viral polyproteins, we next interrogated whether or not mutant HIV^{PRs} also display altered specificity for host proteins like CARD8.

Mutations at the P1' site of CARD8 immediately flanking the HIV^{PR} cleavage site can alter protease recognition such that an F60A mutation within CARD8 can abrogate HIV^{PR}'s ability to cleave and activate CARD8 (127,149). In addition, we previously demonstrated that HIV^{PR} cannot cleave and activate chimpanzee (cpz) CARD8 (149). Thus, to evaluate differences in CARD8 specificity, we examined whether or not PRi-resistant clones could cleave F60A and cpz CARD8 by co-expressing different CARD8 variants with either HIV-1_{LAI} or PRi-resistant clones. Like HIV_{LAI}, none of the PRi-resistant clones could cleave the F60A or cpz CARD8 variants (**Figure 3.5A**). Similarly, cleavage assays with F60L and F60S CARD8 variants also did not reveal any differences in altered specificity (data not shown). These data suggest that these PRi-resistant clones seem to not have altered specificity for CARD8 at the HIV^{PR} cleavage site though more comprehensive mutagenesis studies are necessary to strengthen this hypothesis.

As we did not see a notable difference in CARD8 cleavage specificity, we next assessed whether or not differential CARD8 activation between strains could be explained by variations in HIV^{PR} activity, which is activated upon HIV^{gagpol} dimerization. Certain nonnucleoside reverse

transcriptase inhibitors (NNRTIs) have been reported to enforce HIV^{gagpol} dimerization and artificially induce HIV^{PR} activation including efavirenz and rilpivirine (RPV) (152,209–211). Thus, we tested whether or not RPV treatment, which stimulates more HIV^{PR} activation, could rescue CARD8 activation in the PRi-resistant clones that were less efficient at cleaving CARD8, CA122805 and CA96458. We first assayed differential CARD8 cleavage by co-expressing an mCherry-CARD8 construct with either HIV-1_{LAI} or PRi-resistant clones identified in **Figure 3.4** then either treated with DMSO or RPV. With RPV treatment, we observed an enhancement in CARD8 cleavage to wildtype HIV-1_{LAI} levels in CA122805 and CA96458 which previously exhibited attenuated CARD8 cleavage (**Figure 3.5B**). If RPV treatment had been unable to rescue CARD8 cleavage in the mutant HIV^{PRs}, it may have implied that CA122805 and CA96458 have an inherent difference in specificity for CARD8. However, since RPV enhanced CARD8 cleavage in these mutant HIV^{PRs}, it demonstrates that CA122805 and CA96458 may have the capacity to recognize and cleave CARD8 with similar specificity to wildtype HIV-1_{LAI} and CA96451 and CA20392-1, as suggested in **Figure 3.5A**, but do not exhibit comparable CARD8 cleavage because they do not dimerize as efficiently *in vitro*.

We also assessed the effects of RPV-treatment on subsequent inflammasome activation in HIV-1_{LAI} and PRi-resistant clones using HEK293T cells reconstituted with functional inflammasome pathways as performed in **Figure 3.4B**. RPV treatment significantly enhanced inflammasome activation, as measured by IL-1 β secretion, with all tested HIV-1 proviruses (**Figure 3.5C**). However, CA122805 and CA96458, which display minimal inflammasome activation on their own, exhibited the most dramatic fold change in IL-1 β secretion upon RPV treatment, rescuing IL-1 β secretion to the same levels as the more efficient PRi-resistant clones, CA96451 and CA20392-1 (**Figure 3.5D**). These results suggest that differential CARD8 cleavage displayed by the PRi-resistant clones is due to the capacity for these proteases to dimerize and activate

rather than a difference in specificity for CARD8. However, even upon NNRTI treatment inflammasome activation of HIV-1_{LAI} and CA122805 is markedly lower than the NNRTI-treated CA96458, CA96451, and CA20392.1 HIV^{PR}s, indicating that there may still be uncharacterized alterations in HIV^{PR} specificity for CARD8 or additional variables that confer this differential activation (**Figure 3.5C**).

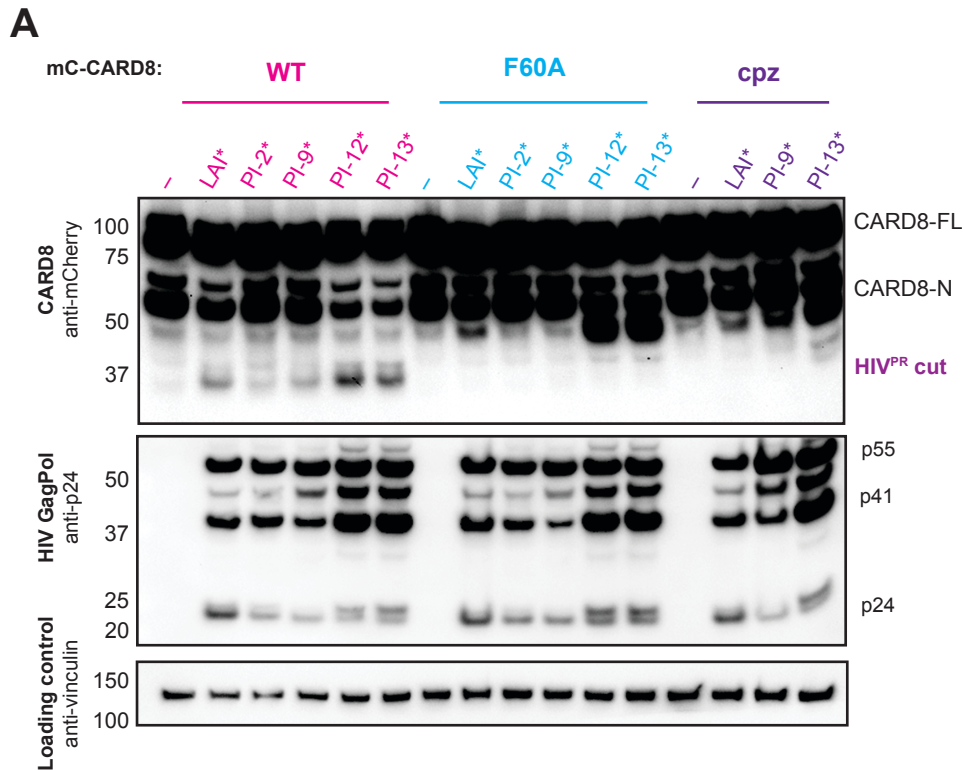


Fig 3.5: Protease inhibitor resistant clones exhibit variable protease activation efficiency
 (A) HEK293T cells were transfected with either wildtype human mCherry-CARD8 (mC-CARD8), human mC-CARD8 F60A, or mC-chimpanzee (cpz) CARD8 and indicated HIV-1 proviral constructs. Top: Immunoblotting using anti-mCherry antibody to detect mCherry-CARD8. The full-length (CARD8-FL) and FIIND-processed (CARD8-N) bands are indicated as well as the HIV^{PR} cleavage product. Bottom: Immunoblotting with an anti-p24^{gag} antibody showing HIV-1^{gag} cleavage products p41^{gag} and p24^{gag}, and/or full-length HIV-1^{gag}, p55^{gag}.

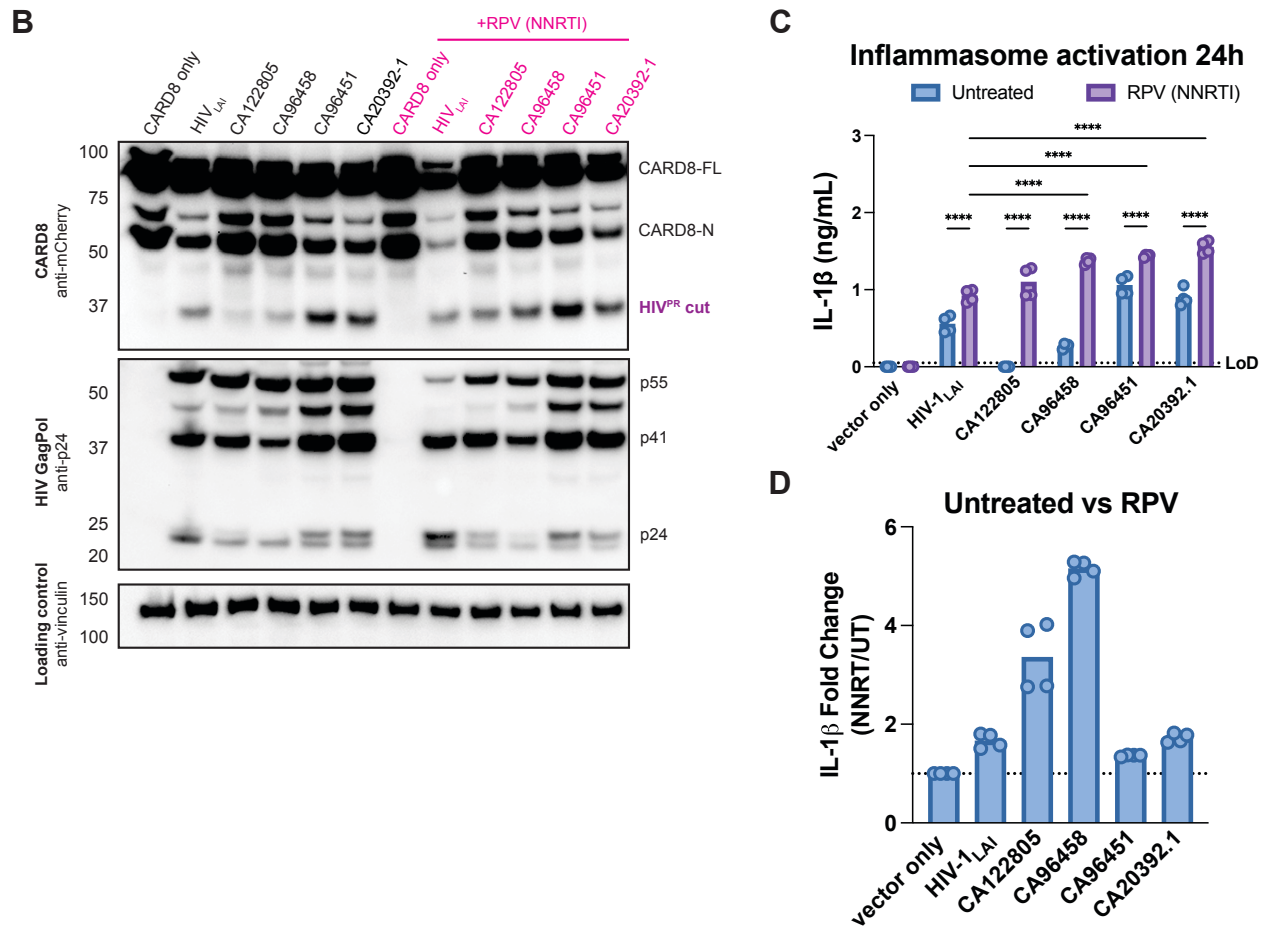


Fig 3.5: Protease inhibitor resistant clones exhibit variable protease activation efficiency (continued) (B) HEK293T cells were transfected and immunoblotted as in (A) with mCherry-CARD8 and indicated HIV-1 proviral constructs and either mock treated with DMSO or treated with the nonnucleoside reverse transcriptase inhibitor (NNRTI) rilpivirine (RPV) at 5 μ M 18 hours post-transfection. Lysates were harvested 6 hours after RPV was added. (C) HEK293T cells were transfected with human caspase 1 and human IL-1 β , and either carrier vector or indicated HIV-1 proviruses then treated with RPV as in (B) and probed for IL-1 β secretion 6 hours post-treatment via IL-1R reporter assay. Dotted line indicates limit of detection (LoD). Datasets represent mean \pm SD ($n=4$ biological replicates). p -Values were determined by two-way ANOVA with Tukey's test using GraphPad Prism 10. ns = not significant, * $p<0.05$, ** $p<0.01$, *** $p<0.001$, **** $p<0.0001$. (D) Relative fold change in IL-1 β secretion between untreated and RPV-treated conditions calculated from C. Dotted line indicates vector only control fold change.

DISCUSSION

While the mechanisms governing HIV-dependent CD4⁺ T cell depletion is extensively studied and debated, innate sensing of HIV-1 in other HIV-1 target cell types is less appreciated. We demonstrate that cell-to-cell transmission of HIV-1 to myeloid cells yields CARD8-dependent inflammasome activation via the HIV-1^{PR}. This activation occurs in a largely ASC-independent manner, suggesting that neither NLRP3 nor IFI16 are necessary for activation in these cell types despite being previously implicated as innate HIV sensors activators in CD4⁺ T cells (131,133). We postulate that under certain physiological conditions, cell-to-cell transmission can cause HIV^{PR} activation of the CARD8 inflammasome when sufficiently high HIV^{gagpol} concentrations are achieved during the influx of HIV^{PR} across the viral synapse. In addition, we identified protease inhibitor resistant strains of HIV-1 that differentially cleave and activate the CARD8 inflammasome. Using this resource, our data suggest that differential CARD8 sensing is incurred by a difference in the ability of HIV^{gagpol} to dimerize rather than an alteration in specificity for CARD8. Thus, HIV^{PR} mutants selected for their resistance to different inhibitors also affect their ability to cleave host proteins including the inflammasome-forming sensor CARD8.

T cell to macrophage cell-to-cell transmission and implications for HIV-1 pathogenesis

Two major hallmarks of HIV-1 pathogenesis are CD4⁺ T cell depletion and chronic immune activation, ultimately resulting in immune destruction and susceptibility to opportunistic infections. CD4⁺ T cell depletion is thought to be driven primarily by inflammasome-dependent pyroptosis of bystander resting CD4⁺ T cells facilitated by IFI16 and NLRP3 in lymphoid- and blood-derived CD4⁺ T cells, respectively (131,133). However, CARD8, which is expressed and functional in naïve and memory CD4⁺ and CD8⁺ T cells, has recently been implicated as a driver of resting CD4⁺ T cell depletion during HIV-1 infection in primary human blood- and lymphoid-derived CD4⁺ T cells and humanized mouse models (125,160). Chronic immune

activation, the other major source of HIV-1 pathogenesis, is primarily caused by microbial translocation induced by depletion of specialized Th17 CD4⁺ T cell subsets in the gut mucosa, resulting in circulating microbial ligands that can prime inflammasome responses (4,54). Here, we investigated the potential role of CARD8 inflammasome activation in contributing to HIV-dependent chronic immune activation in primary monocyte-derived macrophages.

Cell-free infection of macrophages is inefficient; thus, macrophages are thought to be primarily infected through phagocytosis of infected CD4⁺ T cells or cell-to-cell transmission (194,212,213). We demonstrate that unlike CD4⁺ T cells, which are rapidly depleted by HIV-1 infection and do not release pro-inflammatory IL-1 β or IL-18 (125), primary macrophages can sense and induce pro-inflammatory cytokine release in response to HIV^{PR} during cell-to-cell infection (**Figure 3.1C**), thus representing a potential source of sustained IL-1 β and subsequent chronic immune activation. In addition to promoting chronic immune activation, HIV-dependent IL-1 β release from macrophages may further contribute to HIV-1 pathogenesis by activating nearby CD4⁺ T cells, rendering them susceptible to becoming infected with HIV-1, and thus promoting CD4⁺ T cell depletion. Collectively with our prior work demonstrating that human CARD8 and not chimpanzee CARD8 has the unique propensity to respond to HIV^{PR}, our findings provide further evidence that CARD8 inflammasome activation may be a potential driver of HIV-1 pathogenesis.

Inflammasome activation from HIV-1 is largely ASC-independent

In prior work, both IFI16 and NLRP3 have been associated with promoting CD4⁺ T cell depletion via inflammasome-driven pyroptosis using lymphoid-derived and blood-derived CD4⁺ T cells, respectively (131,133). IFI16 has been reported to induce inflammasome activation upon sensing abortive HIV transcripts in the cytoplasm of CD4⁺ T cells (131). However, HIV-1 reverse transcription is now thought to occur largely in the capsid and completed in the nucleus,

rather the cytoplasm. Thus, IFI16 cytoplasmic sensing of HIV-1 transcripts is likely a low frequency event (27). Furthermore, IFI16 has been reported to not be an inflammasome-forming sensor (75), and instead a nuclear transcriptional regulator of antiviral genes including type I interferons and RIG-I (134,135). Here, we observed that HIV-dependent inflammasome activation in our myeloid cell infection models occurs largely independent of ASC-forming inflammasomes, including IFI16 and NLRP3. Instead, we find that IL-1 β release is dampened in ASC KO compared to WT THP-1 cells (**Figure 3.3**), suggesting a secondary amplification role for the NLRP3 inflammasome downstream of CARD8. NLRP3 is well known to be activated upon GSDMD pore formation (214,215), thus we reason that NLRP3 amplifies pro-inflammatory cytokine levels after CARD8-dependent pyroptosis induced by the HIV^{PR} (94). In addition, we noticed that *CARD8* KO THP-1 cells respond to the NLRP3 agonist nigericin more dramatically than WT THP-1 cells (**Figure 3.3A**), which is consistent with prior reports that CARD8 may negatively regulate NLRP3 or rather NLRP3 may guard the function of CARD8 (81,216) .

Protease inhibitor resistant mutants of HIV^{PR} may cleave CARD8 with different efficiencies than wildtype HIV^{PR}

RNA viruses have a remarkable capacity to adapt to selective pressures, including antiviral drugs. Here, we used HIV-1 strains that are resistant to multiple protease inhibitors and assessed the consequences of these adaptations on HIV^{gagpol} dimerization and CARD8 cleavage specificity. We demonstrate that PRI-resistance mutations in HIV^{PRs} can either enhance or diminish HIV^{gagpol} dimerization efficiency relative to WT HIV-1_{LAI} while maintaining similar specificity for CARD8 (**Figure 3.5**). To our knowledge, this is the first demonstration that HIV^{PR} mutants that arose in response to resistance to protease inhibitors also exhibit differences in cleavage activity towards a host protein.

Proper timing and order of HIV^{gag} and HIV^{gagpol} polyprotein processing by HIV^{PR} is crucial to achieve successful viral maturation (30). In addition, along with processing its own genome, HIV^{PR} has been reported to cleave host translation initiation factors to inhibit cap-dependent translation and coopt host translation machinery for IRES-mediated HIV-1 translation (217–220). Thus, variations in HIV^{gagpol} dimerization and subsequent HIV^{PR} activation could have significant impacts on viral replication. For example, hypoactive HIV^{PR} strains that cannot efficiently dimerize may evade innate detection of HIV^{PR} but may consequently exhibit inefficient viral maturation, irregular virion morphology (221), reduced viral infectivity (222,223) and viral protein production. Similarly, HIV^{PR} is also known to cleave regulators of other cell death pathways including Bcl-2 (224), procaspase 8 (225), and RIPK1 and RIPK2 (226) to modulate apoptosis and necroptosis (219,220,227). Thus, enhanced HIV^{gagpol} dimerization could be disadvantageous for HIV-1 by triggering CARD8-dependent pyroptosis or other cell death pathways and clearing HIV's replicative niche.

Ongoing work

Since there are no known inhibitors of the CARD8 inflammasome, a limitation of our study is the inference that cell-to-cell transmission of HIV-1 in MDMs was CARD8-dependent based on HIV^{PR} and CASP1 inhibitors but not reverse transcriptase or NLRP3 inhibitors abrogating inflammasome activation along with complementary data from *CARD8* and *ASC* genetic knockouts in THP-1 cells. However, genetic editing of MDMs to knockout *CARD8* and *ASC* (228) would offer further evidence that this cell-to-cell transmission within myeloid cells is CARD8-dependent. Similarly, we hope to further illustrate that cell-to-cell contact is necessary for CARD8-dependent activation by disrupting viral synapse formation via blocking antibodies, targeting actin-mediated adhesion molecules, including integrin LFA-1 and its cognate ligand ICAM-1 (129,188,229,230). In future studies, we plan to advance our coculture system to utilize CD4⁺ T cells as the viral producer line rather than SUPT1 cells and investigate subsequent

CARD8-dependent responses in both MDMs and tissue resident macrophages. Lastly, the PRi-resistant mutant strains identified in this study provide a unique opportunity to decouple viral replication from CARD8 inflammasome activation and establish whether or not CARD8 inflammasome activation restricts HIV-1 replication in future studies. Regardless of whether or not CARD8 inflammasome activation restricts HIV-1 at the cellular level, we posit that CARD8 sensing of HIV^{PR} in myeloid cells contributes to HIV-1 pathogenesis by promoting chronic immune activation.

METHODS

Plasmids and Reagents

pMD2.G used for HIV-1_{LAI-VSVG} production was a gift from Didier Trono (Addgene). HIV-1_{LAI} has been previously described (179). The following reagents were obtained through the NIH HIV Reagent Program, Division of AIDS, NIAID, NIH: rilpivirine (RPV), lopinavir (LPV), nevirapine (NVP), Human Immunodeficiency Virus 1 (HIV-1) NL4-3 BaL Infectious Molecular Clone (p20-36) (HIV-1_{NL4.3-BaL}), ARP-11442, contributed by Dr. Bruce Chesebro (231–234), and Panel of Multi-Protease Inhibitor Resistant Infectious Molecular Clones, HRP-12740, contributed by Dr. Robert Shafer (207). Mutant HIV^{PR} sequences were amplified from clinically-derived viral cDNA encoding protease genes with resistance to multiple PRIs then cloned into an NL4.3 backbone with overhangs including the 3' end of gag with the gag cleavage site and the 5' end of RT as previously described (207). CARD8 variant constructs were cloned as previously described (149). VX765 was sourced from Invivogen (cat: inh-vx765i-1).

Cell culture

SUPT1 (ATCC) and THP-1 cells (ATCC) were cultured in RPMI (Invitrogen) with 10% FBS, 1% penicillin/streptomycin antibiotics, 10 mM HEPES, 0.11 g/L sodium pyruvate, 4.5 g/L D-glucose and 1% Glutamax. Primary monocytes were cultured in RPMI (Invitrogen) with 10% FBS, and 1% penicillin/streptomycin antibiotics and differentiated in the presence of 20ng/mL GM-CSF (Peprotech cat: 300-03) and 10ng/mL M-CSF (Peprotech cat: 300-25). HEK293T (ATCC) lines were cultured in DMEM (Invitrogen) with 10% FBS and 1% penicillin/streptomycin antibiotics. All lines routinely tested negative for mycoplasma bacteria (Fred Hutch Specimen Processing & Research Cell Bank).

HIV-1_{LAI}, HIV-1_{LAI-VSVG}, and HIV-1_{NL4.3-BaL} production

293T cells were seeded at $2-3 \times 10^5$ cells/well in six-well plates the day before transfection using TransIT-LT1 reagent (Mirus Bio LLC) at 3 μ L transfection reagent/well as previously described (185). For HIV-1 production, 293Ts were transfected with 1 μ g/well HIV_{LAI} or HIV-1_{NL4.3-BaL} proviral DNA or 1 μ g/well HIV_{LAI} Δ env DNA and 500 ng/well pMD2.G for HIV-1_{LAI}, HIV-1_{NL4.3-BaL}, and HIV-1_{LAI-VSVG}, respectively. One day post-transfection, media was replaced. Two days post-transfection, viral supernatants were collected and filtered through a 20 μ m filter and aliquots were frozen at -80°C . HIV-1_{LAI} and HIV-1_{LAI-VSVG} proviruses were previously described (179,186,187).

Cell-free and cell-to-cell coculture HIV-1 infection

Cell-free infections with HIV-1_{LAI-VSVG} was done as previously described (149). Subsequent cell death was assessed by incubating in media containing propidium iodide dye, diluted 1:100, for 5 minutes at room temperature then washed once with PBS before fixing with BD CytoFix/Cytoperm (cat:BDB554714) for flow cytometry. In the HIV-1 cell-to-cell transmission system, SUPT1 cells were spinoculated at 1100g for 30min with either HIV-1_{LAI} or HIV-1_{NL4.3-BaL} in the presence of 20 μ g/mL DEAE-dextran. After 24 hours, mock or HIV-1 infected SUPT1 cells were washed three times in PBS such that DEAE-dextran and cell-free virus were washed away before starting coculture with THP-1 cells or MDMs. THP-1 cells and MDMs were seeded at 5×10^5 cells/well and primed with 500ng/mL Pam3CSK4 (Invivogen) for 16-24 hours before coculture. Mock or infected SUPT1 cells were seeded at 5×10^5 cells/well. Cultured supernatants from coculture were harvested for IL-1R reporter assay 48 hours after starting the coculture.

Transwell coculture HIV-1 infection

SUPT1 cells were spinoculated at 1100g for 30min with HIV-1_{LAI} in the presence of 20ug/mL DEAE-dextran. After 24 hours, mock or HIV-1 infected SUPT1 cells were washed 3 times in PBS and either mixed in a 24-well with THP-1 cells or placed in a transwell insert above target THP-1 cells at a concentration of 5×10^5 infected SUPT1 cells and 2.5×10^5 THP-1 cells per well. THP-1 cells were primed overnight with 500ng/mL Pam3CSK4 before starting coculture. The transwell insert has a $0.4\mu\text{m}$ membrane at the bottom of the well (ThinCert™ Tissue Culture Inserts, Sterile, Greiner Bio-One cat:665640), allowing virus to pass out of the transwell but not the infected cell. Reverse transcriptase activity in viral supernatants was measured using the RT activity assay as described (235,236). A stock of HIV-1_{LAI} virus was titered multiple times, aliquoted at -80°C and used as the standard curve in all assays.

Monocyte-derived macrophage isolation/differentiation

Primary monocytes were isolated via positive selection using the EasySep™ Human CD14 Positive Selection Kit II (Easy Sep, 1×10^9) (Stem Cell Technologies) according to the manufacturers protocols from PBMCs collected from healthy donors. Upon isolation, monocytes were seeded at 5×10^5 cell/well in 24-well plates and differentiated for 5 days in the presence of media containing 20ng/mL GM-CSF (Peprotech cat: 300-03) and 10ng/mL M-CSF (Peprotech cat: 300-25), refreshing media every other day.

IL-1R reporter assay

IL-1 β secretion was assayed using HEK-Blue-1 β reporter cells (Invivogen) as previously described (149). In brief, HEK-Blue-1 β reporter cells are engineered such that binding of IL-1 β to the surface receptor IL-1R1 results in the downstream activation of NF- κB and subsequent production of secreted embryonic alkaline phosphatase (SEAP) in a dose-dependent manner

(104). Culture supernatant from infected/treated cells was transferred to HEK-Blue 1 β reporter cells, and on the same plate, serial dilutions of recombinant human IL-1 β (Peprotech) were added to generate a standard curve for each assay. After overnight incubation, SEAP levels were assayed using QUANTI-Blue colorimetric substrate via absorbance at OD655.

ASC KO and CARD8/ASC DKO generation

ASC knockout (KO) and *CARD8/ASC* double KO (DKO) were generated similarly to *NLRP1* KO described in (104). *CARD8/ASC* DKO were made using previously generated *CARD8* KO cells as the parental line (149).

CARD8 cleavage assay

HEK293T cells were seeded at $1-1.5 \times 10^5$ cells/well in 24-well plates the day before transfection using TransIT-LT1 reagent at 1.5 μ L transfection reagent/well (Mirus Bio LLC). One hundred ng of indicated constructs encoding an N-terminal mCherry-tagged *CARD8* were co-transfected into HEK293T cells with empty vector ('-'), HIV_{LAI} or PRi-resistant provirus. To normalize HIV^{gag} expression between HIV-1_{LAI} and the PRi-resistant clones, which are in a different vector backbone, 400ng of HIV-1_{LAI} and 200ng of all PRi-resistant clones were transfected. All conditions were normalized with empty vector to contain the same amount of DNA. Cytoplasmic lysates were harvested 24 hr post-transfection and immunoblotted as previously described (149). For cleavage blots with NNRTI treatment, NNRTI was added 18 hours post-transfection and then harvested at 24 hours post-transfection or 6 hours post-NNRTI treatment.

HEK reconstitution assay

HEK293T cells, which endogenously express CARD8, were seeded at 2.25×10^5 cell/well in 24-well plates the day before transfection using TransIT-LT1 reagent at 1.5uL transfection reagent/well (Mirus Bio LLC). Functional inflammasomes were reconstituted by transfecting in 5ng human CASP1 and 100ng human IL-1 β . To assess the effects of different viral proteases on inflammasome activation, HIV-1_{LAI} or PRi-resistant clones were co-transfected in with CASP1 and IL-1 β . As with the CARD8 cleavage assay, a higher amount of 250ng HIV-1_{LAI} was added relative to the PRi-resistant clones, which were all added at 125ng, to normalize HIV^{gag} expression between the different vector backbones. All conditions were normalized with empty vector to contain the same amount of DNA. Cultured supernatant was harvested 24 hours post-transfection to assay for IL-1 β secretion via IL-1R reporter assay. The NNRTI-treated HEK293T reconstitution experiment was treated as described above in the CARD8 cleavage assay.

CHAPTER 4: CONCLUSIONS, PERSPECTIVES, AND FUTURE DIRECTIONS

SUMMARY

In this thesis, I demonstrate that human CARD8, but not chimpanzee CARD8, can sense a range of lentiviral proteases including HIV-1 protease (HIV^{PR}). Additionally, I identified various mutant HIV^{PRs}, selected for resistance to protease inhibitors, that can differentially cleave and activate the CARD8 inflammasome. CARD8 inflammasome activation during acute HIV-1 infection in myeloid cells results in pyroptotic cell death and release of pro-inflammatory cytokines. My work suggests a model whereby human-specific sensing of HIV^{PR} by CARD8 and subsequent inflammatory activation in myeloid cells may contribute to HIV-1 pathogenesis by promoting chronic immune activation. Here, I speculate on the implications and potential applications of CARD8-dependent sensing of HIV^{PR} along with possible areas that warrant further investigation and possible experiments.

CARD8 SENSING OF INCOMING HIV PROTEASE

The majority of the literature characterizing HIV^{PR} function focuses on its vital role in proteolytic processing of HIV^{gag} and HIV^{gagpol} during viral maturation in the final stage of viral replication. Proper spatiotemporal proteolytic processing of HIV^{gagpol} by HIV^{PR} is crucial to producing mature infectious virions such that incomplete processing results in defective capsid formation and unprocessed HIV^{gag} intermediates, which can trans-dominantly inhibit viral infectivity (237,238). HIV^{PR} activation requires HIV^{gagpol} dimerization to form its active site, and the resulting HIV^{PR} dimers are highly stable (239–241). Nascent virions consist of approximately 2400 HIV^{gag} molecules and 120 HIV^{gagpol} molecules (30). Thus, since HIV^{PR} requires two HIV^{gagpol} molecules, there are only about 60 functional units of HIV^{PR} dimers in the virion, which limits but does not eliminate the possibility of delivery of active HIV^{PR} dimers into the host cytosol following viral fusion, which I refer to as “incoming” HIV^{PR}. However, early HIV^{PR} characterization studies

report conflicting conclusions on the potential activity and effects of incoming HIV^{PR} dimers (242–246). In this work, I establish that CARD8 can sense incoming HIV^{PR} during acute HIV-1 infection, providing some of the first direct evidence of cytosolic active incoming HIV^{PR}.

In addition to incoming HIV^{PR} activity, the localization of HIV^{PR} after viral maturation is also enigmatic. The HIV capsid core, formed during viral maturation, consists of the RNA genome associated with nucleocapsid and viral enzymes including reverse transcriptase and integrase. In illustrations of HIV replication, HIV^{PR} is typically depicted either as within the matrix shell but excluded from the capsid core or completely omitted from mature virion illustrations (238,247,248); however, to my knowledge, HIV^{PR} localization after viral maturation has never experimentally been shown. Since HIV capsid uncoating occurs primarily in the nucleus and I observed CARD8 sensing of incoming HIV^{PR} in the cytosol, active HIV^{PR} dimers are likely localized outside the capsid and can be immediately sensed upon viral fusion and entry. However, it is also possible that some active HIV^{PR} is also included in the HIV capsid core. To test this, I reasoned that destabilizing the capsid with the capsid inhibitor lenacapavir would expose the contents of the capsid to innate proteins in the cytosol including CARD8. Thus, if there was active HIV^{PR} in the core, I would observe enhanced CARD8-dependent inflammasome activation in lenacapavir-treated cells at early timepoints of HIV infection. In unpublished preliminary work, I did not observe enhanced CARD8 activation upon lenacapavir treatment (data not shown), suggesting that incoming HIV^{PR} dimers are excluded from the HIV capsid which is consistent with the fact that there are no reported host targets of HIV^{PR} in the nucleus. Similarly, future studies leveraging HIV strains with destabilizing capsid mutations (249–251) could provide further evidence of HIV^{PR} presence or absence from the HIV capsid core.

CARD8 SENSING OF DE NOVO SYNTHESIZED HIV PROTEASE

HIV^{PR} proteolytic processing is canonically thought to occur only during viral maturation after viral egress; however, some studies report HIV^{gag} processing in cytoplasmic lysates of HIV-1 infected cells and recent studies using highly sensitive technology, including nanoscale flow cytometry and instant structured illumination microscopy, have indicated that HIV^{PR} activation occurs within infected cells before viral budding (32,37). Though these studies suggest the presence of cytosolic active HIV^{PR}, it is unclear if cytoplasmic HIV^{PR} exists in only its precursor form or in both its precursor and mature form. The immature precursor HIV^{PR} embedded within HIV^{gagpol} is activated in *cis* and accomplishes the initial cleavage events of HIV^{gag} and HIV^{gagpol} processing when high HIV^{gagpol} concentrations are achieved to allow for dimerization. Eventually, the HIV^{gagpol} polyprotein is rapidly processed in *trans* to free the mature HIV^{PR} dimer. In this work, I report that CARD8 senses active cytoplasmic HIV^{PR} originating from both incoming and *de novo* synthesized HIV^{PR} early and late in viral replication. While the incoming HIV^{PR} is already in its mature form, it is not known whether the *de novo* translated HIV^{PR} sensed by CARD8 is in its immature precursor form or if both forms are present in the cytosol.

Despite having identical amino acid sequences, precursor and mature HIV^{PR} exhibit differential proteolytic function, hypothesized to be driven by allosteric regulations (252). My findings regarding CARD8 sensing of incoming HIV^{PR} indicate that the mature form of HIV^{PR} has the capacity to cleave and activate CARD8, but precursor HIV^{PR} has a more limited cleavage capacity relative to mature HIV^{PR} such that precursor HIV^{PR} can efficiently cleave only four of the ten HIV^{gagpol} proteolytic processing sites (253,254). Thus, the reduced proteolytic activity exhibited in precursor HIV^{PR} may extend beyond the viral polyprotein such that precursor HIV^{PR} also demonstrates altered cleavage function toward host proteins including CARD8. Despite hundreds of available crystal structures of mature HIV^{PR} in complex with many different protease inhibitors, much less is known about the structure and substrate specificity of

precursor HIV^{PR} due to its poor solubility and structural heterogeneity. To evaluate whether or not precursor HIV^{PR} is able to cleave CARD8, I could co-transfect HEK293T cells with mCherry-CARD8 and a mutant HIV construct that locks HIV^{PR} into its precursor state by preventing HIV^{PR} processing (32) and assess subsequent CARD8 cleavage by western blot.

An orthogonal approach to determine whether or not CARD8 senses the precursor and/or mature *de novo* synthesized HIV^{PR} during infection is to utilize selective protease inhibitors targeting either precursor or mature HIV^{PR}. Multiple groups have reported that precursor HIV^{PR} is significantly less sensitive to catalytic site protease inhibitors than mature HIV^{PR} and may contribute to protease inhibitor resistance (35,255–259). Thus, high-throughput compound screening identified protease inhibitors that inhibit both precursor and mature HIV^{PR} along with protease inhibitors that selectively inhibit the mature but not the precursor form of HIV^{PR} (260). Since the mature HIV^{PR} is a product of processed precursor HIV^{PR}, there are no inhibitors that can selectively inhibit the precursor HIV^{PR} without also inhibiting mature HIV^{PR}. Thus, I could leverage the protease inhibitors that selectively inhibit mature HIV^{PR} and assess if HIV-dependent CARD8 inflammasome activation persists in the presence of these inhibitors (256,260,261). If inflammasome activation is abrogated by treatment with a mature HIV^{PR} inhibitor, it would suggest that cytoplasmic precursor HIV^{PR} is unable to cleave CARD8, but there is cytoplasmic mature HIV^{PR}, which CARD8 can sense. In contrast, if inflammasome activation persists in the presence of the mature HIV^{PR} inhibitor to the same level as untreated conditions, it would suggest that there is no mature cytoplasmic HIV^{PR} and CARD8 exclusively senses precursor HIV^{PR}. Reduced levels of inflammasome activation upon selective mature HIV^{PR} inhibitor treatment would indicate that both precursor and mature HIV^{PR} are present and active in the cytosol and both forms can contribute to CARD8 activation during acute HIV-1 infection. Therefore, these follow-up studies could elucidate not only additional viral

determinants of CARD8 activation but also clarify an unclear aspect of HIV^{PR} dynamics during HIV-1 replication.

DIFFERENTIAL CLEAVAGE OF OTHER HOST TARGETS OF HIV PROTEASE

In addition to cleaving CARD8, there is increasing evidence that HIV^{PR} modulates other host proteins during viral replication. One class of host proteins implicated as targets of HIV^{PR} are proteins involved in host translation initiation and regulation including eIF4D, eIF4G, PABP, and GCN2 such that cleavage of these host factors shut down host translation and may assist in viral protein translation (217,219,262,263). Similarly, HIV^{PR} is also known to cleave regulators of other programmed cell death pathways including Bcl-2 (224), procaspase 8 (225), and RIPK1 and RIPK2 (226), which control apoptosis and necroptosis (219,220,227). In addition, HIV^{PR} has also been reported to cleave virion-associated host antiviral proteins incorporated into nascent virions. These host antiviral proteins include a unique splice variant of cytidine deaminase APOBEC3H known as A3H haplotype II SV200 (264), which hypermutates the viral genome, and the m⁶A RNA modification reader YTHDF3 (265), which detects m⁶A modifications that are abundant on HIV RNA. These additional host targets suggest that HIV^{PR} may possess functions other than viral maturation to facilitate viral replication.

In Chapter 3, I identified various mutant HIV^{PRs} that could differentially cleave and activate CARD8. Preliminary follow-up studies characterizing the mechanism responsible for these differences suggest that there is no obvious difference in the specificity of these mutant HIV^{PRs} for CARD8 at the HIV^{PR} cleavage site, but rather differences are conferred by its capacity to dimerize and activate HIV^{PR} (**Figure 3.4, 3.5**). However, I tested only a small number of CARD8 variants for differential cleavage by the mutant HIV^{PRs}. Thus, I could more thoroughly assess the specificity of the mutant HIV^{PRs} by screening peptide libraries fused to a fluorescently quenched reporter that is activated upon proteolytic cleavage (266). Additionally, I would also be interested

in assessing whether or not mutant HIV^{PRs} also exhibit differential cleavage of known host cell protein targets of HIV^{PR} other than CARD8 with a particular focus on those involved in cell death pathways. For example, I could assess differential HIV^{PR}-mediated cleavage of Bcl-2 or procaspase 8, which both induce apoptosis, with mutant strains that were hypo- or hyperactive for cleaving CARD8 using the HEK293T cell overexpression and western blot pipeline I optimized for evaluating CARD8 cleavage by SIV/HIV^{PR} (**Figure 2.1B-C**). If the mutant HIV^{PRs} exhibit similar preferences for Bcl-2 and procaspase 8 as CARD8, it would provide further evidence that the mutant HIV^{PRs} have similar substrate specificity and that differences are instead rendered by its ability to activate HIV^{PR}. However, if the mutant HIV^{PRs} preferences for Bcl-2 and procaspase 8 do not phenocopy its CARD8 preferences, it could suggest a difference in substrate specificity between mutant HIV^{PRs} and could inform future CARD8 mutagenesis studies.

Interestingly, altered mutant HIV^{PR} substrate preference for Bcl-2 and procaspase 8 relative to CARD8 could also hint at an innate host failsafe for sensing HIV-1 infection via HIV^{PR} such that HIV^{PR} specificity could skew an infected cell toward either pyroptosis or apoptosis. For example, mutant HIV^{PRs} that exhibit reduced cleavage for CARD8 may exhibit increased cleavage for other host cell targets like Bcl-2 or procaspase 8 to induce apoptosis instead. Since both pyroptosis and apoptosis result in removal of HIV's replicative niche, it suggests that programmed cell death is antiviral. However, further studies assessing relative viral load in cells that can or cannot readily undergo pyroptosis and/or apoptosis (i.e., GSDMD KO or caspase 1 KO to inhibit pyroptosis and caspase 3 KO to inhibit apoptosis) are necessary to strengthen that hypothesis. Taken together, these musings and speculations highlight the largely underappreciated but potentially pivotal role of HIV^{PR} may play in host regulation during HIV-1 infection.

EFFECTS OF TISSUE MICROENVIRONMENT ON CARD8 ACTIVATION

There have been conflicting reports in the literature as to whether or not CD4⁺ T cells can pyroptose and induce IL-1 β secretion in response to HIV-1 infection. Blood-derived resting CD4⁺ T cells infected with HIV-1 seem resistant to pyroptosis (132) whereas lymphoid-derived resting CD4⁺ T cells readily undergo pyroptosis (128). Some of this discrepancy may be due to differences in cytokine exposure in blood-derived versus lymphoid-derived cells. Cytokines can drastically alter the gene expression profile of a cell. For example, exposure to interferon can upregulate hundreds of antiviral genes and transcriptionally reprogram the cell into an antiviral state. Similarly, transcriptional 'priming' is a known prerequisite for inflammasome activation, inducing the expression of IL-1 β and/or inflammasome components before challenge with an inflammasome activator. Indeed, in Chapter 2, I demonstrate that toll-like receptor (TLR) priming of target myeloid cells is essential to elicit IL-1 β release in response to CARD8 inflammasome activation by HIV^{PR} and Val-boroPro, a known CARD8 agonist (**Figure 2.4B**). In addition, in Chapter 3, I observed inflammasome activation, as measured by IL-1 β secretion, upon cell-to-cell transmission of HIV-1 from SUPT1 T cell lymphoma cells to primary blood monocyte-derived macrophages when the macrophages were TLR-primed (**Figure 3.1C**).

Given the importance of cytokines in defining innate responses, I would be intrigued to explore the importance of cellular microenvironments in altering CARD8 responses when using CD4⁺ T cells and macrophages from different cellular compartments. To test this, I could assess CARD8 activation in cell-to-cell transmission cocultures using either blood- or lymphoid-derived CD4⁺ T cells as the viral producer line and either monocyte-derived or tissue-resident macrophages as the target cells. When used as the viral producer line, I would anticipate that blood- and lymphoid- derived CD4⁺ T cells should behave similar to one another, unless the cytokine cues of the tissue microenvironment alter the cell's ability to form a viral synapse to deliver virions

into the target cell. In contrast, monocyte-derived macrophages and tissue resident macrophages may vary widely in propensity to activate and elicit inflammatory cytokines. In fact, macrophages are so heavily influenced by tissue microenvironment that I would anticipate that tissue-resident macrophages originating from different organs, including Kupffer cells in the liver, alveolar macrophages in the lungs, and macrophages localized at mucosal barriers like the vagina, urethra, and intestine, would likely exhibit differential responses to cell-to-cell transmission of HIV. In this way, macrophages from the blood and tissues may differentially contribute to HIV-associated chronic inflammation and immune activation.

CARD8 INFLAMMASOME ACTIVATION AS A DRIVER OF HIV-1 PATHOGENESIS

Although SIVcpz infection of chimpanzees causes AIDS-like immunopathogenesis (59), HIV-1 infection of humans is markedly more pathogenic and inflammatory than SIVcpz-infected chimpanzees. In this work, I posit that this differential pathogenesis is driven by CARD8 sensing of HIV^{PR}, conferred by the human-specific FF motif within CARD8. I demonstrate that CARD8 inflammasome activation readily occurs in HIV-1 infected myeloid cells upon both cell-free and cell-to-cell infection. In Chapter 3, I propose multiple mechanisms by which CARD8 inflammasome activation in myeloid cells may be contributing to HIV-1 pathogenesis. To recap, HIV-dependent CARD8 inflammasome activation induces pro-inflammatory cytokine release in myeloid cells, which may promote chronic immune activation. Additionally, these pro-inflammatory cytokines may activate nearby CD4⁺ T cells, rendering them susceptible to HIV-1 infection and thus may also contribute to viral dissemination.

Since the entirety of this work was accomplished in *in vitro* systems of infection, *in vivo* animal studies are necessary to provide more concrete evidence of CARD8-dependent HIV pathogenesis. Indeed, recent work using humanized mouse models suggests that CARD8 activation drives CD4⁺ T cell depletion (160). Non-human primate studies demonstrating

CARD8-driven HIV pathogenesis could be pivotal to bolstering interest in leveraging HIV-dependent CARD8 activation for developing novel HIV therapeutics. However, currently, there are no known selective CARD8 inflammasome inhibitors or potent selective CARD8 activators, which may make designing non-human primate studies challenging. In addition to animal models, data mining early clinical outcomes and inflammatory biomarkers from people living with HIV (PLWH) harboring protease inhibitor resistant strains of HIV^{PRs} that differentially activate CARD8 may also provide insights into the pathogenic potential of HIV-dependent CARD8 inflammasome activation. For example, given the model for CARD8-driven pathogenesis, I would anticipate that PLWH harboring HIV^{PRs} with hyperactivity toward CARD8 would present with enhanced chronic immune activation as measured by elevated serum pro-inflammatory cytokines and other inflammatory cytokines. Conversely, I might expect that PLWH harboring HIV^{PRs} with hypoactivity toward CARD8 would have reduced chronic immune activation relative to the hyperactive HIV^{PRs}.

EXPLORING OTHER NON-HUMAN PRIMATE CARD8

In this work, I characterize human and chimpanzee CARD8 responsiveness to HIV/SIV^{PR} and speculate on potential consequences of this activation on HIV-1 and SIVcpz pathogenesis. However, other non-human primates that exhibit both pathogenic and nonpathogenic SIV infection also express CARD8 in varying degrees. Thus, I would be interested in determining whether or not the proposed model of CARD8 activation driving pathogenesis may extend to nonpathogenic and pathogenic SIV infections. SIVagm and SIVsmm infection of African green monkeys and sooty mangabeys, respectively, are the best studied examples of SIVs that yield nonpathogenic infection in their natural host despite reaching high viral loads. Therefore, future characterization of CARD8 variants from African green monkeys and sooty mangabeys are of particular interest in characterizing the potential role of CARD8 activation or suppression in allowing for tolerance of SIV infection. Similarly, rhesus macaques develop pathogenic SIV

infection, characterized by CD4+ T cell depletion, high viremia, and progression to AIDS-like immunopathology (267–270). Thus, assessing rhesus macaque CARD8 activation to SIV infection could provide further insights into CARD8 sensing's pathogenetic potential.

Multiple non-human primates, including rhesus macaques, sooty mangabeys, and African green monkeys possess CARD8 gene duplications with various truncations and indels that remain to be fully characterized. However, at the time of writing this dissertation, a new published study reported that one copy of rhesus CARD8 can induce inflammasome activation in response to HIV/SIV^{PR} while the other copy possesses a large N-terminal truncation that ablates FIIND auto-processing, which is necessary for oligomerization, and thus cannot form an inflammasome (160). As rhesus macaques exhibit pathogenic SIV infection, the finding that rhesus CARD8 can sense and activate in response to HIV/SIV^{PR} is consistent with the hypothesis that CARD8 inflammasome activation promotes HIV/SIV pathogenesis. Similarly, while the N-terminus could be cleaved by HIV/SIV^{PR}, African green monkey and sooty mangabey CARD8 could not form an inflammasome due to deletions or large truncations in the C-terminal CARD necessary for caspase 1 recruitment, once more consistent with CARD8 activation mediating SIV pathogenesis. Additionally, chimeras fusing the nonpathogenic sooty mangabey or African green monkey N-terminus with the functional rhesus CARD8 C-terminal CARD was sufficient to rescue inflammasome activation *in vitro*, suggesting that sooty mangabeys and African green monkeys evolved away from possessing a functional CARD8 inflammasome (160). Taken together, these findings are consistent with the working model that CARD8 inflammasome activation is a driving factor in conferring inflammatory pathogenesis in HIV and SIV infections.

Despite this latest evidence of CARD8-dependent pathogenesis, non-human primate *in vivo* studies inhibiting HIV/SIV-dependent CARD8 inflammasome activation are necessary to draw stronger conclusions about the pathogenic implications of CARD8 activation. Additionally,

though microbial translocation and immune activation can be recapitulated in African green monkeys during acute SIV_{agm} infection when the gut mucosa is chemically damaged by dextran sulfate sodium, AIDS-like immunopathology has never been recapitulated in non-pathogenic hosts (65). Thus, since the sooty/rhesus and African green monkey/rhesus chimeras were sufficient to confer HIV/SIV-dependent CARD8 activation *in vitro*, it would be interesting to test whether or not genetically engineered expression of rhesus CARD8 or Old World monkey/rhesus chimeras in an SIV-infected but nonpathogenic host like African green monkeys or sooty mangabeys can also confer AIDS-like immunopathogenesis.

Recently, owl monkeys, which are New World monkeys, have garnered interest in potentially being an alternative non-human primate animal model for pathogenic SIV/HIV infection (271,272). CARD8 variants from neither prosimians nor New World monkeys like owl monkeys have been characterized for capacity to form inflammasomes or respond to lentiviral proteases. Thus, if CARD8 activation is necessary for conferring HIV/SIV pathogenesis, characterizing whether or not owl monkey CARD8 exhibits HIV/SIV-dependent inflammasome activation like humans could provide further evidence in favor of or against using owl monkeys as an alternative HIV/SIV animal model.

THE ORIGINS OF CARD8 INFLAMMASOME ACTIVATION BY HIV-1 PROTEASE

Since the FF motif at the HIV^{PR} cleavage site in CARD8 is conserved across all humans and Neanderthals but not chimpanzees, there was likely a selective sweep in favor for F60 before the species divergence between Neanderthals and *Homo sapiens* but after divergence of humans and chimpanzees (between approximately 800,000 and 7 million years ago) (273). As HIV only arose in the past hundred years (48), it is too young of a virus to have driven evolution of the HIV^{PR} cleavage site in human CARD8. Nonetheless, despite conservation at position 60, human CARD8 is highly polymorphic, and multiple residues within the N-terminal tripwire of

CARD8, including those that allow CARD8 sensing of extant human pathogenic viruses like coronaviruses and picornaviruses, show strong evidence of positive selection, an evolutionary signature consistent with a history of host-pathogen conflict (121,136). In fact, the HIV^{PR} cleavage site in CARD8 overlaps with a site that is cleaved by the coronavirus 3CL protease, and a single amino acid polymorphism around this site is sufficient to switch the host specificity from sensing coronavirus to preferentially sensing picornavirus instead. These seemingly minor alterations conferring drastic changes in host sensing specificity highlights the plasticity and capacity of the N-terminus CARD8 to harbor a wide range of viral protease or general pathogen effector substrates (121). Although it is possible that the human-specific F60 was fixed stochastically or as a passenger mutation, I favor a scenario in which human CARD8 sensing of HIV^{PR} arose as a consequence of CARD8 adaptation to an ancient virus such that F60 rendered humans more fit for survival (121,124).

First reported as an inflammasome-forming sensor in 2018, CARD8 is a relatively newly discovered inflammasome and thus, the breadth of its activators is incomplete. Further characterization of the pathogens CARD8 can sense within its N-terminal tripwire may reveal the pathogen or its modern descendant that drove the selective sweep for the FF motif in CARD8. Though CARD8 has been reported to sense only viral proteases thus far, it is possible that CARD8 can also detect other pathogen effectors like bacterial or fungal toxins. To identify additional CARD8 activators to follow-up on, one could develop a library of human pathogenic effector proteins to conduct a high-throughput screen for capacity to activate CARD8. This could provide a powerful unbiased approach to identify novel CARD8 agonists and with some modifications, potentially classify other inflammasome agonists. Alternatively, as many computational tools exist for predicting protease-specific target substrate, including PoPS (274), SitePrediction (275), PROSPERous (276), and Procleave (277), one could consider a computational approach and utilize these protease cleavage site algorithms to predict other viral

proteases that may cleave CARD8 to help guide future hypothesis-driven experimental studies in the wet lab (278). Whether it be through high-throughput or individual studies, I anticipate that more CARD8 inflammasome agonists will be identified in the years to come and perhaps hint at the pathogenic effector, or effector family if the actual pathogen no longer exists in our modern world, that drove the FF motif in CARD8.

CARD8 ACTIVATION FOR HIV CURE

Though combination antiretroviral (cART) therapy can control HIV replication and disease progression, there is no absolute cure for HIV infection. The primary barrier to HIV cure is the presence of a latent HIV reservoir persisting in long-lived memory CD4+ T cells (7,9,279), introduced during integration into the host genome in the course of initial viral replication. These latently infected cells often remain dormant and hidden from the immune system but can become reactivated upon encountering its cognate antigen (280,281) or through other mechanisms, resulting in productive HIV infection and infectious virion release in a process known as viral rebound (282). Thus, people living with HIV (PLWH) must remain on cART indefinitely to prevent disease progression associated with viral rebound.

One strategy proposed to clear the latent reservoir is known as “shock and kill” whereby a latency reversal agent (LRA) is administered to “shock” the provirus out of latency to reveal to the host immune system which cells are harboring HIV then “killed” presumably through immune-mediated clearance mechanisms. Currently, most kill approaches involve targeting HIV-infected cells through delivery of an extrinsic executioner like engineered CAR-T cells or broadly neutralizing antibodies. However, application of CARD8-dependent inflammasome activation by HIV^{PR} may provide an intriguing intrinsic “kill” strategy for shock and kill that does not require recognition of a HIV-specific epitope on the cell surface.

Indeed, by facilitating intracellular HIV^{PR} activation through artificial HIV^{gagpol} dimerization, non-nucleoside reverse transcriptase inhibitors (NNRTIs) treatment at high concentrations can induce pyroptotic lytic cell death in HIV-infected cells in a CARD8-dependent manner (127,153). Follow-up studies revealed that the NNRTI concentration required for NNRTI-induced cell killing could be lowered to more physiologically relevant concentrations similar to those measured in plasma of PLWH on cART if cells were first sensitized to CARD8 inflammasome activation with Valbora-Pro (VbP), a known CARD8 agonist. In this way, researchers demonstrated improved clearance of latently infected CD4+ T cells isolated from PLWH through co-treatment with VbP and NNRTIs relative to NNRTIs alone (142). As a result of these promising results, industry researchers at Merck & Co. conducted studies to identify and develop new NNRTIs that dimerize HIV^{gagpol} more efficiently to further enhance CARD8-dependent killing of HIV-1-infected cells, highlighting the importance of basic science research in providing a basis for translational solutions to disease (141).

Similarly, as VbP can activate both the NLRP1 and CARD8 inflammasome in certain cell types, selectively CARD8-specific activators should be assessed for sensitization to NNRTI-induced killing to avoid off-target effects. Recently, CQ31 was identified as the first CARD8-specific inflammasome activator; however, it requires high micromolar concentrations (122,123). Thus, there is a clear need for development of more potent and specific CARD8 inflammasome activators in order for NNRTI-induced killing to become more therapeutically viable.

Nonetheless, CARD8 inflammasome activation by HIV-1 protease may prove to be a powerful tool for immune-mediated clearance of HIV-1. In addition to HIV-1, I also demonstrated that HIV-2 protease has the capacity to cleave CARD8, suggesting that NNRTI-induced cell killing may also be a viable strategy for HIV-2 elimination. Similarly, identification of additional viral proteases that can be sensed by CARD8 may provide additional candidates for CARD8-mediated viral clearance.

CONCLUDING REMARKS

The work outlined in this dissertation underscores the power of using evolution guided approaches to understand host/pathogen interactions. I have speculated on a few of the many implications of CARD8 sensing of HIV^{PR}, ranging from driving HIV-1 pathogenesis to curing HIV-1. As CARD8 research is a burgeoning field, future studies continuing my initial characterization of CARD8 sensing of HIV^{PR} may uncover additional mechanisms of CARD8 inflammasome activation and inspire therapeutic strategies for controlling other pathogenic infections.

Bibliography

1. WHO [Internet]. [cited 2024 Feb 2]. HIV. Available from: <https://www.who.int/data/gho/data/themes/hiv-aids>
2. Collman R, Godfrey B, Cutilli J, Rhodes A, Hassan NF, Sweet R, et al. Macrophage-tropic strains of human immunodeficiency virus type 1 utilize the CD4 receptor. *J Virol*. 1990 Sep;64(9):4468–76.
3. Collman R, Hassan NF, Walker R, Godfrey B, Cutilli J, Hastings JC, et al. Infection of monocyte-derived macrophages with human immunodeficiency virus type 1 (HIV-1). Monocyte-tropic and lymphocyte-tropic strains of HIV-1 show distinctive patterns of replication in a panel of cell types. *J Exp Med*. 1989 Oct 1;170(4):1149–63.
4. Brenchley JM, Paiardini M, Knox KS, Asher AI, Cervasi B, Asher TE, et al. Differential Th17 CD4 T-cell depletion in pathogenic and nonpathogenic lentiviral infections. *Blood*. 2008 Oct 1;112(7):2826–35.
5. Gosselin A, Monteiro P, Chomont N, Diaz-Griffero F, Said EA, Fonseca S, et al. Peripheral Blood CCR4+CCR6+ and CXCR3+CCR6+ CD4+ T Cells Are Highly Permissive to HIV-1 Infection. *J Immunol*. 2009 Dec 30;184(3):1604–16.
6. Rodriguez-Garcia M, Barr FD, Crist SG, Fahey JV, Wira CR. Phenotype and susceptibility to HIV infection of CD4+ Th17 cells in the human female reproductive tract. *Mucosal Immunol*. 2014 Nov 1;7(6):1375–85.
7. Chun TW, Finzi D, Margolick J, Chadwick K, Schwartz D, Siliciano RF. In vivo fate of HIV-1-infected T cells: Quantitative analysis of the transition to stable latency. *Nat Med*. 1995 Dec;1(12):1284–90.
8. Chun TW, Stuyver L, Mizell SB, Ehler LA, Mican JAM, Baseler M, et al. Presence of an inducible HIV-1 latent reservoir during highly active antiretroviral therapy. *Proc Natl Acad Sci*. 1997 Nov 25;94(24):13193–7.
9. Chun TW, Carruth L, Finzi D, Shen X, DiGiuseppe JA, Taylor H, et al. Quantification of latent tissue reservoirs and total body viral load in HIV-1 infection. *Nature*. 1997 May;387(6629):183–8.
10. Dalglish AG, Beverley PC, Clapham PR, Crawford DH, Greaves MF, Weiss RA. The CD4 (T4) antigen is an essential component of the receptor for the AIDS retrovirus. *Nature*. 1984 Jan 20;312(5996):763–7.
11. Klatzmann D, Champagne E, Chamaret S, Gruest J, Guetard D, Hercend T, et al. T-lymphocyte T4 molecule behaves as the receptor for human retrovirus LAV. *Nature*. 1984 Jan 20;312(5996):767–8.

12. Feng Y, Broder CC, Kennedy PE, Berger EA. HIV-1 entry cofactor: functional cDNA cloning of a seven-transmembrane, G protein-coupled receptor. *Science*. 1996 May 10;272(5263):872–7.
13. Alkhatib G, Combadiere C, Broder CC, Feng Y, Kennedy PE, Murphy PM, et al. CC CKR5: A RANTES, MIP-1 α , MIP-1 β Receptor as a Fusion Cofactor for Macrophage-Tropic HIV-1. *Science*. 1996 Jun 28;272(5270):1955–8.
14. Dragic T, Litwin V, Allaway GP, Martin SR, Huang Y, Nagashima KA, et al. HIV-1 entry into CD4+ cells is mediated by the chemokine receptor CC-CKR-5. *Nature*. 1996 Jun;381(6584):667–73.
15. Doranz BJ, Rucker J, Yi Y, Smyth RJ, Samson M, Peiper SC, et al. A dual-tropic primary HIV-1 isolate that uses fusin and the beta-chemokine receptors CKR-5, CKR-3, and CKR-2b as fusion cofactors. *Cell*. 1996 Jun 28;85(7):1149–58.
16. Deng H, Liu R, Ellmeier W, Choe S, Unutmaz D, Burkhart M, et al. Identification of a major co-receptor for primary isolates of HIV-1. *Nature*. 1996 Jun;381(6584):661–6.
17. Choe H, Farzan M, Sun Y, Sullivan N, Rollins B, Ponath PD, et al. The β -Chemokine Receptors CCR3 and CCR5 Facilitate Infection by Primary HIV-1 Isolates. *Cell*. 1996 Jun 28;85(7):1135–48.
18. Bannert N, Schenten D, Craig S, Sodroski J. The Level of CD4 Expression Limits Infection of Primary Rhesus Monkey Macrophages by a T-Tropic Simian Immunodeficiency Virus and Macrophagetropic Human Immunodeficiency Viruses. *J Virol*. 2000 Dec;74(23):10984–93.
19. Wang J, Crawford K, Yuan M, Wang H, Gorry PR, Gabuzda D. Regulation of CC Chemokine Receptor 5 and CD4 Expression and Human Immunodeficiency Virus Type 1 Replication in Human Macrophages and Microglia by T Helper Type 2 Cytokines. *J Infect Dis*. 2002 Apr 1;185(7):885–97.
20. Duenas-Decamp MJ, Peters PJ, Burton D, Clapham PR. Determinants Flanking the CD4 Binding Loop Modulate Macrophage Tropism of Human Immunodeficiency Virus Type 1 R5 Envelopes. *J Virol*. 2009 Mar 15;83(6):2575–83.
21. Dunfee RL, Thomas ER, Gorry PR, Wang J, Taylor J, Kunstman K, et al. The HIV Env variant N283 enhances macrophage tropism and is associated with brain infection and dementia. *Proc Natl Acad Sci*. 2006 Oct 10;103(41):15160–5.
22. Dunfee RL, Thomas ER, Wang J, Kunstman K, Wolinsky SM, Gabuzda D. Loss of the N-linked glycosylation site at position 386 in the HIV envelope V4 region enhances macrophage tropism and is associated with dementia. *Virology*. 2007 Oct 10;367(1):222–34.

23. Collman R, Balliet JW, Gregory SA, Friedman H, Kolson DL, Nathanson N, et al. An infectious molecular clone of an unusual macrophage-tropic and highly cytopathic strain of human immunodeficiency virus type 1. *J Virol*. 1992 Dec;66(12):7517–21.
24. Scarlatti G, Tresoldi E, Björndal A, Fredriksson R, Colognesi C, Deng HK, et al. In vivo evolution of HIV-1 co-receptor usage and sensitivity to chemokine-mediated suppression. *Nat Med*. 1997 Nov;3(11):1259–65.
25. Xiao L, Rudolph DL, Owen SM, Spira TJ, Lal RB. Adaptation to promiscuous usage of CC and CXCR4-chemokine coreceptors in vivo correlates with HIV-1 disease progression. *AIDS Lond Engl*. 1998 Sep 10;12(13):F137-143.
26. Terrasse R, Memmi M, Palle S, Heyndrickx L, Vanham G, Pozzetto B, et al. Visualization of X4- and R5-Tropic HIV-1 Viruses Expressing Fluorescent Proteins in Human Endometrial Cells: Application to Tropism Study. *PLoS One*. 2017;12(1):e0169453.
27. Dharan A, Bachmann N, Talley S, Zwickelmaier V, Campbell EM. Nuclear pore blockade reveals that HIV-1 completes reverse transcription and uncoating in the nucleus. *Nat Microbiol*. 2020 Sep;5(9):1088–95.
28. Iwasa J. Life Cycle – Science of HIV [Internet]. [cited 2024 Feb 9]. Available from: <https://scienceofhiv.org/wp/life-cycle/>
29. Jacks T, Power MD, Masiarz FR, Luciw PA, Barr PJ, Varmus HE. Characterization of ribosomal frameshifting in HIV-1 gag-pol expression. *Nature*. 1988 Jan 21;331(6153):280–3.
30. Lee SK, Potempa M, Swanstrom R. The Choreography of HIV-1 Proteolytic Processing and Virion Assembly. *J Biol Chem*. 2012 Nov 30;287(49):40867–74.
31. Potempa M, Lee SK, Kurt Yilmaz N, Nalivaika EA, Rogers A, Spielvogel E, et al. HIV-1 Protease Uses Bi-Specific S2/S2' Subsites to Optimize Cleavage of Two Classes of Target Sites. *J Mol Biol*. 2018 Dec 7;430(24):5182–95.
32. Tabler CO, Wegman SJ, Chen J, Shroff H, Alhusaini N, Tilton JC. The HIV-1 Viral Protease Is Activated during Assembly and Budding Prior to Particle Release. *J Virol*. 2022 Apr 19;96(9):e02198-21.
33. Weber IT, Wang YF, Harrison RW. HIV Protease: Historical Perspective and Current Research. *Viruses*. 2021 May 6;13(5):839.
34. Pettit SC, Clemente JC, Jeung JA, Dunn BM, Kaplan AH. Ordered Processing of the Human Immunodeficiency Virus Type 1 GagPol Precursor Is Influenced by the Context of the Embedded Viral Protease. *J Virol*. 2005 Aug 15;79(16):10601–7.

35. Pettit SC, Everitt LE, Choudhury S, Dunn BM, Kaplan AH. Initial Cleavage of the Human Immunodeficiency Virus Type 1 GagPol Precursor by Its Activated Protease Occurs by an Intramolecular Mechanism. *J Virol.* 2004 Aug 15;78(16):8477–85.
36. Pettit SC, Gulnik S, Everitt L, Kaplan AH. The Dimer Interfaces of Protease and Extra-Protease Domains Influence the Activation of Protease and the Specificity of GagPol Cleavage. *J Virol.* 2003 Jan;77(1):366–74.
37. Kaplan AH, Manchester M, Swanstrom R. The activity of the protease of human immunodeficiency virus type 1 is initiated at the membrane of infected cells before the release of viral proteins and is required for release to occur with maximum efficiency. *J Virol.* 1994 Oct;68(10):6782–6.
38. De Luca A. The impact of resistance on viral fitness and its clinical implications. In: Geretti AM, editor. *Antiretroviral Resistance in Clinical Practice* [Internet]. London: Mediscript; 2006 [cited 2024 Feb 6]. Available from: <http://www.ncbi.nlm.nih.gov/books/NBK2244/>
39. Martinez-Picado J, Savara AV, Sutton L, D'Aquila RT. Replicative fitness of protease inhibitor-resistant mutants of human immunodeficiency virus type 1. *J Virol.* 1999 May;73(5):3744–52.
40. Prado JG, Wrin T, Beauchaine J, Ruiz L, Petropoulos CJ, Frost SDW, et al. Amprenavir-resistant HIV-1 exhibits lopinavir cross-resistance and reduced replication capacity. *AIDS Lond Engl.* 2002 May 3;16(7):1009–17.
41. Resch W, Ziermann R, Parkin N, Gamarnik A, Swanstrom R. Nelfinavir-resistant, amprenavir-hypersusceptible strains of human immunodeficiency virus type 1 carrying an N88S mutation in protease have reduced infectivity, reduced replication capacity, and reduced fitness and process the Gag polyprotein precursor aberrantly. *J Virol.* 2002 Sep;76(17):8659–66.
42. Harris KS, Reddigari SR, Nicklin MJ, Hämmerle T, Wimmer E. Purification and characterization of poliovirus polypeptide 3CD, a proteinase and a precursor for RNA polymerase. *J Virol.* 1992 Dec;66(12):7481–9.
43. Towner JS, Ho TV, Semler BL. Determinants of Membrane Association for Poliovirus Protein 3AB *. *J Biol Chem.* 1996 Oct 25;271(43):26810–8.
44. Walsh D, Mohr I. Viral subversion of the host protein synthesis machinery. *Nat Rev Microbiol.* 2011 Dec;9(12):860–75.
45. Lin JY, Chen TC, Weng KF, Chang SC, Chen LL, Shih SR. Viral and host proteins involved in picornavirus life cycle. *J Biomed Sci.* 2009 Nov 20;16(1):103.
46. Sharp PM, Hahn BH. Origins of HIV and the AIDS Pandemic. *Cold Spring Harb Perspect Med.* 2011 Sep;1(1):a006841.

47. Aghokeng AF, Bailes E, Loul S, Courgnaud V, Mpoudi-Ngolle E, Sharp PM, et al. Full-length sequence analysis of SIVmus in wild populations of mustached monkeys (*Cercopithecus cephus*) from Cameroon provides evidence for two co-circulating SIVmus lineages. *Virology*. 2007 Apr 10;360(2):407–18.
48. Sharp PM, Hahn BH. The evolution of HIV-1 and the origin of AIDS. *Philos Trans Biol Sci*. 2010;365(1552):2487–94.
49. Brand CM, White FJ, Rogers AR, Webster TH. Estimating bonobo (*Pan paniscus*) and chimpanzee (*Pan troglodytes*) evolutionary history from nucleotide site patterns. *Proc Natl Acad Sci*. 2022 Apr 26;119(17):e2200858119.
50. Stone AC, Battistuzzi FU, Kubatko LS, Perry GH, Trudeau E, Lin H, et al. More reliable estimates of divergence times in *Pan* using complete mtDNA sequences and accounting for population structure. *Philos Trans R Soc B Biol Sci*. 2010 Oct 27;365(1556):3277–88.
51. Takehisa J, Kraus MH, Ayoub A, Bailes E, Van Heuverswyn F, Decker JM, et al. Origin and Biology of Simian Immunodeficiency Virus in Wild-Living Western Gorillas. *J Virol*. 2009 Feb;83(4):1635–48.
52. Sauter D, Schindler M, Specht A, Landford WN, Münch J, Kim KA, et al. Tetherin-driven adaptation of Vpu and Nef function and the evolution of pandemic and nonpandemic HIV-1 strains. *Cell Host Microbe*. 2009 Nov 19;6(5):409–21.
53. Wang X, Xu H, Alvarez X, Pahar B, Moroney-Rasmussen T, Lackner AA, et al. Distinct expression patterns of CD69 in mucosal and systemic lymphoid tissues in primary SIV infection of rhesus macaques. *PloS One*. 2011;6(11):e27207.
54. Brenchley JM, Price DA, Schacker TW, Asher TE, Silvestri G, Rao S, et al. Microbial translocation is a cause of systemic immune activation in chronic HIV infection. *Nat Med*. 2006 Dec;12(12):1365–71.
55. Stacey AR, Norris PJ, Qin L, Haygreen EA, Taylor E, Heitman J, et al. Induction of a Striking Systemic Cytokine Cascade prior to Peak Viremia in Acute Human Immunodeficiency Virus Type 1 Infection, in Contrast to More Modest and Delayed Responses in Acute Hepatitis B and C Virus Infections. *J Virol*. 2009 Apr 15;83(8):3719–33.
56. Nazli A, Chan O, Dobson-Belair WN, Ouellet M, Tremblay MJ, Gray-Owen SD, et al. Exposure to HIV-1 directly impairs mucosal epithelial barrier integrity allowing microbial translocation. *PLoS Pathog*. 2010 Apr 8;6(4):e1000852.
57. Blackburn SD, Shin H, Haining WN, Zou T, Workman CJ, Polley A, et al. Coregulation of CD8+ T cell exhaustion by multiple inhibitory receptors during chronic viral infection. *Nat Immunol*. 2009 Jan;10(1):29–37.

58. Fenwick C, Joo V, Jacquier P, Noto A, Banga R, Perreau M, et al. T-cell exhaustion in HIV infection. *Immunol Rev.* 2019 Nov;292(1):149–63.
59. Keele BF, Jones JH, Terio KA, Estes JD, Rudicell RS, Wilson ML, et al. Increased mortality and AIDS-like immunopathology in wild chimpanzees infected with SIVcpz. *Nature.* 2009 Jul;460(7254):515–9.
60. Kaur A, Grant RM, Means RE, McClure H, Feinberg M, Johnson RP. Diverse Host Responses and Outcomes following Simian Immunodeficiency Virus SIVmac239 Infection in Sooty Mangabeys and Rhesus Macaques. *J Virol.* 1998 Dec;72(12):9597–611.
61. Hirsch VM, Dapolito G, Johnson PR, Elkins WR, London WT, Montali RJ, et al. Induction of AIDS by simian immunodeficiency virus from an African green monkey: species-specific variation in pathogenicity correlates with the extent of in vivo replication. *J Virol.* 1995 Feb;69(2):955–67.
62. Joas S, Parrish EH, Gnanadurai CW, Lump E, Stürzel CM, Parrish NF, et al. Species-specific host factors rather than virus-intrinsic virulence determine primate lentiviral pathogenicity. *Nat Commun.* 2018 Apr 10;9(1):1371.
63. Jasinska AJ, Apetrei C, Pandrea I. Walk on the wild side: SIV infection in African non-human primate hosts—from the field to the laboratory. *Front Immunol* [Internet]. 2023 [cited 2023 Jun 23];13. Available from: <https://www.frontiersin.org/articles/10.3389/fimmu.2022.1060985>
64. Barrenas F, Raetz K, Xu C, Law L, Green RR, Silvestri G, et al. Macrophage-associated wound healing contributes to African green monkey SIV pathogenesis control. *Nat Commun.* 2019 Nov 8;10(1):5101.
65. Hao XP, Lucero CM, Turkbey B, Bernardo ML, Morcock DR, Deleage C, et al. Experimental colitis in SIV-uninfected rhesus macaques recapitulates important features of pathogenic SIV infection. *Nat Commun.* 2015 Aug 18;6:8020.
66. Yuan J, Ofengeim D. A guide to cell death pathways. *Nat Rev Mol Cell Biol.* 2023 Dec 18;1–17.
67. Dhuriya YK, Sharma D. Necroptosis: a regulated inflammatory mode of cell death. *J Neuroinflammation.* 2018 Jul 6;15(1):199.
68. Fink SL, Cookson BT. Apoptosis, Pyroptosis, and Necrosis: Mechanistic Description of Dead and Dying Eukaryotic Cells. *Infect Immun.* 2005 Apr;73(4):1907–16.
69. Broz P, Dixit VM. Inflammasomes: mechanism of assembly, regulation and signalling. *Nat Rev Immunol.* 2016 Jul;16(7):407–20.

70. Kayagaki N, Kornfeld OS, Lee BL, Stowe IB, O'Rourke K, Li Q, et al. NINJ1 mediates plasma membrane rupture during lytic cell death. *Nature*. 2021 Mar;591(7848):131–6.
71. Tartey S, Kanneganti TD. Inflammasomes in the pathophysiology of autoinflammatory syndromes. *J Leukoc Biol*. 2020 Mar;107(3):379–91.
72. Kaneko N, Kurata M, Yamamoto T, Morikawa S, Masumoto J. The role of interleukin-1 in general pathology. *Inflamm Regen*. 2019 Jun 6;39(1):12.
73. Dinarello CA. Overview of the IL-1 family in innate inflammation and acquired immunity. *Immunol Rev*. 2018 Jan;281(1):8–27.
74. Broderick L, Hoffman HM. IL-1 and autoinflammatory disease: biology, pathogenesis and therapeutic targeting. *Nat Rev Rheumatol*. 2022 Aug;18(8):448–63.
75. Hornung V, Ablasser A, Charrel-Dennis M, Bauernfeind F, Horvath G, Caffrey DR, et al. AIM2 recognizes cytosolic dsDNA and forms a caspase-1 activating inflammasome with ASC. *Nature*. 2009 Mar 26;458(7237):514–8.
76. Zhao Y, Yang J, Shi J, Gong YN, Lu Q, Xu H, et al. The NLRC4 inflammasome receptors for bacterial flagellin and type III secretion apparatus. *Nature*. 2011 Sep;477(7366):596–600.
77. Hara H, Seregin SS, Yang D, Fukase K, Chamaillard M, Alnemri ES, et al. The NLRP6 Inflammasome Recognizes Lipoteichoic Acid and Regulates Gram-Positive Pathogen Infection. *Cell*. 2018 Nov 29;175(6):1651-1664.e14.
78. Muñoz-Planillo R, Kuffa P, Martínez-Colón G, Smith BL, Rajendiran TM, Núñez G. K⁺ efflux is the common trigger of NLRP3 inflammasome activation by bacterial toxins and particulate matter. *Immunity*. 2013 Jun 27;38(6):1142–53.
79. Xu H, Yang J, Gao W, Li L, Li P, Zhang L, et al. Innate immune sensing of bacterial modifications of Rho GTPases by the Pyrin inflammasome. *Nature*. 2014 Sep 11;513(7517):237–41.
80. Xue Y, Enosi Tuipulotu D, Tan WH, Kay C, Man SM. Emerging Activators and Regulators of Inflammasomes and Pyroptosis. *Trends Immunol*. 2019 Nov 1;40(11):1035–52.
81. Remick BC, Gaidt MM, Vance RE. Effector-Triggered Immunity. *Annu Rev Immunol*. 2023;41(1):453–81.
82. Chisholm ST, Coaker G, Day B, Staskawicz BJ. Host-Microbe Interactions: Shaping the Evolution of the Plant Immune Response. *Cell*. 2006 Feb 24;124(4):803–14.

83. Jones JDG, Dangl JL. The plant immune system. *Nature*. 2006 Nov;444(7117):323–9.
84. Nguyen QM, Iswanto ABB, Son GH, Kim SH. Recent Advances in Effector-Triggered Immunity in Plants: New Pieces in the Puzzle Create a Different Paradigm. *Int J Mol Sci*. 2021 Apr 29;22(9):4709.
85. Yue JX, Meyers BC, Chen JQ, Tian D, Yang S. Tracing the origin and evolutionary history of plant nucleotide-binding site-leucine-rich repeat (NBS-LRR) genes. *New Phytol*. 2012 Mar;193(4):1049–63.
86. Urbach JM, Ausubel FM. The NBS-LRR architectures of plant R-proteins and metazoan NLRs evolved in independent events. *Proc Natl Acad Sci U S A*. 2017 Jan 31;114(5):1063–8.
87. Black DS, Bliska JB. The RhoGAP activity of the *Yersinia pseudotuberculosis* cytotoxin YopE is required for antiphagocytic function and virulence. *Mol Microbiol*. 2000 Aug;37(3):515–27.
88. Shao F, Dixon JE. YopT is a cysteine protease cleaving Rho family GTPases. *Adv Exp Med Biol*. 2003;529:79–84.
89. Craven RR, Gao X, Allen IC, Gris D, Bubeck Wardenburg J, McElvania-Tekippe E, et al. *Staphylococcus aureus* alpha-hemolysin activates the NLRP3-inflammasome in human and mouse monocytic cells. *PLoS One*. 2009 Oct 14;4(10):e7446.
90. McCoy AJ, Koizumi Y, Toma C, Higa N, Dixit V, Taniguchi S, et al. Cytotoxins of the human pathogen *Aeromonas hydrophila* trigger, via the NLRP3 inflammasome, caspase-1 activation in macrophages. *Eur J Immunol*. 2010 Oct;40(10):2797–803.
91. Bhakdi S, Mannhardt U, Muhly M, Hugo F, Ronneberger H, Hungerer KD. Human hyperimmune globulin protects against the cytotoxic action of staphylococcal alpha-toxin in vitro and in vivo. *Infect Immun*. 1989 Oct;57(10):3214–20.
92. Ichinohe T, Pang IK, Iwasaki A. Influenza virus activates inflammasomes via its intracellular M2 ion channel. *Nat Immunol*. 2010 May;11(5):404–10.
93. Pandey KP, Zhou Y. Influenza A Virus Infection Activates NLRP3 Inflammasome through Trans-Golgi Network Dispersion. *Viruses*. 2022 Jan 5;14(1):88.
94. Snyder AG, Oberst A. The Antisocial Network: Cross Talk Between Cell Death Programs in Host Defense. *Annu Rev Immunol*. 2021;39(1):77–101.
95. Bedoui S, Herold MJ, Strasser A. Emerging connectivity of programmed cell death pathways and its physiological implications. *Nat Rev Mol Cell Biol*. 2020 Nov;21(11):678–95.

96. Bertheloot D, Latz E, Franklin BS. Necroptosis, pyroptosis and apoptosis: an intricate game of cell death. *Cell Mol Immunol*. 2021 May;18(5):1106–21.
97. cesari S, Bernoux M, Moncuquet P, Kroj T, Dodds PN. A novel conserved mechanism for plant NLR protein pairs: the 'integrated decoy' hypothesis. *Front Plant Sci* [Internet]. 2014 [cited 2024 Feb 8];5. Available from: <https://www.frontiersin.org/journals/plant-science/articles/10.3389/fpls.2014.00606>
98. Sarris PF, Duxbury Z, Huh SU, Ma Y, Segonzac C, Sklenar J, et al. A Plant Immune Receptor Detects Pathogen Effectors that Target WRKY Transcription Factors. *Cell*. 2015 May 21;161(5):1089–100.
99. Le Roux C, Huet G, Jauneau A, Camborde L, Trémousaygue D, Kraut A, et al. A receptor pair with an integrated decoy converts pathogen disabling of transcription factors to immunity. *Cell*. 2015 May 21;161(5):1074–88.
100. D'Osualdo A, Weichenberger CX, Wagner RN, Godzik A, Wooley J, Reed JC. CARD8 and NLRP1 Undergo Autoproteolytic Processing through a ZU5-Like Domain. *PLOS ONE*. 2011 Nov 8;6(11):e27396.
101. Taabazuing CY, Griswold AR, Bachovchin DA. The NLRP1 and CARD8 inflammasomes. *Immunol Rev*. 2020;297(1):13–25.
102. Robinson KS, Teo DET, Tan KS, Toh GA, Ong HH, Lim CK, et al. Enteroviral 3C protease activates the human NLRP1 inflammasome in airway epithelia. *Science*. 2020 Dec 4;370(6521):eaay2002.
103. Sandstrom A, Mitchell PS, Goers L, Mu EW, Lesser CF, Vance RE. Functional degradation: A mechanism of NLRP1 inflammasome activation by diverse pathogen enzymes. 2019;11.
104. Tsu BV, Beierschmitt C, Ryan AP, Agarwal R, Mitchell PS, Daugherty MD. Diverse viral proteases activate the NLRP1 inflammasome. *eLife*. 2021 Jan 7;10:e60609.
105. Tsu BV, Fay EJ, Nguyen KT, Corley MR, Hosuru B, Dominguez VA, et al. Running With Scissors: Evolutionary Conflicts Between Viral Proteases and the Host Immune System. *Front Immunol* [Internet]. 2021 [cited 2022 Aug 16];12. Available from: <https://www.frontiersin.org/articles/10.3389/fimmu.2021.769543>
106. Planès R, Pinilla M, Santoni K, Hessel A, Passemar C, Lay K, et al. Human NLRP1 is a sensor of pathogenic coronavirus 3CL proteases in lung epithelial cells. *Mol Cell*. 2022 Jul 7;82(13):2385-2400.e9.
107. Okondo MC, Johnson DC, Sridharan R, Go EB, Chui AJ, Wang MS, et al. DPP8 and DPP9 inhibition induces pro-caspase-1-dependent monocyte and macrophage pyroptosis. *Nat Chem Biol*. 2017 Jan;13(1):46–53.

108. Okondo MC, Rao SD, Taabazuing CY, Chui AJ, Poplawski SE, Johnson DC, et al. Inhibition of Dpp8/9 Activates the Nlrp1b Inflammasome. *Cell Chem Biol.* 2018 Mar;25(3):262-267.e5.
109. Johnson DC, Taabazuing CY, Okondo MC, Chui AJ, Rao SD, Brown FC, et al. DPP8/9 inhibitor-induced pyroptosis for treatment of acute myeloid leukemia. *Nat Med.* 2018 Aug;24(8):1151–6.
110. Johnson DC, Okondo MC, Orth EL, Rao SD, Huang HC, Ball DP, et al. DPP8/9 inhibitors activate the CARD8 inflammasome in resting lymphocytes. *Cell Death Dis.* 2020 Aug;11(8):628.
111. Zurawek M, Fichna M, Januszkiewicz-Lewandowska D, Gryczyńska M, Fichna P, Nowak J. A coding variant in NLRP1 is associated with autoimmune Addison's disease. *Hum Immunol.* 2010 May;71(5):530–4.
112. Levandowski CB, Mailloux CM, Ferrara TM, Gowan K, Ben S, Jin Y, et al. NLRP1 haplotypes associated with vitiligo and autoimmunity increase interleukin-1 β processing via the NLRP1 inflammasome. *Proc Natl Acad Sci.* 2013 Feb 19;110(8):2952–6.
113. Pontillo A, Laurentino W, Crovella S, Pereira AC. NLRP1 haplotypes associated with leprosy in Brazilian patients. *Infect Genet Evol J Mol Epidemiol Evol Genet Infect Dis.* 2013 Oct;19:274–9.
114. Pontillo A, Reis EC, Liphaut BL, Silva CA, Carneiro-Sampaio M. Inflammasome polymorphisms in juvenile systemic lupus erythematosus. *Autoimmunity.* 2015;48(7):434–7.
115. Shamsabadi RM, Basafa S, Yarahmadi R, Goorani S, Khani M, Kamarehei M, et al. Elevated expression of NLRP1 and IPAF are related to oral pemphigus vulgaris pathogenesis. *Inflammation.* 2015 Feb;38(1):205–8.
116. Grandemange S, Sanchez E, Louis-Plence P, Tran Mau-Them F, Bessis D, Coubes C, et al. A new autoinflammatory and autoimmune syndrome associated with NLRP1 mutations: NAIAD (NLRP1-associated autoinflammation with arthritis and dyskeratosis). *Ann Rheum Dis.* 2017 Jul;76(7):1191–8.
117. Silva LM, de Sousa JR, Hirai KE, Dias LB, Furlaneto IP, Carneiro FRO, et al. The inflammasome in leprosy skin lesions: an immunohistochemical evaluation. *Infect Drug Resist.* 2018;11:2231–40.
118. Zhong FL, Mamaï O, Sborgi L, Bousofara L, Hopkins R, Robinson K, et al. Germline NLRP1 Mutations Cause Skin Inflammatory and Cancer Susceptibility Syndromes via Inflammasome Activation. *Cell.* 2016 Sep 22;167(1):187-202.e17.

119. Robinson KS, Toh GA, Rozario P, Chua R, Bauernfried S, Sun Z, et al. ZAK α -driven ribotoxic stress response activates the human NLRP1 inflammasome. *Science*. 2022 Jul 15;377(6603):328–35.
120. Broz P, von Moltke J, Jones JW, Vance RE, Monack DM. Differential Requirement for Caspase-1 Autoproteolysis in Pathogen-Induced Cell Death and Cytokine Processing. *Cell Host Microbe*. 2010 Dec 16;8(6):471–83.
121. Tsu BV, Agarwal R, Gokhale NS, Kulsuptrakul J, Ryan AP, Fay EJ, et al. Host-specific sensing of coronaviruses and picornaviruses by the CARD8 inflammasome. *PLOS Biol*. 2023 Jun 8;21(6):e3002144.
122. Kulsuptrakul J, Mitchell PS. XaaP-ing DPP8/9 for CARD8 activation. *Nat Chem Biol*. 2022 May;18(5):439–40.
123. Rao SD, Chen Q, Wang Q, Orth-He EL, Saoi M, Griswold AR, et al. M24B aminopeptidase inhibitors selectively activate the CARD8 inflammasome. *Nat Chem Biol*. 2022 May;18(5):565–74.
124. Nadkarni R, Chu WC, Lee CQE, Mohamud Y, Yap L, Toh GA, et al. Viral proteases activate the CARD8 inflammasome in the human cardiovascular system. *J Exp Med*. 2022 Sep 21;219(10):e20212117.
125. Linder A, Bauernfried S, Cheng Y, Albanese M, Jung C, Keppler OT, et al. CARD8 inflammasome activation triggers pyroptosis in human T cells. *EMBO J*. 2020 Oct 1;39(19):e105071.
126. Balibar CJ, Klein DJ, Zamlynny B, Diamond TL, Fang Z, Cheney CA, et al. Potent targeted activator of cell kill molecules eliminate cells expressing HIV-1. *Sci Transl Med*. 2023 Feb 22;15(684):eabn2038.
127. Wang Q, Gao H, Clark KM, Mugisha CS, Davis K, Tang JP, et al. CARD8 is an inflammasome sensor for HIV-1 protease activity. *Science*. 2021 Mar 19;371(6535):eabe1707.
128. Doitsh G, Galloway NL, Geng X, Yang Z, Monroe KM, Zepeda O, et al. Pyroptosis drives CD4 T-cell depletion in HIV-1 infection. *Nature*. 2014 Jan 23;505(7484):509–14.
129. Galloway NLK, Doitsh G, Monroe KM, Yang Z, Muñoz-Arias I, Levy DN, et al. Cell-to-Cell Transmission of HIV-1 Is Required to Trigger Pyroptotic Death of Lymphoid-Tissue-Derived CD4 T Cells. *Cell Rep*. 2015 Sep 8;12(10):1555–63.
130. Doitsh G, Cavrois M, Lassen KG, Zepeda O, Yang Z, Santiago ML, et al. Abortive HIV Infection Mediates CD4 T Cell Depletion and Inflammation in Human Lymphoid Tissue. *Cell*. 2010 Nov 24;143(5):789–801.

131. Monroe KM, Yang Z, Johnson JR, Geng X, Doitsh G, Krogan NJ, et al. IFI16 DNA Sensor Is Required for Death of Lymphoid CD4 T-cells Abortively Infected with HIV. *Science*. 2014 Jan 24;343(6169):428–32.
132. Muñoz-Arias I, Doitsh G, Yang Z, Sowinski S, Ruelas D, Greene WC. Blood-Derived CD4 T Cells Naturally Resist Pyroptosis During Abortive HIV-1 Infection. *Cell Host Microbe*. 2015 Oct 14;18(4):463–70.
133. Zhang C, Song JW, Huang HH, Fan X, Huang L, Deng JN, et al. NLRP3 inflammasome induces CD4⁺ T cell loss in chronically HIV-1–infected patients. *J Clin Invest* [Internet]. 2021 Mar 15 [cited 2021 Jun 24];131(6). Available from: <https://www.jci.org/articles/view/138861>
134. Thompson MR, Sharma S, Atianand M, Jensen SB, Carpenter S, Knipe DM, et al. Interferon γ -inducible Protein (IFI) 16 Transcriptionally Regulates Type I Interferons and Other Interferon-stimulated Genes and Controls the Interferon Response to both DNA and RNA Viruses. *J Biol Chem*. 2014 Aug 22;289(34):23568–81.
135. Jiang Z, Wei F, Zhang Y, Wang T, Gao W, Yu S, et al. IFI16 directly senses viral RNA and enhances RIG-I transcription and activation to restrict influenza virus infection. *Nat Microbiol*. 2021 Jul;6(7):932–45.
136. Daugherty MD, Malik HS. Rules of Engagement: Molecular Insights from Host-Virus Arms Races. 2012;27.
137. Parrish CR, Holmes EC, Morens DM, Park EC, Burke DS, Calisher CH, et al. Cross-Species Virus Transmission and the Emergence of New Epidemic Diseases. *Microbiol Mol Biol Rev*. 2008 Sep;72(3):457–70.
138. Harapas CR, Steiner A, Davidson S, Masters SL. An Update on Autoinflammatory Diseases: Inflammasomopathies. *Curr Rheumatol Rep*. 2018 Jul;20(7):40.
139. D’Oswaldo A, Weichenberger CX, Wagner RN, Godzik A, Wooley J, Reed JC. CARD8 and NLRP1 Undergo Autoproteolytic Processing through a ZU5-Like Domain. Wang T, editor. *PLoS ONE*. 2011 Nov 8;6(11):e27396.
140. Sharif H, Hollingsworth LR, Griswold AR, Hsiao JC, Wang Q, Bachovchin DA, et al. Dipeptidyl peptidase 9 sets a threshold for CARD8 inflammasome formation by sequestering its active C-terminal fragment. *Immunity*. 2021 Jul 13;54(7):1392-1404.e10.
141. Balibar CJ, Klein DJ, Zamlynny B, Diamond TL, Fang Z, Cheney CA, et al. Potent targeted activator of cell kill molecules eliminate cells expressing HIV-1. *Sci Transl Med*. 2023 Feb 22;15(684):eabn2038.
142. Clark KM, Kim JG, Wang Q, Gao H, Presti RM, Shan L. Chemical inhibition of DPP9 sensitizes the CARD8 inflammasome in HIV-1-infected cells. *Nat Chem Biol*. 2022 Nov 10;1–9.

143. Robinson KS, Teo DET, Tan KS, Toh GA, Ong HH, Lim CK, et al. Enteroviral 3C protease activates the human NLRP1 inflammasome in airway epithelia. *Science*. 2020 Dec 4;370(6521):eaay2002.
144. Sandstrom A, Mitchell PS, Goers L, Mu EW, Lesser CF, Vance RE. Functional degradation: A mechanism of NLRP1 inflammasome activation by diverse pathogen enzymes. 2019;11.
145. Tsu BV, Beierschmitt C, Ryan AP, Agarwal R, Mitchell PS, Daugherty MD. Diverse viral proteases activate the NLRP1 inflammasome. *eLife*. 2021 Jan 7;10:e60609.
146. Castro LK, Daugherty MD. Tripping the wire: sensing of viral protease activity by CARD8 and NLRP1 inflammasomes. *Curr Opin Immunol*. 2023 Aug 1;83:102354.
147. Green RE, Krause J, Briggs AW, Maricic T, Stenzel U, Kircher M, et al. A Draft Sequence of the Neandertal Genome. *Science*. 2010 May 7;328(5979):710–22.
148. Hsiao JC, Neugroschl AR, Chui AJ, Taabazuing CY, Griswold AR, Wang Q, et al. A ubiquitin-independent proteasome pathway controls activation of the CARD8 inflammasome. *J Biol Chem*. 2022 May 14;298(7):102032.
149. Kulsuptrakul J, Turcotte EA, Emerman M, Mitchell PS. A human-specific motif facilitates CARD8 inflammasome activation after HIV-1 infection. Kirchhoff F, Davenport MP, Kirchhoff F, editors. *eLife*. 2023 Jul 7;12:e84108.
150. Barbian HJ, Decker JM, Bibollet-Ruche F, Galimidi RP, West AP, Learn GH, et al. Neutralization Properties of Simian Immunodeficiency Viruses Infecting Chimpanzees and Gorillas. *mBio*. 2015 Apr 21;6(2):e00296-15.
151. Keele BF, Van Heuverswyn F, Li Y, Bailes E, Takehisa J, Santiago ML, et al. Chimpanzee Reservoirs of Pandemic and Nonpandemic HIV-1. *Science*. 2006 Jul 28;313(5786):523–6.
152. Figueiredo A, Moore KL, Mak J, Sluis-Cremer N, Bethune MP de, Tachedjian G. Potent Nonnucleoside Reverse Transcriptase Inhibitors Target HIV-1 Gag-Pol. *PLOS Pathog*. 2006 Nov 10;2(11):e119.
153. Trinité B, Zhang H, Levy DN. NNRTI-induced HIV-1 protease-mediated cytotoxicity induces rapid death of CD4 T cells during productive infection and latency reversal. *Retrovirology*. 2019 Jun 26;16(1):17.
154. Álvarez E, Castelló A, Menéndez-Arias L, Carrasco L. HIV protease cleaves poly(A)-binding protein. *Biochem J*. 2006 Jun 1;396(Pt 2):219–26.
155. Linder A, Bauernfried S, Cheng Y, Albanese M, Jung C, Keppler OT, et al. CARD8 inflammasome activation triggers pyroptosis in human T cells. *EMBO J*. 2020 Oct 1;39(19):e105071.

156. Ball DP, Taabazuing CY, Griswold AR, Orth EL, Rao SD, Kotliar IB, et al. Caspase-1 interdomain linker cleavage is required for pyroptosis. *Life Sci Alliance* [Internet]. 2020 Mar 1 [cited 2021 Nov 12];3(3). Available from: <https://www.life-science-alliance.org/content/3/3/e202000664>
157. Mohammadi P, Desfarges S, Bartha I, Joos B, Zangger N, Muñoz M, et al. 24 Hours in the Life of HIV-1 in a T Cell Line. *PLOS Pathog*. 2013 Jan 31;9(1):e1003161.
158. Moore KP, Schwaid AG, Tudor M, Park S, Beshore DC, Converso A, et al. A Phenotypic Screen Identifies Potent DPP9 Inhibitors Capable of Killing HIV-1 Infected Cells. *ACS Chem Biol*. 2022 Sep 16;17(9):2595–604.
159. Sparrer KMJ, Kirchhoff F. HIV protease: late action to prevent immune detection. *Signal Transduct Target Ther*. 2021 Apr 16;6(1):1–2.
160. Wang Q, Clark KM, Tiwari R, Raju N, Tharp GK, Rogers J, et al. The CARD8 inflammasome dictates HIV/SIV pathogenesis and disease progression. *Cell*. 2024 Feb 29;187(5):1223-1237.e16.
161. Chan AH, Schroder K. Inflammasome signaling and regulation of interleukin-1 family cytokines. *J Exp Med*. 2019 Oct 14;217(1):e20190314.
162. Sandler NG, Douek DC. Microbial translocation in HIV infection: causes, consequences and treatment opportunities. *Nat Rev Microbiol*. 2012 Sep;10(9):655–66.
163. Kim JG, Shan L. Beyond Inhibition: A Novel Strategy of Targeting HIV-1 Protease to Eliminate Viral Reservoirs. *Viruses*. 2022 Jun;14(6):1179.
164. Lim ES, Malik HS, Emerman M. Ancient adaptive evolution of tetherin shaped the functions of Vpu and Nef in human immunodeficiency virus and primate lentiviruses. *J Virol*. 2010 Jul;84(14):7124–34.
165. Bibollet-Ruche F, Heigele A, Keele BF, Easlick JL, Decker JM, Takehisa J, et al. Efficient SIVcpz replication in human lymphoid tissue requires viral matrix protein adaptation. *J Clin Invest*. 2012 May 1;122(5):1644–52.
166. Zhang Z, Gu Q, de Manuel Montero M, Bravo IG, Marques-Bonet T, Häussinger D, et al. Stably expressed APOBEC3H forms a barrier for cross-species transmission of simian immunodeficiency virus of chimpanzee to humans. *PLoS Pathog*. 2017 Dec;13(12):e1006746.
167. Etienne L, Hahn BH, Sharp PM, Matsen FA, Emerman M. Gene Loss and Adaptation to Hominids Underlie the Ancient Origin of HIV-1. *Cell Host Microbe*. 2013 Jul;14(1):85–92.

168. Binning JM, Chesarino NM, Emerman M, Gross JD. Structural Basis for a Species-Specific Determinant of an SIV Vif Protein toward Hominid APOBEC3G Antagonism. *Cell Host Microbe*. 2019 Dec 11;26(6):739-747.e4.
169. Muema DM, Akilimali NA, Ndumnego OC, Rasehlo SS, Durgiah R, Ojwach DBA, et al. Association between the cytokine storm, immune cell dynamics, and viral replicative capacity in hyperacute HIV infection. *BMC Med*. 2020 Mar 25;18(1):81.
170. Arditi M, Kabat W, Yogev R. Serum tumor necrosis factor alpha, interleukin 1-beta, p24 antigen concentrations and CD4+ cells at various stages of human immunodeficiency virus 1 infection in children. *Pediatr Infect Dis J*. 1991 Jun;10(6):450-4.
171. Zhang C, Song JW, Huang HH, Fan X, Huang L, Deng JN, et al. NLRP3 inflammasome induces CD4⁺ T cell loss in chronically HIV-1-infected patients. *J Clin Invest* [Internet]. 2021 Mar 15 [cited 2022 Aug 12];131(6). Available from: <https://www.jci.org/articles/view/138861>
172. Chung Y, Chang SH, Martinez GJ, Yang XO, Nurieva R, Kang HS, et al. Critical Regulation of Early Th17 Cell Differentiation by Interleukin-1 Signaling. *Immunity*. 2009 Apr 17;30(4):576-87.
173. Rider P, Carmi Y, Guttman O, Braiman A, Cohen I, Voronov E, et al. IL-1 α and IL-1 β Recruit Different Myeloid Cells and Promote Different Stages of Sterile Inflammation. *J Immunol*. 2011 Nov 1;187(9):4835-43.
174. Paiardini M, Müller-Trutwin M. HIV-associated chronic immune activation. *Immunol Rev*. 2013 Jul;254(1):78-101.
175. Busnadiego I, Kane M, Rihn SJ, Preugschas HF, Hughes J, Blanco-Melo D, et al. Host and Viral Determinants of Mx2 Antiretroviral Activity. *J Virol*. 2014 Jul 15;88(14):7738-52.
176. Haddox HK, Dingens AS, Hilton SK, Overbaugh J, Bloom JD. Mapping mutational effects along the evolutionary landscape of HIV envelope. Chakraborty AK, editor. *eLife*. 2018 Mar 28;7:e34420.
177. Poss M, Overbaugh J. Variants from the Diverse Virus Population Identified at Seroconversion of a Clade A Human Immunodeficiency Virus Type 1-Infected Woman Have Distinct Biological Properties. *J Virol*. 1999 Jul;73(7):5255-64.
178. Guyader M, Emerman M, Sonigo P, Clavel F, Montagnier L, Alizon M. Genome organization and transactivation of the human immunodeficiency virus type 2. *Nature*. 1987 Apr 16;326(6114):662-9.
179. Peden K, Emerman M, Montagnier L. Changes in growth properties on passage in tissue culture of viruses derived from infectious molecular clones of HIV-1LAI, HIV-1MAL, and HIV-1ELI. *Virology*. 1991 Dec 1;185(2):661-72.

180. Rogel ME, Wu LI, Emerman M. The human immunodeficiency virus type 1 vpr gene prevents cell proliferation during chronic infection. *J Virol.* 1995 Feb;69(2):882–8.
181. Labun K, Montague TG, Krause M, Torres Cleuren YN, Tjeldnes H, Valen E. CHOPCHOP v3: expanding the CRISPR web toolbox beyond genome editing. *Nucleic Acids Res.* 2019 Jul 2;47(W1):W171–4.
182. Schmid-Burgk JL, Schmidt T, Gaidt MM, Pelka K, Latz E, Ebert TS, et al. OutKnocker: a web tool for rapid and simple genotyping of designer nuclease edited cell lines. *Genome Res.* 2014 Oct;24(10):1719–23.
183. Schmidt T, Schmid-Burgk JL, Ebert TS, Gaidt MM, Hornung V. Designer Nuclease-Mediated Generation of Knockout THP1 Cells. In: Kühn R, Wurst W, Wefers B, editors. TALENs [Internet]. New York, NY: Springer New York; 2016 [cited 2022 Sep 26]. p. 261–72. (Methods in Molecular Biology; vol. 1338). Available from: http://link.springer.com/10.1007/978-1-4939-2932-0_19
184. Montoya VR, Ready TM, Felton A, Fine SR, OhAinle M, Emerman M. A Virus-Packageable CRISPR System Identifies Host Dependency Factors Co-Opted by Multiple HIV-1 Strains. *mBio.* 2023 Feb 6;14(1):e00009-23.
185. OhAinle M, Helms L, Vermeire J, Roesch F, Humes D, Basom R, et al. A virus-packageable CRISPR screen identifies host factors mediating interferon inhibition of HIV. Nussenzweig MC, Sundquist WI, editors. *eLife.* 2018 Dec 6;7:e39823.
186. Bartz SR, Vodicka MA. Production of High-Titer Human Immunodeficiency Virus Type 1 Pseudotyped with Vesicular Stomatitis Virus Glycoprotein. *Methods.* 1997 Aug 1;12(4):337–42.
187. Gummuluru S, Rogel M, Stamatatos L, Emerman M. Binding of Human Immunodeficiency Virus Type 1 to Immature Dendritic Cells Can Occur Independently of DC-SIGN and Mannose Binding C-Type Lectin Receptors via a Cholesterol-Dependent Pathway. *J Virol.* 2003 Dec;77(23):12865–74.
188. Chen P, Hübner W, Spinelli MA, Chen BK. Predominant mode of human immunodeficiency virus transfer between T cells is mediated by sustained Env-dependent neutralization-resistant virological synapses. *J Virol.* 2007 Nov;81(22):12582–95.
189. Iwami S, Takeuchi JS, Nakaoka S, Mammano F, Clavel F, Inaba H, et al. Cell-to-cell infection by HIV contributes over half of virus infection. Chakraborty AK, editor. *eLife.* 2015 Oct 6;4:e08150.
190. Martin N, Welsch S, Jolly C, Briggs JAG, Vaux D, Sattentau QJ. Virological Synapse-Mediated Spread of Human Immunodeficiency Virus Type 1 between T Cells Is Sensitive to Entry Inhibition. *J Virol.* 2010 Apr;84(7):3516–27.

191. Agosto LM, Herring MB, Mothes W, Henderson AJ. HIV-1-Infected CD4+ T Cells Facilitate Latent Infection of Resting CD4+ T Cells through Cell-Cell Contact. *Cell Rep*. 2018 Aug 21;24(8):2088–100.
192. Baxter AE, Russell RA, Duncan CJA, Moore MD, Willberg CB, Pablos JL, et al. Macrophage infection via selective capture of HIV-1-infected CD4+ T cells. *Cell Host Microbe*. 2014 Dec 10;16(6):711–21.
193. Lopez P, Koh WH, Hnatiuk R, Murooka TT. HIV Infection Stabilizes Macrophage-T Cell Interactions To Promote Cell-Cell HIV Spread. *J Virol*. 2019 Aug 28;93(18):e00805-19.
194. Dupont M, Sattentau QJ. Macrophage Cell-Cell Interactions Promoting HIV-1 Infection. *Viruses*. 2020 May;12(5):492.
195. Agosto LM, Uchil PD, Mothes W. HIV cell-to-cell transmission: effects on pathogenesis and antiretroviral therapy. *Trends Microbiol*. 2015 May;23(5):289–95.
196. Russell RA, Martin N, Mitar I, Jones E, Sattentau QJ. Multiple proviral integration events after virological synapse-mediated HIV-1 spread. *Virology*. 2013 Aug 15;443(1):143–9.
197. Del Portillo A, Tripodi J, Najfeld V, Wodarz D, Levy DN, Chen BK. Multiploid Inheritance of HIV-1 during Cell-to-Cell Infection ∇ . *J Virol*. 2011 Jul;85(14):7169–76.
198. Duncan CJA, Russell RA, Sattentau QJ. High multiplicity HIV-1 cell-to-cell transmission from macrophages to CD4+ T cells limits antiretroviral efficacy. *AIDS*. 2013 Sep 10;27(14):2201.
199. Jolly C, Booth NJ, Neil SJD. Cell-Cell Spread of Human Immunodeficiency Virus Type 1 Overcomes Tetherin/BST-2-Mediated Restriction in T cells. *J Virol*. 2010 Dec;84(23):12185–99.
200. Zhong P, Agosto LM, Ilinskaya A, Dorjbal B, Truong R, Derse D, et al. Cell-to-Cell Transmission Can Overcome Multiple Donor and Target Cell Barriers Imposed on Cell-Free HIV. *PLOS ONE*. 2013 Jan 7;8(1):e53138.
201. Xie M, Leroy H, Mascarau R, Woottum M, Dupont M, Ciccone C, et al. Cell-to-Cell Spreading of HIV-1 in Myeloid Target Cells Escapes SAMHD1 Restriction. *mBio*. 2019 Nov 19;10(6):10.1128/mbio.02457-19.
202. Richardson MW, Carroll RG, Stremlau M, Korokhov N, Humeau LM, Silvestri G, et al. Mode of Transmission Affects the Sensitivity of Human Immunodeficiency Virus Type 1 to Restriction by Rhesus TRIM5 α . *J Virol*. 2008 Nov 15;82(22):11117–28.

203. Abela IA, Berlinger L, Schanz M, Reynell L, Günthard HF, Rusert P, et al. Cell-Cell Transmission Enables HIV-1 to Evade Inhibition by Potent CD4bs Directed Antibodies. *PLOS Pathog.* 2012 Apr 5;8(4):e1002634.
204. Dufloo J, Bruel T, Schwartz O. HIV-1 cell-to-cell transmission and broadly neutralizing antibodies. *Retrovirology.* 2018 Jul 28;15(1):51.
205. Sigal A, Kim JT, Balazs AB, Dekel E, Mayo A, Milo R, et al. Cell-to-cell spread of HIV permits ongoing replication despite antiretroviral therapy. *Nature.* 2011 Sep;477(7362):95–8.
206. Agosto LM, Zhong P, Munro J, Mothes W. Highly Active Antiretroviral Therapies Are Effective against HIV-1 Cell-to-Cell Transmission. *PLOS Pathog.* 2014 Feb 27;10(2):e1003982.
207. Varghese V, Mitsuya Y, Fessel WJ, Liu TF, Melikian GL, Katzenstein DA, et al. Prototypical Recombinant Multi-Protease-Inhibitor-Resistant Infectious Molecular Clones of Human Immunodeficiency Virus Type 1. *Antimicrob Agents Chemother.* 2013 Sep;57(9):4290–9.
208. Stanford - HIV Drug Resistance Database [Internet]. [cited 2024 Feb 10]. Available from: <https://hivdb.stanford.edu/page/release-notes/#consensusubsequences>
209. Tachedjian G, Orlova M, Sarafianos SG, Arnold E, Goff SP. Nonnucleoside reverse transcriptase inhibitors are chemical enhancers of dimerization of the HIV type 1 reverse transcriptase. *Proc Natl Acad Sci U S A.* 2001 Jun 19;98(13):7188–93.
210. Venezia CF, Howard KJ, Ignatov ME, Holladay LA, Barkley MD. Effects of efavirenz binding on the subunit equilibria of HIV-1 reverse transcriptase. *Biochemistry.* 2006 Mar 7;45(9):2779–89.
211. Sharaf NG, Xi Z, Ishima R, Gronenborn AM. The HIV-1 p66 homodimeric RT exhibits different conformations in the binding-competent and -incompetent NNRTI site. *Proteins Struct Funct Bioinforma.* 2017;85(12):2191–7.
212. Martínez-Méndez D, Rivera-Toledo E, Ortega E, Licona-Limón I, Huerta L. Monocyte-lymphocyte fusion induced by the HIV-1 envelope generates functional heterokaryons with an activated monocyte-like phenotype. *Exp Cell Res.* 2017 Mar 1;352(1):9–19.
213. Orenstein JM. In Vivo Cytolysis and Fusion of Human Immunodeficiency Virus Type 1-Infected Lymphocytes in Lymphoid Tissue. *J Infect Dis.* 2000 Jul 1;182(1):338–42.
214. Kayagaki N, Warming S, Lamkanfi M, Walle LV, Louie S, Dong J, et al. Non-canonical inflammasome activation targets caspase-11. *Nature.* 2011 Nov;479(7371):117–21.

215. Cunha LD, Silva ALN, Ribeiro JM, Mascarenhas DPA, Quirino GFS, Santos LL, et al. AIM2 Engages Active but Unprocessed Caspase-1 to Induce Noncanonical Activation of the NLRP3 Inflammasome. *Cell Rep.* 2017 Jul 25;20(4):794–805.
216. Ito S, Hara Y, Kubota T. CARD8 is a negative regulator for NLRP3 inflammasome, but mutant NLRP3 in cryopyrin-associated periodic syndromes escapes the restriction. *Arthritis Res Ther.* 2014;16(1):R52.
217. Ventoso I, Blanco R, Perales C, Carrasco L. HIV-1 protease cleaves eukaryotic initiation factor 4G and inhibits cap-dependent translation. *Proc Natl Acad Sci.* 2001 Nov 6;98(23):12966–71.
218. Guerrero S, Batisse J, Libre C, Bernacchi S, Marquet R, Paillart JC. HIV-1 Replication and the Cellular Eukaryotic Translation Apparatus. *Viruses.* 2015 Jan 19;7(1):199–218.
219. Jäger S, Cimermancic P, Gulbahce N, Johnson JR, McGovern KE, Clarke SC, et al. Global landscape of HIV–human protein complexes. *Nature.* 2012 Jan;481(7381):365–70.
220. Impens F, Timmerman E, Staes A, Moens K, Ariën KK, Verhasselt B, et al. A catalogue of putative HIV-1 protease host cell substrates. 2012;17.
221. Mattei S, Anders M, Konvalinka J, Kräusslich HG, Briggs JAG, Müller B. Induced Maturation of Human Immunodeficiency Virus. *J Virol.* 2014 Dec;88(23):13722–31.
222. Kräusslich HG. Human immunodeficiency virus proteinase dimer as component of the viral polyprotein prevents particle assembly and viral infectivity. *Proc Natl Acad Sci U S A.* 1991 Apr 15;88(8):3213–7.
223. Pan YY, Wang SM, Huang KJ, Chiang CC, Wang CT. Placement of leucine zipper motifs at the carboxyl terminus of HIV-1 protease significantly reduces virion production. *PLoS One.* 2012;7(3):e32845.
224. Strack PR, Frey MW, Rizzo CJ, Cordova B, George HJ, Meade R, et al. Apoptosis mediated by HIV protease is preceded by cleavage of Bcl-2. *Proc Natl Acad Sci.* 1996 Sep 3;93(18):9571–6.
225. Nie Z, Bren GD, Vlahakis SR, Schimnich AA, Brenchley JM, Trushin SA, et al. Human Immunodeficiency Virus Type 1 Protease Cleaves Procaspase 8 In Vivo. *J Virol.* 2007 Jul;81(13):6947–56.
226. Wagner RN, Reed JC, Chanda SK. HIV-1 protease cleaves the serine-threonine kinases RIPK1 and RIPK2. *Retrovirology.* 2015 Aug 22;12(1):74.
227. Centazzo M, Manganaro L, Alvisi G. Cellular Targets of HIV-1 Protease: Just the Tip of the Iceberg? *Viruses.* 2023 Mar;15(3):712.

228. Freund EC, Lock JY, Oh J, Maculins T, Delamarre L, Bohlen CJ, et al. Efficient gene knockout in primary human and murine myeloid cells by non-viral delivery of CRISPR-Cas9. *J Exp Med*. 2020 Jul 6;217(7):e20191692.
229. Jolly C, Mitar I, Sattentau QJ. Requirement for an intact T-cell actin and tubulin cytoskeleton for efficient assembly and spread of human immunodeficiency virus type 1. *J Virol*. 2007 Jun;81(11):5547–60.
230. Jolly C, Kashefi K, Hollinshead M, Sattentau QJ. HIV-1 Cell to Cell Transfer across an Env-induced, Actin-dependent Synapse. *J Exp Med*. 2004 Jan 19;199(2):283–93.
231. Chesebro B, Nishio J, Perryman S, Cann A, O'Brien W, Chen IS, et al. Identification of human immunodeficiency virus envelope gene sequences influencing viral entry into CD4-positive HeLa cells, T-leukemia cells, and macrophages. *J Virol*. 1991 Nov;65(11):5782–9.
232. Chesebro B, Wehrly K, Nishio J, Perryman S. Macrophage-tropic human immunodeficiency virus isolates from different patients exhibit unusual V3 envelope sequence homogeneity in comparison with T-cell-tropic isolates: definition of critical amino acids involved in cell tropism. *J Virol*. 1992 Nov;66(11):6547–54.
233. Toohey K, Wehrly K, Nishio J, Perryman S, Chesebro B. Human immunodeficiency virus envelope V1 and V2 regions influence replication efficiency in macrophages by affecting virus spread. *Virology*. 1995 Oct 20;213(1):70–9.
234. Walter BL, Wehrly K, Swanstrom R, Platt E, Kabat D, Chesebro B. Role of low CD4 levels in the influence of human immunodeficiency virus type 1 envelope V1 and V2 regions on entry and spread in macrophages. *J Virol*. 2005 Apr;79(8):4828–37.
235. Roesch F, OhAinle M, Emerman M. A CRISPR screen for factors regulating SAMHD1 degradation identifies IFITMs as potent inhibitors of lentiviral particle delivery. *Retrovirology*. 2018 Mar 20;15(1):26.
236. Vermeire J, Naessens E, Vanderstraeten H, Landi A, Iannucci V, Van Nuffel A, et al. Quantification of reverse transcriptase activity by real-time PCR as a fast and accurate method for titration of HIV, lenti- and retroviral vectors. *PLoS One*. 2012;7(12):e50859.
237. Müller B, Anders M, Akiyama H, Welsch S, Glass B, Nikovics K, et al. HIV-1 Gag processing intermediates trans-dominantly interfere with HIV-1 infectivity. *J Biol Chem*. 2009 Oct 23;284(43):29692–703.
238. Freed EO. HIV-1 assembly, release and maturation. *Nat Rev Microbiol*. 2015 Aug;13(8):484–96.
239. Ishima R, Ghirlando R, Tözsér J, Gronenborn AM, Torchia DA, Louis JM. Folded Monomer of HIV-1 Protease *. *J Biol Chem*. 2001 Dec 28;276(52):49110–6.

240. Strisovsky K, Tessmer U, Langner J, Konvalinka J, Kräusslich HG. Systematic mutational analysis of the active-site threonine of HIV-1 proteinase: Rethinking the “fireman’s grip” hypothesis. *Protein Sci.* 2000 Sep;9(9):1631–41.
241. Weber IT. Comparison of the crystal structures and intersubunit interactions of human immunodeficiency and Rous sarcoma virus proteases. *J Biol Chem.* 1990 Jun 25;265(18):10492–6.
242. Jacobsen H, Ahlborn-Laake L, Gugel R, Mous J. Progression of early steps of human immunodeficiency virus type 1 replication in the presence of an inhibitor of viral protease. *J Virol.* 1992 Aug;66(8):5087–91.
243. Stefanidou M, Herrera C, Armanasco N, Shattock RJ. Saquinavir inhibits early events associated with establishment of HIV-1 infection: potential role for protease inhibitors in prevention. *Antimicrob Agents Chemother.* 2012 Aug;56(8):4381–90.
244. Uchida H, Maeda Y, Mitsuya H. HIV-1 protease does not play a critical role in the early stages of HIV-1 infection. *Antiviral Res.* 1997 Oct 1;36(2):107–13.
245. Kaplan AH, Manchester M, Smith T, Yang YL, Swanstrom R. Conditional human immunodeficiency virus type 1 protease mutants show no role for the viral protease early in virus replication. *J Virol.* 1996 Sep;70(9):5840–4.
246. Nagy K, Young M, Baboonian C, Merson J, Whittle P, Oroszlan S. Antiviral activity of human immunodeficiency virus type 1 protease inhibitors in a single cycle of infection: evidence for a role of protease in the early phase. *J Virol.* 1994 Feb;68(2):757–65.
247. Sundquist WI, Kräusslich HG. HIV-1 Assembly, Budding, and Maturation. *Cold Spring Harb Perspect Med.* 2012 Jul;2(7):a006924.
248. Novikova M, Zhang Y, Freed EO, Peng K. Multiple Roles of HIV-1 Capsid during the Virus Replication Cycle. *Virol Sin.* 2019 Apr 26;34(2):119–34.
249. Hulme AE, Kelley Z, Okocha EA, Hope TJ. Identification of Capsid Mutations That Alter the Rate of HIV-1 Uncoating in Infected Cells. *J Virol.* 2014 Dec 16;89(1):643–51.
250. Eschbach JE, Elliott JL, Li W, Zadrozny KK, Davis K, Mohammed SJ, et al. Capsid Lattice Destabilization Leads to Premature Loss of the Viral Genome and Integrase Enzyme during HIV-1 Infection. *J Virol.* 2020 Dec 22;95(2):e00984-20.
251. Saito A, Yamashita M. HIV-1 capsid variability: viral exploitation and evasion of capsid-binding molecules. *Retrovirology.* 2021 Oct 26;18(1):32.
252. Huang L, Chen C. Understanding HIV-1 protease autoprocessing for novel therapeutic development. *Future Med Chem.* 2013 Jul;5(11):10.4155/fmc.13.89.

253. Pettit SC, Clemente JC, Jeung JA, Dunn BM, Kaplan AH. Ordered Processing of the Human Immunodeficiency Virus Type 1 GagPol Precursor Is Influenced by the Context of the Embedded Viral Protease. *J Virol*. 2005 Aug 15;79(16):10601–7.
254. Ludwig C, Leiherer A, Wagner R. Importance of protease cleavage sites within and flanking human immunodeficiency virus type 1 transframe protein p6* for spatiotemporal regulation of protease activation. *J Virol*. 2008 May;82(9):4573–84.
255. Louis JM, Clore GM, Gronenborn AM. Autoprocessing of HIV-1 protease is tightly coupled to protein folding. *Nat Struct Biol*. 1999 Sep;6(9):868–75.
256. Humpolíčková J, Weber J, Starková J, Mašínová E, Günterová J, Flaisigová I, et al. Inhibition of the precursor and mature forms of HIV-1 protease as a tool for drug evaluation. *Sci Rep*. 2018 Jul 11;8(1):10438.
257. Louis JM, Aniana A, Weber IT, Sayer JM. Inhibition of autoprocessing of natural variants and multidrug resistant mutant precursors of HIV-1 protease by clinical inhibitors. *Proc Natl Acad Sci*. 2011 May 31;108(22):9072–7.
258. Huang L, Chen C. Autoprocessing of human immunodeficiency virus type 1 protease miniprecursor fusions in mammalian cells. *AIDS Res Ther*. 2010 Jul 28;7(1):27.
259. Huang L, Li Y, Chen C. Flexible catalytic site conformations implicated in modulation of HIV-1 protease autoprocessing reactions. *Retrovirology*. 2011 Oct 10;8:79.
260. Huang L, Li L, Tien C, LaBarbera DV, Chen C. Targeting HIV-1 Protease Autoprocessing for High-throughput Drug Discovery and Drug Resistance Assessment. *Sci Rep*. 2019 Jan 22;9(1):301.
261. Tien C, Huang L, Watanabe SM, Speidel JT, Carter CA, Chen C. Context-dependent autoprocessing of human immunodeficiency virus type 1 protease precursors. *PLoS One*. 2018;13(1):e0191372.
262. Alvarez E. HIV protease cleaves poly(A)-binding protein [Internet]. 2006 [cited 2022 Sep 16]. Available from: <https://www.ncbi.nlm.nih.gov/pmc/articles/PMC1462710/>
263. Pino J del, Jiménez JL, Ventoso I, Castelló A, Muñoz-Fernández MÁ, Haro C de, et al. GCN2 Has Inhibitory Effect on Human Immunodeficiency Virus-1 Protein Synthesis and Is Cleaved upon Viral Infection. *PLOS ONE*. 2012 Oct 23;7(10):e47272.
264. Genetic and mechanistic basis for APOBEC3H alternative splicing, retrovirus restriction, and counteraction by HIV-1 protease | *Nature Communications* [Internet]. [cited 2024 Feb 23]. Available from: <https://www.nature.com/articles/s41467-018-06594-3>

265. Jurczynszak D, Zhang W, Terry SN, Kehrer T, González MCB, McGregor E, et al. HIV protease cleaves the antiviral m6A reader protein YTHDF3 in the viral particle. *PLOS Pathog.* 2020 Feb 13;16(2):e1008305.
266. Poreba M, Szalek A, Rut W, Kasperkiewicz P, Rutkowska-Wlodarczyk I, Snipas SJ, et al. Highly sensitive and adaptable fluorescence-quenched pair discloses the substrate specificity profiles in diverse protease families. *Sci Rep.* 2017 Feb 23;7(1):43135.
267. He X, Aid M, Ventura JD, Borducchi E, Lifton M, Liu J, et al. Rapid Loss of CD4 T Cells by Pyroptosis during Acute SIV Infection in Rhesus Macaques. *J Virol.* 2022 Aug 24;0(0):e00808-22.
268. Picker LJ, Hagen SI, Lum R, Reed-Inderbitzin EF, Daly LM, Sylwester AW, et al. Insufficient Production and Tissue Delivery of CD4+Memory T Cells in Rapidly Progressive Simian Immunodeficiency Virus Infection. *J Exp Med.* 2004 Nov 15;200(10):1299–314.
269. Finkel TH, Tudor-Williams G, Banda NK, Cotton MF, Curiel T, Monks C, et al. Apoptosis occurs predominantly in bystander cells and not in productively infected cells of HIV- and SIV-infected lymph nodes. *Nat Med.* 1995 Feb;1(2):129–34.
270. Harouse JM, Gettie A, Tan RCH, Blanchard J, Cheng-Mayer C. Distinct Pathogenic Sequela in Rhesus Macaques Infected with CCR5 or CXCR4 Utilizing SHIVs. *Science.* 1999 Apr 30;284(5415):816–9.
271. Meyerson NR, Sharma A, Wilkerson GK, Overbaugh J, Sawyer SL. Identification of Owl Monkey CD4 Receptors Broadly Compatible with Early-Stage HIV-1 Isolates. *J Virol.* 2015 Aug;89(16):8611–22.
272. Warren CJ, Meyerson NR, Dirasantho O, Feldman ER, Wilkerson GK, Sawyer SL. Selective use of primate CD4 receptors by HIV-1. *PLOS Biol.* 2019 Jun 10;17(6):e3000304.
273. Foley RA, Lahr MM. Ghosts of extinct apes: genomic insights into African hominid evolution. *Trends Ecol Evol [Internet].* 2024 Jan 31 [cited 2024 Feb 21];0(0). Available from: [https://www.cell.com/trends/ecology-evolution/abstract/S0169-5347\(23\)00347-6](https://www.cell.com/trends/ecology-evolution/abstract/S0169-5347(23)00347-6)
274. Boyd SE, Pike RN, Rudy GB, Whisstock JC, Garcia de la Banda M. PoPS: a computational tool for modeling and predicting protease specificity. *J Bioinform Comput Biol.* 2005 Jun;3(3):551–85.
275. Verspurten J, Gevaert K, Declercq W, Vandenabeele P. SitePredicting the cleavage of proteinase substrates. *Trends Biochem Sci.* 2009 Jul;34(7):319–23.

276. Song J, Li F, Leier A, Marquez-Lago TT, Akutsu T, Haffari G, et al. PROSPERous: high-throughput prediction of substrate cleavage sites for 90 proteases with improved accuracy. *Bioinformatics*. 2018 Feb 15;34(4):684–7.
277. Li F, Leier A, Liu Q, Wang Y, Xiang D, Akutsu T, et al. Procleave: Predicting Protease-specific Substrate Cleavage Sites by Combining Sequence and Structural Information. *Genomics Proteomics Bioinformatics*. 2020 Feb;18(1):52–64.
278. Li F, Wang Y, Li C, Marquez-Lago TT, Leier A, Rawlings ND, et al. Twenty years of bioinformatics research for protease-specific substrate and cleavage site prediction: a comprehensive revisit and benchmarking of existing methods. *Brief Bioinform*. 2018 Aug 29;20(6):2150–66.
279. Chun TW, Stuyver L, Mizell SB, Ehler LA, Mican JA, Baseler M, et al. Presence of an inducible HIV-1 latent reservoir during highly active antiretroviral therapy. *Proc Natl Acad Sci U S A*. 1997 Nov 25;94(24):13193–7.
280. Douek DC, Betts MR, Brenchley JM, Hill BJ, Ambrozak DR, Ngai KL, et al. A novel approach to the analysis of specificity, clonality, and frequency of HIV-specific T cell responses reveals a potential mechanism for control of viral escape. *J Immunol Baltim Md 1950*. 2002 Mar 15;168(6):3099–104.
281. Wang Z, Gurule EE, Brennan TP, Gerold JM, Kwon KJ, Hosmane NN, et al. Expanded cellular clones carrying replication-competent HIV-1 persist, wax, and wane. *Proc Natl Acad Sci*. 2018 Mar 13;115(11):E2575–84.
282. Cohn LB, Chomont N, Deeks SG. The Biology of the HIV-1 Latent Reservoir and Implications for Cure Strategies. *Cell Host Microbe*. 2020 Apr 8;27(4):519–30.